Imperial College London

A Top-Down Approach to Understand the Fire Performance of Building Facades Using Standard Test Data

A thesis submitted in partial fulfilment of the

requirements for the degree of

Doctor of Philosophy

in

Mechanical Engineering

by

Matthew Bonner

2020

Supervised by Prof. Guillermo Rein

Declaration of Originality

I declare that this thesis and the work described within have been completed solely by myself under the supervision of Prof. Guillermo Rein. Where others have contributed or other sources are quoted, full references are given.

Matthew Bonner

2020

Copyright Declaration

To my loving family.

ABSTRACT

A Top-Down Approach to Understand the Fire Performance of Building Facades Using Standard Test Data

by

Matthew Bonner

Doctor of Philosophy in Mechanical Engineering

Imperial College London, 2020

Supervised by Prof. Guillermo Rein

Designing the outer walls of a building – its facade – is a complex, multi-objective problem. While some design objectives, like weight, are easily quantified others, like fire safety, are harder to assess, making it difficult to compare facades in that objective. A move to more complex facades with novel materials has led the number of facade fires to quadruple over the last 3 decades. Current fire safety literature has no way to accurately predict the performance of a facade from its individual components, therefore the only way to test whether a facade system is safe is to run a large-scale fire test. Thousands of these tests are run internationally each year, subjecting different facades to different fire scenarios depending on the country, but data from these tests are locked away, missing an opportunity to learn from this untapped source of knowledge. This thesis taps into that source for the first time by presenting a unique database of 384 facade tests, named KRESNIK. We analysed this database using a top-down, statistical approach, and found that facades with combustible cladding and a cavity generally performed worse in these tests. These trends were investigated further in a parametric series of 20 intermediate-scale experiments on facades with different cladding and insulation materials, with and without a cavity. These experiments were analysed using a novel method to measure the heat released through visible flames in a fire from regular camera footage. We refer to this quantity as *visual fire power*. KRESNIK was also used to compare, for the first time, the behaviour of similar facades tested using different test standards, finding that different standards could not agree on how to rank the same facades. This work demonstrates the power of a top-down approach to tackle fire safety using data that already exists.

ACKNOWLEDGEMENTS

In the four years and three months it took to undertake the work in this thesis I have received incalculable help and support from friends, colleagues, and family. While I cannot possibly thank everyone here, I will do my best.

I would like to thank EPSRC and Ove Arup and Partners for sponsoring this research, and Imperial College London for providing everything I could need to complete this work successfully. Thank you also to ITB for being such close collaborators during this work, particularly to Dr Wojciech Wegrzynski for getting the whole thing started – without those post-conference drinks, I doubt this PhD would exist in its current form.

Thank you to all of my colleagues in Hazelab, both past and present, who are an inestimable source of expertise, and also great company. Thank you particularly to Egle, for getting me into cameras; to Francesco, for being a general font of knowledge and wisdom; to Nieves, for letting me know that researchers are human too; to Nils, for letting me use your coffee machine; to Iza, for your emotional support and for sharing my video game enthusiasm; to Yuqi for introducing me to Baiju; to Franz for being the best flatmate; to Eirik for our many enlightening discussions; to Ben and Francesca for being the facade research dream-team; and to everyone else for making the Hazelab such a wonderful place to work. Special thanks to honorary Hazelab member Christos Trapezaris for collecting damage profiles from photos taken before and after 252 different facade tests. That saved me a lot of effort.

Now onto the extracurricular acknowledgments. Thank you in general to the communities of the Imperial College Book Club and Imperial College Buddhist Society. Although there are too many individuals to thank, you made Imperial feel like more than just an office. Those thanks are also extended to all my friends in the Mechanical Engineering Department, particularly to Lisa for hosting so many amazing dinner parties.

To all of the friends who offered me emotional support through these years, you have my deepest gratitude. I surely can't mention everyone individually, but thanks to Mike, Shibani, Ryan, Mikaela, and all those mentioned elsewhere. Thank you as well to Issi, for everything.

Thank you to all my friends from the UCL Comedy Club for being a constant source of joy and laughter through these years, and for encouraging me to take one of my favourite holidays of these last four years. Thank you also to the beer boys for a series of get togethers that can only be titled “How I learned to stop worrying and love sour beer”; and particularly to Jeremy, who has managed to stay friends with me despite everything.

My particular gratitude goes to my old flatmates from Buchanan Gardens – I guess that suffering really does produce strong friendships. Thank you, Hugo, for constantly teaching me about another area of knowledge I didn’t know existed; Emrys, for being master of the obscure recommendation; Oli, for always being up for a philosophy debate; Miguel, for being the best DM, along with everything else; and to honorary Buchanan Gardens flatmate Arthur, for everything, but most relevantly the figures he made for this thesis.

Thank you to all of my family who have given me their love, generosity, and kindness over the years. I would like to mention Ara in particular, in the hope it might encourage her to get into science. Of course, my deepest thanks go to my parents and sisters, not least for letting me live with them for the last 9 months of this research. I owe them for everything, and this thesis is dedicated to them.

Lastly, I would like to extend special thanks to my supervisor, and the guiding hand behind this thesis, Guillermo. I started this PhD with very little knowledge of fire safety or academia, and you have provided guidance, passion, and support throughout. Despite teaching 2 undergraduate courses and having at least another 12 PhD students to look after, you seem to care for every one of your students. I have had so many opportunities to travel and learn during this project, and that is in large part down to you. Thank you.

TABLE OF CONTENTS

LIST OF FIGURES

LIST OF TABLES

NOMENCLATURE

Symbols

T	Temperature
β	Linear Model Parameter
k	Thermal Conductivity
ρ	Density
c	Specific Heat
ΔH	Heat of Combustion
Δx	Layer Thickness
L	Flame Height
$\Delta\theta^*$	Dimensionless Excess Temperature
ΔL^*	Dimensionless Excess Flame Height
Q^*	Dimensionless Heat Release Rate
g	Acceleration due to gravity
D	Characteristic length of fire source

Subscripts

∞	Ambient conditions
p	Peak
f	With respect to flame
s	Relating to fire source
e	External

i	Insulation

Abbreviations

ACP	Aluminium Composite Panel
AI	Artificial Intelligence
EPS	Expanded Polystyrene
ERD	Entity Relationship Diagram
ETICS	External Thermally Insulating Composite System
FR	Fire Retardant
GRC	Glass Reinforced Concrete
HPL	High Pressure Laminate
PE	Polyethylene
PIR	Polyisocyanurate
PUR	Polyurethane
WPC	Wood Polymer Composite

PREFACE

This thesis contains 7 chapters. Chapter 1 provides an introduction and context to the thesis. Chapter 7 provides the overall conclusions of the thesis. The other chapters are either based on already published manuscripts, or partially completed manuscripts that will be submitted for publication.

Chapter 2 is based on the published paper:

M. Bonner and G. Rein, Flammability and Multi-Objective Performance of Building Facades: Towards Optimum Design, IJHRB, 7 (4), 2018, https://doi.org/10.21022/IJHRB.2018.7.4.363

Chapter 3 is based on the published paper:

M. Bonner, W. Wegrzynski, B. K. Papis, and G. Rein, KRESNIK: A top-down, statistical approach to understand the fire performance of building facades using standard test data, Building and Environment, 169, 2019 https://doi.org/10.1016/j.buildenv.2019.106540

Chapter 4 is based on a paper in progress:

M. Bonner, W. Wegrzynski, B. K. Papis, B. Khoo, F. Lugaresi, and G. Rein, Fires in the Walls of Tall Buildings: A Parametric Study and 3D Reconstruction of Intermediate-Scale Facade Experiments Containing Combustible Components (To be submitted)

Chapter 5 is based on a paper in progress:

M. Bonner and G. Rein, A Novel Method for Measuring Heat Released Through Visible Flaming in Regular Camera Footage (to be submitted)

Chapter 6 is based on a paper in progress:

M. Bonner, W. Wegrzynski, B.K. Papis, and G. Rein, KRESNIK: Comparing the Performance of Similar Facades Across Different International Fire Test Standards. (to be submitted)

Publications produced outside of this thesis

The following publications were co-authored during the course of this PhD on fire related topics but are not part of this thesis.

D. M. J. Purnomo, F. Richter, M. Bonner, R. Vaidyanathan, and G. Rein, Role of optimisation method on kinetic inverse modelling of biomass pyrolysis at the microscale, Fuel, 262, 2020, https://doi.org/10.1016/j.fuel.2019.116251.

D. M. J. Purnomo, M. Bonner, S. Moafi, and G. Rein, Using cellular automata to simulate field-scale flaming and smouldering wildfires in tropical peatlands, Proceedings of the Combustion Institute, 2020, https://doi.org/10.1016/j.proci.2020.08.052

E. Rackauskaite, M. Bonner, F. Restuccia, N. Fernandez-Anez, E. G. Christensen, N. Roenner, W. Wegrzynski, P. Tofilo, M. Heidari, P. Kotsovinos, I. Vermesi, F. Richter, Y. Hu, C. Jeanneret, R. Wadhwani, and G. Rein, Fire Experiment inside a Very Large and Open-Plan Compartment: x-ONE, Fire Technology (submitted)

Chapter 1

Introduction

The outer walls of a building – its facade – represent one of the most complex and expensive parts of such a construction project, sometimes accounting for up to 25% of the total cost [1]. They must achieve multiple objectives of benefit to the building's occupants, maximising positive traits, such as the sustainability and aesthetics of the building, while minimising negative traits, such as the build-up of condensation in the walls or the overall fire risk of the building. These objectives are not independent however and improving one objective (e.g., improving a facade's moisture control) may require a trade-off in another (e.g., its ability to limit the spread of fire).

Over the last 30 years there have been over 50 fires in skyscrapers around the world where the fire has spread via the building's facade (see Chapter 2). These kinds of fires are becoming more frequent, with half of those fire having occurred since 2012. In many of these fires, the facade was ignited and contributed to the fire. A desire for taller, energy efficient buildings has led to facades being built with newer materials that can provide greater strength-to-weight ratios and better insulating properties. Most of these new materials are polymer-based, and thus have the potential to be flammable.

A material's flammability is "the ease with which a material is ignited, the intensity with which it burns and releases heat once ignited, its propensity to spread fire, and the rate at which it generates smoke and toxic combustion products during gasification and burning" [2]. The flammability of a facade can be seen in the same way – the ease at which the entire system is ignited, promotes flame spread, and generates smoke. In both cases, the flammability of a material or system is also dependent on the external conditions, for instance the size and location of the fire the system is experiencing. However, it is useful to be able to discuss the flammability of a material or system independently of these external conditions, as is the case when the term is used colloquially. Therefore, the flammability of a facade can be thought of as the ease at which that facade is ignited, promotes flame spread, and generates smoke *across all the fire scenarios it could likely experience in its lifetime*.

Being able to quantify a facade's flammability is important. The Grenfell Tower fire in 2017 claimed 72 lives [3], but this was not the only building in the UK with a flammable facade. The UK government has vowed to spend billions [4] to fix what has been named a "cladding crisis", by replacing or adapting the facades of buildings deemed at risk. Selecting which facades should be prioritised is a difficult problem that would be made easier if their relative flammability could be quantified, and therefore easily compared. When designing new facades, the ability to quantify flammability could also allow more sophisticated approaches to optimising the many objectives a facade needs to achieve.

One approach to quantifying facade flammability would be to fully understand how the materials in each component react to fire, then how each component in the facade system reacts to fire, then combine this with knowledge how the components interact with each other and the geometry of the facade system across different fires to then be able to fully parameterise the problem. In this thesis, I refer to this procedure as the *bottom-up* approach to understanding facade flammability. The flammability defined here would be a fuzzy variable, as deciding on the weights of each factor that makes up flammability (ease of ignition, amount of smoke produced) is subjective, as is selecting the range of fires that the facade would likely experience. The state-of-the-art of fire science is a long way from being able to do this for complex facade systems, however this approach is crucial for understanding facade flammability in the long term, as the predictions it makes can be extended to novel materials and designs.

In contrast, this thesis presents a *top-down* approach to quantifying the flammability of building facades. This approach analyses a large number of examples of the fire behaviour of entire facade systems and uses statistics and machine learning to identify empirical trends in the data. These trends can be used to predict the behaviour of new facades that are similar to those in the dataset, or to identify trends in the data that could be investigated using a more traditional bottom-up approach. This top-down approach is common in other research fields with complex behaviour, such as a medicine or economics, and has already been applied in other areas of fire safety (see Section 2.5). However, this approach still requires a definition of flammability that will be inherently fuzzy, as in the bottom-up case. It also requires a range of examples from different types of fire to produce generalised results.

Finding large quantities of existing data on the fire behaviour of facades presents another large challenge, however. Existing literature on facade fires is still relatively sparse – and was even more so when this research project began in 2016 (see Chapter 2). Therefore, the data available from published experiments is much smaller than the amount usually required for machine learning; in addition, each experimental setup is unique – making it harder to compare between them. In many countries however, for a facade to be approved for use on a building it may undergo a fire safety test according to some national standard. These facade fire safety tests subject a mock-up of a facade to one kind of fire that it might experience during its lifespan and measure certain criteria to decide whether a facade can or cannot be used on a building. There are at least 14 different national facade fire test standards used globally, and each one uses a different kind of fire, different measurements, or different criteria to decide whether a facade has passed. Whether the criteria in these tests adequately assess whether a facade should or should not be used on a building is a matter of debate, however in either case thousands of these tests are performed every year, meaning they represent a large source of existing data on the fire behaviour of facades in different fire conditions. Unfortunately, the data from these tests are stored in unstructured reports, as opposed to the structured data used for top-down analysis. If this data could be analysed using a top-down approach, it could be valuable source of scientific knowledge.

1.1 Aims and Objectives

The aim of this research was to transform standardised facade fire tests into a useful source of scientific knowledge and to present the top-down approach as a potential path to quantifying facade flammability as a design objective. To achieve this aim, the following objectives were identified: (i) to create a structured database of standard facade fire tests from the previously unstructured data in standard test reports; (ii) to analyse this data for what design factors correlate with different factors related to facade flammability; (iii) to identify ways to improve the data collected in standard facade tests; (iv) to find methods for comparing the data from different national test standards; (v) to propose a method for converting the structured data from these tests into a way to quantify flammability.

1.2 Layout of Thesis

Chapter 2 presents a review of the literature on fire safety in facades, covering the different categories of facade, the different objectives that facades are expected to fulfil, and the different components that make up a facade. It also discusses the role of optimisation in facade design and the advantages of explicitly quantifying facade flammability

Chapter 3 addresses objectives (i) and (ii) and presents the design and preliminary analysis of a database of 252 commercial facade tests, named KRESNIK. The data in this chapter came from a single test house: Instytut Techniki Budowlanej (ITB) from Poland using the Polish national facade test standard. It explains the decisions taken in the structure of the database, and the trends that emerged from looking at this initial dataset.

Chapter 4 addresses objective (iii) and presents a detailed explanation and validation of a novel methodology for predicting the heat released from visible flaming, the visual fire power, during a well-ventilated, turbulent diffusion fire. Results from a series of calibration experiments using fires with known heat release rates are presented alongside an explanation of the algorithms used.

Chapter 5 presents a parametric series of 22 experiments on rainscreen facades, using a similar method to the Polish national standard, but with a higher resolution of data recorded. The results from these experiments are compared to the trends from Chapter 3, in order to assess whether the analysis was reasonable and to address gaps in the original dataset. This chapter also uses estimates of the visual fire power taken during the experiments, using the method explained in Chapter 4.

Chapter 6 addresses objective (iv) and presents a methodology for comparing between data from national facade test standards that use fire sources with different heat release rates and geometries. This is done using an updated version of the database in Chapter 3, containing an additional 168 tests across 3 different test standards. This new database, named KRESNIK II, is also used to train a simple AI model, which can be used to predict the outcome of a facade test based on the facade's structure and materials and the test standard used.

Chapter 7 presents the conclusions from this thesis and suggestions for future work. It also discusses how an AI model, such as the one presented in Chapter 6, could be used as a way to quantify flammability when optimising design objectives, addressing objective (v) of the research.

Chapter 2

Literature Review of Facade Flammability and Multi-Objective Optimisation

Summary[1]

This chapter presents a review of the previous literature on facade fire safety. We discuss the multiple objectives that need to be considered when designing a facade, and how a shifted focus towards the objectives of energy efficiency and thermal insulation has led to an increase in the use of polymeric materials in facades, increasing facade flammability. We discuss previous research done into different types of facades, moving from simple monolithic facades, such as brick walls, to complex rainscreen facades with cladding, insulation, and ventilated cavities, and show that as facades have become more complex, so too has their potential flammability increased. Finally, we discuss previous research done to try and explicitly quantify the flammability of facade systems, and the advantages this could bring through the use of optimum design.

2.1 Introduction

The facade is an important part of a building, its principal front facing the open space. A facade performs multiple objectives of value to its occupants, like protecting from wind, rain, sunlight, heat, cold, and sound, on top of its aesthetic significance. Facade systems are complex, and represent one of the largest construction costs for high-rise buildings, sometimes as much as 20-25% of the total [1]. Modern facades, especially in tall buildings, have become high-performance systems, designed by advanced engineering, and resulting in much greater complexity than the traditional monolithic stone, brick, or concrete facades of earlier times.

However, fires involving the facade have never been more prevalent [5]. In an online search of news in the English language, the number of fires in tall buildings worldwide

[1] This chapter is based on the published paper: M. Bonner and G. Rein, Flammability and Multi-Objective Performance of Building Facades: Towards Optimum Design, IJHRB, 7 (4), pp 363-374, https://doi.org/10.21022/IJHRB.2018.7.4.363

with spread via the external wall was found to be, on average, 4 per year over the last 5 years – a 5 times increase from the yearly average from 30 years ago (Figure 2.1). These data are biased towards large fires that were reported by the media, so many smaller facade fires may not have been included, but the trend is clear: facade fires in high-rise buildings are becoming more frequent.

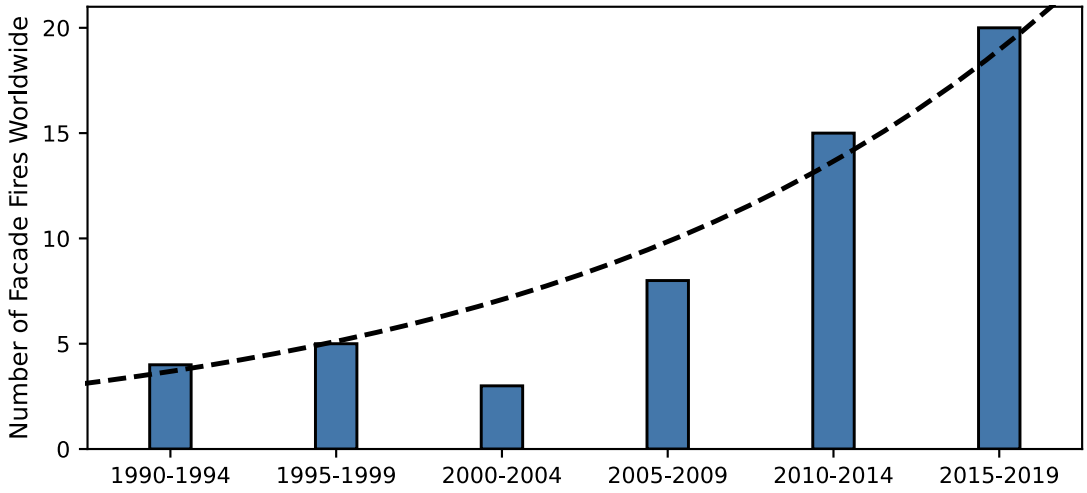

Figure 2.1: Data showing the frequency of large facade fires worldwide from 1990 to November 2019. Data found from news articles online. This data has since been made available online [6], [7].

The primary threat from a facade fire to a building's residents is a potential breach in compartmentation, either vertically (from floor to floor) or horizontally (e.g., from apartment to apartment). Fire strategies for high-rise buildings typically aim for the fire to be confined to its floor of origin for an extended period after its initiation [8], [9]. One potential vertical breach comes from a compartment fire breaking through an opening in the facade, extending up the side of the building, and then igniting material in the compartments above (so called "leap-frogging") [8], [10]. A fire could also spread via the internal wall of the facade if the fire stopping is insufficient or the facade warps and creates paths for the spread of smoke and flame. In modern facades, that may contain varying amounts of flammable components, another possibility is that a facade ignites and directly contributes to a fire, assisting rather than hindering its spread. This ignition could be triggered by direct flame impingement from a compartment fire breaking through an opening in the facade (an externally venting flame or EVF) or from an external fire source such as a car or bin fire or could be triggered from the radiation from another nearby fire, or from faulty electrical circuits within the facade itself.

The flammable components in facades are generally formed from a wide range of polymers such as polyethylene, polycarbonate, phenolics, polyisocyanurate (PIR), polyurethane (PUR) or polystyrene, to name just a few [5]. Different types of polymers will burn very differently. For example, polyethylene will often melt and form pools of liquid fuel, while polyurethane will char and remain solid. Components within a facade system made of these materials may be included in the original engineering design or added at later stages by contractors. They may also be added when a facade is refurbished, or when parts are replaced during the life of a property.

The number of flammable components used in a facade will affect the overall flammability of the system, but it is not the only factor. As mentioned in Chapter 1, the flammability of a material is the "the ease with which a material is ignited, the intensity with which it burns and releases heat once ignited, its propensity to spread fire, and the rate at which it generates smoke and toxic combustion products during gasification and burning" [2]. The flammability of the facade itself can be defined in the same way. In this case, flammability is not only a function of the flammable materials used in the facade. For instance, in the case of a facade with a ventilated cavity, the cavity itself is not flammable but it will increase the facade's propensity to spread fire and smoke, and therefore increase its flammability. A similar argument can be made for the geometry of the facade.

For this reason, it is essential to understand how the whole facade system will perform in the event of a fire, and not only the materials and components independently (Figure 2.2). However, there are significant gaps in our understanding of facade fires. This is for two reasons: firstly, there are a myriad of different design decisions for any facade build-up such that it complies with its multiple objectives within a building; and secondly, there is no theory, model, or comprehensive experimental data series that can reliably explain or predict from first principles how a facade will behave in case of fire. This has led to the situation where, since 2002 in the UK, the only way for designers to assess whether a facade containing flammable components was suitable to use on a building was to subject it to a large-scale fire test [11], [12]; but large-scale testing is prohibitively time consuming, expensive, and the results cannot be extrapolated to other facade designs. Since the Grenfell Tower fire in 2017 (in which the facade had not undergone such large-scale testing) this route to compliance has also been removed as a possibility, restricting designers to only use facades without flammable components [13].

However, a facade's flammability does not only depend on its components, and polymeric materials provide a number of advantages in facade design.

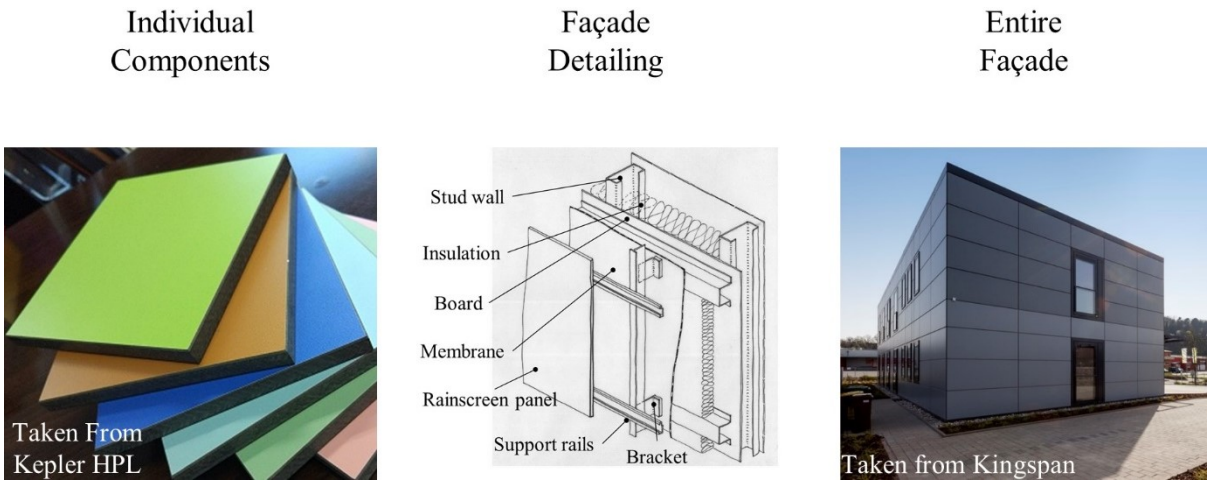

Figure 2.2: Images demonstrating the different levels of analysis when considering a facade. Currently, fire research focuses mainly on individual components, while large-scale fire testing is used to assess facade systems.

2.2 Design Objectives for Facades

Building a facade is a multi-objective problem. A successful facade system must help to bring safety and comfort to a building's occupants by providing protection from wind, moisture, light, heat, cold, and sound. These requirements must be balanced with a facade's aesthetics, sustainability, and return on investment. Overall, these broad goals can be broken down into more specific design objectives, detailed in Table 2.1. These objectives are not independent and improving in one area may require a trade-off in another.

In order to balance these multiple objectives, facade systems combine layers of different materials [14]. The material list will nearly always include polymers in some amount, as they are high-performing, affordable, and their thermal and mechanical properties can be manipulated and tailored to meet different needs. However, all polymers can ignite and promote flame spread to some degree and will increase a facade's flammability.

Table 2.1: Objectives in facade design [14]. Objectives are ordered by whether they are intended to be minimized or maximized, and from those that ensure the building is safe, to those that ensure the building is comfortable.

Objective	Description
Minimal flammability	Reducing flammability reduces a facade's contribution to fire spread.
Minimal moisture ingress	Reducing water in a facade reduces mould and damp in the building.
Minimal weight	Reducing the weight of a facade reduces construction time and the amount of structural support required, allowing for more complex facade geometries.
Minimal thickness	Reducing the thickness of a facade increases the living area available inside the building.
Maximal structural stability	Increasing the stability of a facade increases its ability to withstand all loading conditions e.g., wind, self-weight, other live loads.
Maximal thermal insulation	Increasing the insulating ability of a facade decreases the energy needed to ensure the comfort of the building's occupants.
Maximal lighting comfort	Increasing the quality of sunlight management provided by a facade increases the comfort of the building's occupants.
Maximal sound insulation	Increasing the amount of external noise blocked by a facade increases the comfort of the building's occupants.
Aesthetics	A facade should be beautiful.
Sustainability	A facade should be environmentally sustainable. This could refer to the amount of greenhouse gases released, or the amount of pollution generated, by both the facade's creation and, at the end of its life, its destruction or re-use.
Return on investment	A facade must stay within its allowed budget.

Over time, the amount of polymeric material used in facades has increased. In order to understand why, we need to look at the factors that have driven this change. There are three main drivers.

The first driver is a requirement for energy efficiency. After the oil crises of the 1970s, western countries shifted high-rise building design towards energy saving by reducing thermal losses [15]. Shortly afterwards, polymers entered the building industry, providing generally better thermal performance than other insulation materials.

The second driver is sustainability. The demand for thermal efficiency has increased again in recent years with growing concerns over carbon emissions. Figure 2.3 shows the legal requirements for the insulating ability of external walls in the United Kingdom (UK) over two decades, expressed in terms of their U-Values. The U-Value of a wall quantifies its overall thermal transmittance - a lower value indicating a better insulating performance. The U-Value is measured under steady-state conditions and is therefore only used in countries where the climate is relatively constant (such as the UK). The increasing trend in UK insulation requirements is clear and is the result of government policies targeting energy efficiency and sustainably. This UK trend is representative of legislation across much of the northern hemisphere [16], [17]. Possible solutions to this increased demand on thermal performance are to reduce the number of openings (vents, glazing) on a facade, include thicker insulation in a facade, or to increase the thermal resistance of that insulation. Polymers are suited to meet these requirements because they are good thermal insulators.

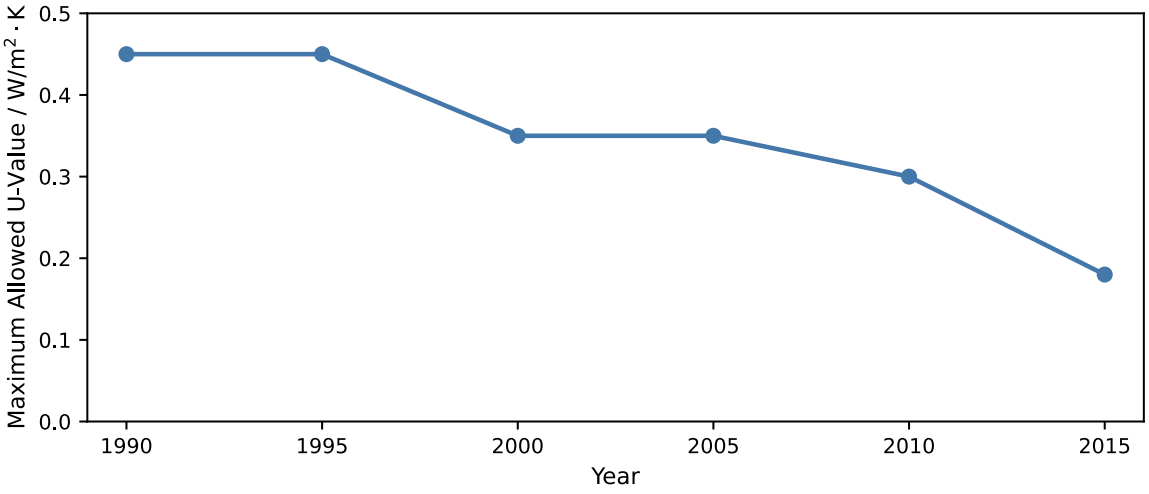

Figure 2.3: Maximum U-Values allowed for external walls in progressive editions of the UK building codes [18].

The third driver is return on investment. In this regard, thinner and lighter facades are more desirable because they allow for more usable floor space and for shorter

construction times. Polymers are suited to meet these requirements because they are light, and as composites they can be made thin while still retaining strength.

The fact that, in general, polymer foams are more flammable but more insulating than mineral insulation [19] has split design philosophy in two. One design philosophy prefers thicker facades with mineral insulation, and the other prefers thinner facades containing polymeric insulation. This, in turn, has led to a split in the insulation market, shown in Figure 2.4. Around 60% of the German market divided between non-combustible mineral wool and more thermally efficient polymeric insulation, which includes both natural polymers (e.g., wood fibre insulation) and foam plastics. Although these data are from the German market, data from the European market in 2010 showed a similar split of 50-60% stone and glass wool and 40-45% foam insulation [20] and data from U.S. manufacturing in 2017 showed a split of 45% stone and glass wool and 40% foam insulation [21] (with the other 15% composed of mechanical insulation materials), suggesting a global trend.

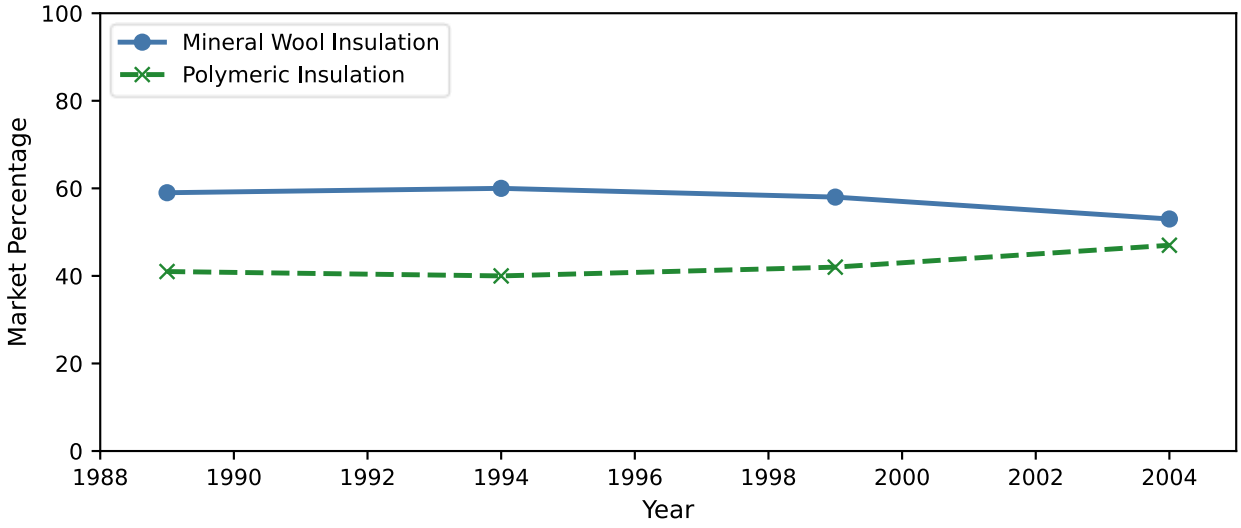

Figure 2.4: Market share of German insulation products from 1989-2004 [22]. The market is divided between non-combustible mineral wool and more thermally efficient polymeric insulation.

2.3 Fire Safety and Testing of Facades

As mentioned, the primary risk of a facade fire is a breach in compartmentation. In cases where parts of the facade can ignite, this opens multiple paths for fire spread. Most commonly in residential buildings, a fire could start inside the building and spread to the facade via openings in the compartment. This is similar to the case in a non-

combustible facade, but the flames can extend further and are fuelled by the facade itself. This has happened in many documented facade fires [5], [23], [24]. There is also the possibility of the fire igniting externally to the building and spreading to the facade, and then from the facade into the interior [5], [25], [26]. In some cases, such as the high-profile fire at The Address Hotel in Dubai [27] a fire can be initiated in the facade itself, and then spread internally. In the case of facades with an air cavity, this gives an additional path for flame spread and can help to extend the flame length and make it easier for fires to spread to additional floors.

Most countries require that a facade meets a minimum standard of fire safety before being allowed on a building. For example, historically in the UK, a facade was deemed safe to use on a building if it either contained no combustible components or passed a standardised facade fire test [28]. In the UK, the test standard used is BS-8414 [11], [12]. These standardised fire tests are common in many countries, and while they vary in method (there is no agreement on the fire source, facade size, or failure criteria of these methods), they all try to simulate one kind of fire that a facade might be subjected to [29]. Work is currently being done to harmonise the large-scale testing across Europe [30], [31], highlighting the disagreements between what is deemed a suitable test across different countries. In theory, all of the tests being considered in the harmonization are assessing whether the facade promotes flame spread and threatens a breach in compartmentation; however, it is debatable whether a single test with a simple pass or fail could decide whether this is the case, because the response of the facade will be different for different types of fires and facade geometries and will depend on whether details such as windows are included.

For large-scale national standards, these tests are also expensive (often more than £10,000 per test), cumbersome to run and, when designing a building there are often many different parts of the facade that would need to be tested. Therefore, countries will often allow a facade to be approved by using expert judgement to explain why a particular facade would meet this minimum safety requirement, based on the results of previous large-scale tests. These are colloquially referred to as “desktop studies”. After the Grenfell Tower fire [32], this kind of approval by expert judgement came under criticism in the UK [33], and at the time of writing no combustible materials of any kind are allowed on building facades [34], though this move has been criticised as having potentially unintended consequences [13]. Part of this criticism was that such studies, and assessments of facade fire safety in general, were not always carried out by

competent fire safety engineers, a similar conclusion to reports in Australia following the Lacrosse fire [35]–[37].

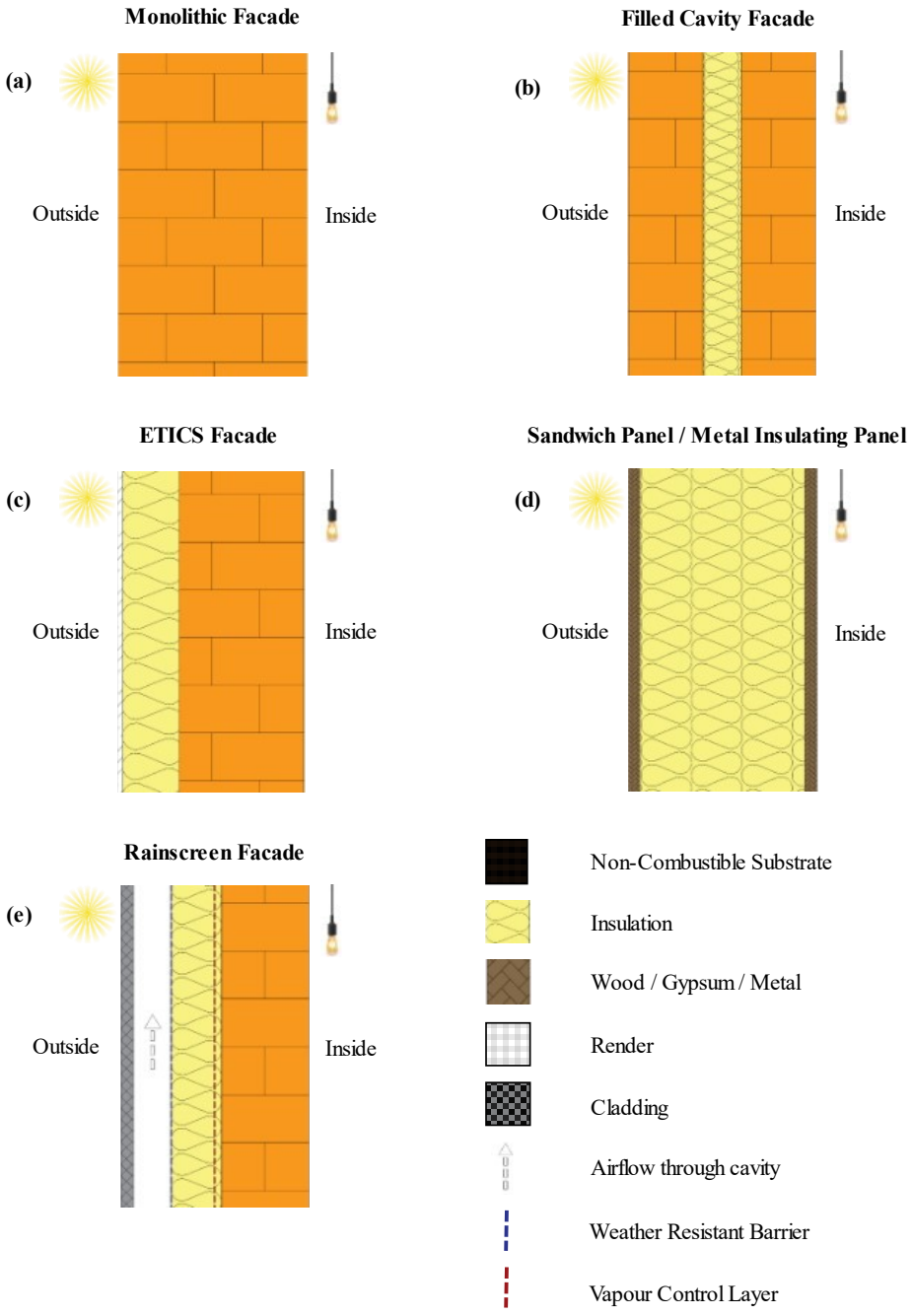

Figure 2.5: Simplified sections of common facade systems: (a) Monolithic Facade, (b) Filled Cavity Facade, (c) External Thermal Insulating Composite System (ETICS) Facade, (d) Sandwich Panel (or Metal Insulated Panel), (e) Rainscreen Facade. Note: The vapor control layer and weather resistant barrier in (e) are shown

on the warm side of the insulation, for a climate that has an annual desire for vapor to flow from inside to outside

2.4 From simple to complex facades

This section provides an introduction to the fire hazards present in different facade systems and suggests that as the complexity of a facade system increases (which is what has happened in real facade systems over time), the potential for a more flammable facade system also increases. Each subsection focuses on a different kind of facade system, shown in Figure 2.5, and each section is ordered by increasing complexity (from simple to complex). The facade types shown in Figure 2.5 are simplified abstractions of reality, and a real facade system will include many details that are not covered in this figure. Some facades are also difficult to categorise. I hope however, that the categories in this section can help to connect the broad range of facade research in a way that supports greater understanding.

2.4.1 Monolithic Facades

This facade system is the simplest type and is made from a single layer of non-combustible material. This could refer to a simple concrete or brick masonry wall, or a glass facade system, such as a glazed curtain wall (in reality, modern curtain walls will contain many additional components). Hollow brick masonry walls have been studied experimentally and numerically [38]–[40] and the main hazards they present in fire are loss of mechanical performance (though facades are often non-loadbearing) and the possibility of spalling. These papers found that spalling was the main cause of loss in mechanical performance. Spalling also produces falling debris, which could harm people standing in the vicinity of a building.

The main hazard presented by glass facades is shattering due to the heat of a fire, which can increase the size of a compartment fire by increasing ventilation and also allow the aforementioned “leap-frogging” of a fire to occur between floors. As such, the majority of fire research into glass facades explores this phenomenon. Many types of glass fixings have been tested [41]–[43], and numerical models have been built to try to predict the onset of cracking or pane fallout [42], [44]. These models suggest that the main factor affecting when cracking occurs is the temperature difference across the glass, as well as the number and location of fixings.

These systems may contain small amounts of combustible material, for instance, combustible insulation in the connecting frames in a glazed curtain wall. However, in terms of flammability, these systems pose a small hazard, as the total fuel load is likely to be small, and often without large, connected areas of combustible material that flame could spread along. These systems though are unlikely to achieve the more stringent energy efficiency requirements of modern facades with just a single material. Therefore, systems with additional complexity are needed.

2.4.2 Insulated Facades

These facade systems have a layer of insulation protected by two layers of usually non-combustible material that in some cases can limit heat transfer to the insulation. This insulation might not be combustible and may have a range of different heat transfer properties. If it is a combustible polymer insulation, it may char and produce pyrolyzates (a thermoset polymer), or it may melt and evaporate (a thermoplastic polymer). The properties of common insulating materials are explored in [45], and the choice of these materials will affect the flammability of a facade system, with thermoplastic polymers being, in general, the most flammable.

2.4.2.1 Filled Cavity Facades

The filled cavity facade has a layer of insulation between two protective layers of material that prevent flames directly impinging on the insulation. This could represent a filled masonry wall, or perhaps pre-cast concrete walls with a filled cavity. These facade systems would more often be used on a low-rise building. In the case of filled masonry walls, if gaps are limited enough to prevent direct flame impingement, then flame spread along the insulation layer is likely to be limited [46]. However, thermoplastic insulation, such as expanded polystyrene (EPS), can melt upon heating and form voids, increasing the rate of flame spread. Alternatively, the burning plastic could drip through gaps in the wall, providing more fuel to the fire or igniting new fires further down the facade.

In [19], [47] the authors argue that the most important parameter in evaluating the flammability of these systems is the depth of the protective layers. The deeper the outer layer, the longer it will take for the insulation to heat up and then pyrolyze or melt [48]. By controlling the depth of these layers, it is therefore possible to limit the time at which substantial amounts of pyrolyzates may be produced, a characteristic that may determine the flammability of these facade systems [19].

2.4.2.2 ETICS Facades

ETICS facades – standing for External Thermal Insulation Composite Systems – have a thin layer of render, approximately 2-12 mm [49]–[51], protecting the insulation from fire. Such a thin layer of protection can be breached more easily than the thicker masonry or pre-cast concrete walls, potentially allowing direct impingement of flames onto the insulation. Flame spread via this insulation is, therefore, much more likely than in the filled cavity facade. This is backed up by large-scale experiments performed on ETICS facades, which found flame spread along even perfectly built constructions [52]. The recommendations from these findings are to add fire barriers to combat the increased fire hazard [50], [51]: layers of non-combustible material designed to limit the spread of flame along a combustible surface. However [53] found that in a large enough fire (in this case one with 2 m height of facade panels already burning) even the thickest fire barriers tested (mineral wool extending horizontally along the facade width and across 40 cm of height) could not prevent further flame spread. The destruction of the outer render can also allow burning droplets of thermoplastic insulation to fall, potentially igniting fires further down the facade.

2.4.2.3 Sandwich Panels

Sandwich panels, sometimes also referred to as Metal Insulated Panels, are another system where a layer of insulation is surrounded by two protective layers. For industrial facilities, these outer layers are usually made of some kind of metal to provide an inert and easily cleaned surface. For low-rise residential buildings, these outer layers can also be made of plywood, gypsum, or cement board [5], [54]. These outer layers are often very thin (about 0.5 mm for metal insulating panels, 10 mm for wood or gypsum panels). If the insulating core of the panel is combustible, then there is a significant risk of it igniting and contributing to a fire.

Of particular concern are the connections and joints between individual panels. These represent a weak point of the panels and is recommended as a point of focus in industrial reports on safely using sandwich panels [55], [56]. It is also where much of the academic research is focused. A recent paper by [57] demonstrated how potential damage to sandwich panels, which can occur during transport or construction, increases their flammability, and the numerical study by [58] found that a larger joint gap between panels increased the mass loss of the insulation within the panels significantly. The thesis of [59] also found that larger gaps reduced the fire resistance time of the panels, and suggested reducing the gap size with intumescent strips.

2.4.3 Rainscreen Facades

As previously mentioned, moisture control in facades is of critical importance during their design (Table 2.1). One common way of making sure moisture doesn't get trapped in a facade is to include an air cavity, creating a ventilated facade system. Due to pressure differences between each side of the outer wall of the cavity, air flows constantly through it, allowing water to evaporate and be carried away from any porous insulation, rather than build up and cause damage. Unfortunately, if a facade system contains combustible material, then the addition of an air cavity will increase its flammability.

The most common type of ventilated facade system in high-rise construction is the rainscreen facade, where a layer of opaque material (the rainscreen) is used as the outer wall of the cavity to protect the insulation from adverse weather conditions and provide a decorative finish for the facade. This outer layer is usually referred to as cladding and can be made of many different materials, including metals, ceramics, or polymers. In the latter case this cladding could contribute to fire spread. Therefore, there are two main factors differentiating the rainscreen facade in terms of flammability, the cladding, and the air cavity.

The effects of a cavity on fire dynamics have been documented for a long time [60], [61]. Qualitatively, three factors enhance flame spread in a cavity vs. a simple vertical surface: radiation being enhanced by the cavity, increased upward spread from the chimney effect (where temperature differences inside and outside of the cavity drive increased upward flow through the cavity), and a decrease in the amount of convective cooling from external air. This has the effect of extending flame heights in a cavity (Colwell & Baker, 2013) and makes the ignition of any combustible materials in the cavity easier [61], which increases the flammability of the facade system.

The sensitivity of these factors to the width of a cavity was quickly realized by researchers. The effect of cavity width on the level of heat flux impinging on a wall was studied first in the 1990s in the context of warehouse fires, and again more recently in the context of ventilated facades [62], [63]. These studies found that the heat flux on parallel walls increased with a smaller distance between them, and that flame height was extended through the cavity. However, line burners were used in these experiments to release heat into the cavities, which resulted in an amount of heat independent of the cavity width (which was greater than the width of the line burner). We hypothesize that in a real fire a larger cavity width could mean that more hot air and flammable gases

were drawn into a cavity, thereby increasing the amount of heat within the cavity, and potentially the rate of flame spread.

Figure 2.6 illustrates this hypothesis with plots showing how the heat release rate into the cavity (influenced by the chimney effect) and the heat flux on the walls of the cavity (influenced by the enhanced radiation) are dependent on the cavity width. These competing effects come together to affect the flammability of a particular system. The authors hypothesize that there is an optimum cavity width at which the two effects converge to minimize the increase in flammability caused by the cavity, however this would be different for different fire conditions.

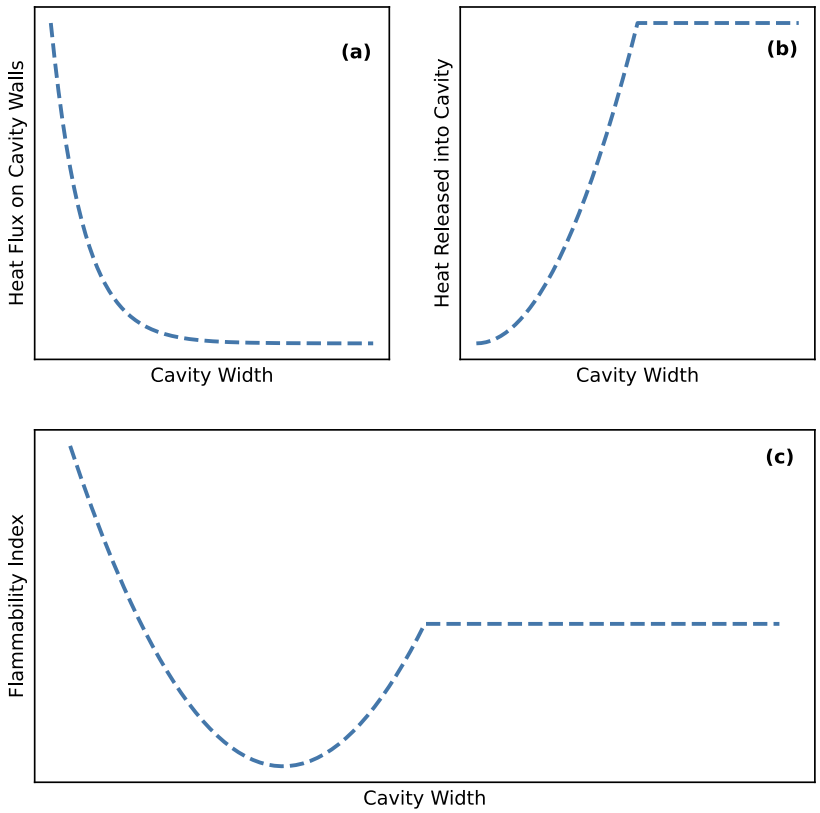

Figure 2.6: Plots illustrating how cavity width could hypothetically affect: (a) the heat flux on the cavity walls (radiation enhancement), (b) the heat released into the cavity (chimney effect), and (c) the total flammability (combination)

The effect of the cladding on the flammability of the facade system will depend on what materials are used. In many recent fires, the cladding consisted of flammable

aluminium composite panels (ACP) [64]. These panels consist of two sheets of aluminium laminated to a plastic core. This plastic layer reduces the volume of aluminium needed to achieve the same structural performance, but also increases the flammability of the panel. This flammability can be reduced by increasing the mineral content within the plastic layer. There are a range of ACP products available on the market, containing cores ranging from 100% plastic to around 10% plastic, with the rest of the core made from minerals and fire retardants [65]. Other metals can be used in place of aluminium too, such as copper or zinc. An increasing concern of flammable cladding has led to increased research into ACPs and similar materials. A report by [66] found that some setups using ACP that passed the UK large-scale fire test did not fare well when subjected to more intense heating conditions, potentially closer to a real fire scenario. Meanwhile, the authors of [67] performed intermediate-scale experiments on systems with plastic and mineral cored ACP and with different types of insulation and found that the results of the test were mainly dependent on the type of ACP used.

High Pressure Laminate (HPL) panels are another type of cladding that can contribute to fire. These panels consist of layers of cellulosic fibres (similar to paper) impregnated with phenolic resin. They are lightweight, weather resistant, and can be printed with almost any design, but are also flammable. Their fire performance seems to vary with thickness and the adhesives used [68]. HPLs have come under scrutiny in the UK after being involved in a fire in student housing [69], and the authors of [70] suggest that this type of cladding could present a significant fire risk in the future.

Given the potential significance of these different cladding materials in contributing to a facade's flammability, the University of Queensland has created a database to catalogue the chemical structure and fire performance of a large number of cladding and insulation materials [71], [72]. Many of the entries in this database come from different ACP or HPL claddings, showing a wide range of fire behaviour depending on their composition.

When employing these systems in colder and wetter countries, the insulation is often also protected by a weather resistant barrier (WRB): a polymer mesh that allows water vapor to pass through and leave the insulation but prevents liquid water from entering. These WRBs are always made of plastic and can therefore ignite. This increases the flammability of the facade system, however, as far as the authors are aware, no published research into their fire behaviour as part of a facade system is available.

The addition of a ventilated cavity, cladding, and a weather resistant barrier offers superior moisture protection to the previous types of facades, while remaining thin and thermally efficient. However, the flammability of these systems increases. This type of system is the most complex in Figure 2.5 the most modern, and also the most flammable. Notably though, these discussions about the cavity were of idealizations of real systems. In a real system cavity barriers and fire stops are usually required to be installed. These can help to limit fire spread through a cavity, though the installation of these barriers, as well as other elements of the system, is not always perfect and can create further challenges to fire protection. Large-scale tests performed with different amounts of cavity barriers in [73] found that increasing the number of cavity barriers had a significant impact on the flame spread on a facade. Similarly, a series of papers that used fire modelling to re-create and investigate the Grenfell Tower fire found that cavity barriers could reduce flame spread along a facade, but only if the facade's cladding did not ignite [74]–[77].

2.4.4 Openings, fixings, and interfaces

The systems in Figure 2.5 are simplified and, in reality, would need to be fixed onto a building's structure. The choice of fixing method for each system adds additional complexity to the problem. Glass curtain walls were mentioned in the section on monolithic facades, but in reality the opaque areas between layers of glass have insulation in them, and the systems are often fixed so that there are voids and cavities present too. [8] also mentions how railing systems could lose integrity and cause parts of the facade to fall. These problems are currently not being tackled in the research.

Different areas of a building can have different facade systems. These systems must connect to each other, leading to additional complexity at the interface. This scenario has not yet been studied from a research perspective and is also not considered in large-scale fire tests for facades, which test each facade system individually rather than seeing how they interact together.

The geometry of a facade can differ from the straight vertical walls shown in Figure 2.5 and present different fire behaviour. [78] notes how a convex sloped facade could trap hot gases from an external fire and experience more severe fire conditions, while [79] found that a concave structure increased vertical flame spread along EPS insulation. Therefore, it seems any deviation from the vertical case has the potential to increase the flammability of a facade, yet our understanding of other geometries and orientations is limited.

Real facades contain windows and openings to allow air and light into the building. Currently, there has been a large body of research detailing how the geometry of an opening will affect the nature of fire impinging on the facade from a compartment fire, which has been reviewed in [80]. However, there is no research into how installing a window changes the flammability of a facade system. Gaps in protection around a window may make the system easier to ignite, or plastic elements used in the window itself could present a problem. The areas where the complexities of construction deviate from idealised design are likely to be one of the weakest points of the facade from a fire safety perspective, but so far there is little research into what problems they may pose.

2.4.5 Other facade types

Not all facade systems have been presented in the diagrams presented in Figure 2.5**.** Double-skin facades are one example, where two layers of glazing are separated by a large cavity. The cavity here is much larger than in a rainscreen system, and it exists to limit heat transfer and control light levels, rather than for moisture control. As there are very few combustible materials present, this facade system does not pose the same hazards to flame spread as the other systems. However, it can provide a channel for enhanced smoke spread between floors, and the physics of the heat and mass transfer has been studied [81]–[83].

Another facade system increasing in popularity is the green facade. These facades are composed of a wall of vegetation growing through a reinforced mesh or growing out of some kind of substrate, which is commonly made of a combustible polymer. Although there is very little formal research into this type of facade, the current fire safety strategy is concerned with making sure the plants do not dry out, and that the types of plants used are generally more difficult to burn [84].

Finally, there is the rise of photovoltaic or solar facade systems, which use solar cells to generate additional power for the building. These cells pose an ignition hazard to combustible materials within a facade system. There is currently little published research on the fire behaviour of vertical solar panels available, but there is currently work to establish safety strategies and test guidelines for these facade systems as they increase in popularity [85].

2.5 Quantifying flammability

It can be seen from the body of research presented in the previous section that the current research into facade systems gives only a partial understanding of how different elements of these systems behave during fire, such as the cladding, insulation, or the effect of a cavity. There are also basic qualitative studies into large-scale systems, but the conclusions are broad, and the experiments are too few to make definitive claims. What is missing is an understanding, or body of theory, of how different elements of a facade system interact with each other, and what parts of a facade system will be more or less important in determining the flammability of the facade as a whole.

While exact prediction of ignition and flame spread in facade systems is probably a long way away, the potential to quantify the relative flammability of these systems is achievable. [19], [47] proposed quantifying the relative flammability of an insulation material as the temperature at which its rate of pyrolysis peaks, and then extended this to the flammability of a larger system by calculating how long heat transfer would take through different choices of a thermal barrier to protect the insulation. This is a simple system, but such approaches could be extended. The NFPA released a tool that ranked the perceived fire risk to buildings with facades containing combustible components, in order to prioritise work on said buildings [65]. It is possible that their approach of collating expert opinion could be extended to a quantification specifically of the factors relating to facade flammability, such as ease of ignition, flame spread, and the generation of toxic products.

Another approach could be to use artificial intelligence (AI) to predict the flammability of a facade based off of a large amount of example data containing different types of fire a facade might be exposed to. This approach has been taken in fire science to try and predict the fire resistance and thermal properties of structural beams [86], [87] and whether or not compartment experiments would reach flashover [88]. It has also been used to try and predict the severity of facade fire incidents in real buildings [89]. However, each of these examples have been limited by small sample sizes due to the difficulty of finding large datasets in fire science. The challenge also remains, as in the cases without artificial intelligence, of selecting a weighting for the different elements that define flammability, such as flame spread and generation of smoke.

Quantifying the flammability of a facade would give an explicit way to evaluate this aspect of the relative hazard posed by different facade designs in a fire. Not only would

this support fire engineers in the difficult task of assuring a building is fire safe but would also open the door for more advanced computational methods for optimising facade design.

Optimization methods are ways of finding points of maxima and minima in usually complex and non-linear functions. If a particular design objective can be quantified as a function – the desire for a facade to be as thin as possible for instance – then optimization can be used to find a design that maximizes that objective within certain constraints – in this case finding the thinnest possible facade that still meets the requirements for thermal performance. The function used to quantify a particular objective is called an *objective function*, and the point where it is maximized or minimized is called an *optimal solution*.

In cases where multiple objectives need to be maximized, multi-objective optimization can be used instead. Here, optimization will try to find permutations of a design where, across multiple objective functions, at least one objective cannot be improved. This can be difficult, as often improving one objective may impair another. Those particular designs where an objective cannot be improved are referred to as *Pareto optimal* solutions, and if enough of these solutions are found then it is possible to plot them on a graph comparing the two objective functions as a *Pareto front*. It is then possible for different parties involved in the design to choose a particular optimal solution from this front, based on how important each objective is.

The advantages of multi-objective optimization in design have been laid out in [90], and it is an approach that has already been applied to the problem of facades [91], [92], though not in the context of their fire safety. Table 2.1 shows how facades are an example of a multi-objective problem, and so an optimization approach could improve modern facade design. Figure 2.7 demonstrates a hypothetical Pareto front of solutions trying to minimize the U-Value and the flammability of a facade. Designers could pick the solution that best reflected what was demanded by a project. For a small building in a cold country with a low-risk of fire and multiple escape routes, one might pick the minimum U-Value without regard to flammability, while for a high-rise residential building a solution that scores lower in flammability would be required. In this case, the U-Value and flammability index are stand-ins for the more holistic objectives of energy efficiency and fire safety, which would have to consider the entire building. Therefore, these techniques can only assist engineering design, not replace it.

This approach to design is referred to by J. Arora in [93] as *Optimum Design*. He distinguishes it as an approach where designers can be certain that they have chosen a design that is close to optimal in some regard, and one where a large focus must be put on the choice of design objectives. While flammability is only one part of the fire hazard posed by the facade (it does not consider the hazard of the facade detaching and falling from the building for instance), and fire hazard is only one objective to be considered during the design of facade systems, a process that encourages a deeper consideration of the interaction between all possible design objectives (Table 2.1) would be a step in the right direction.

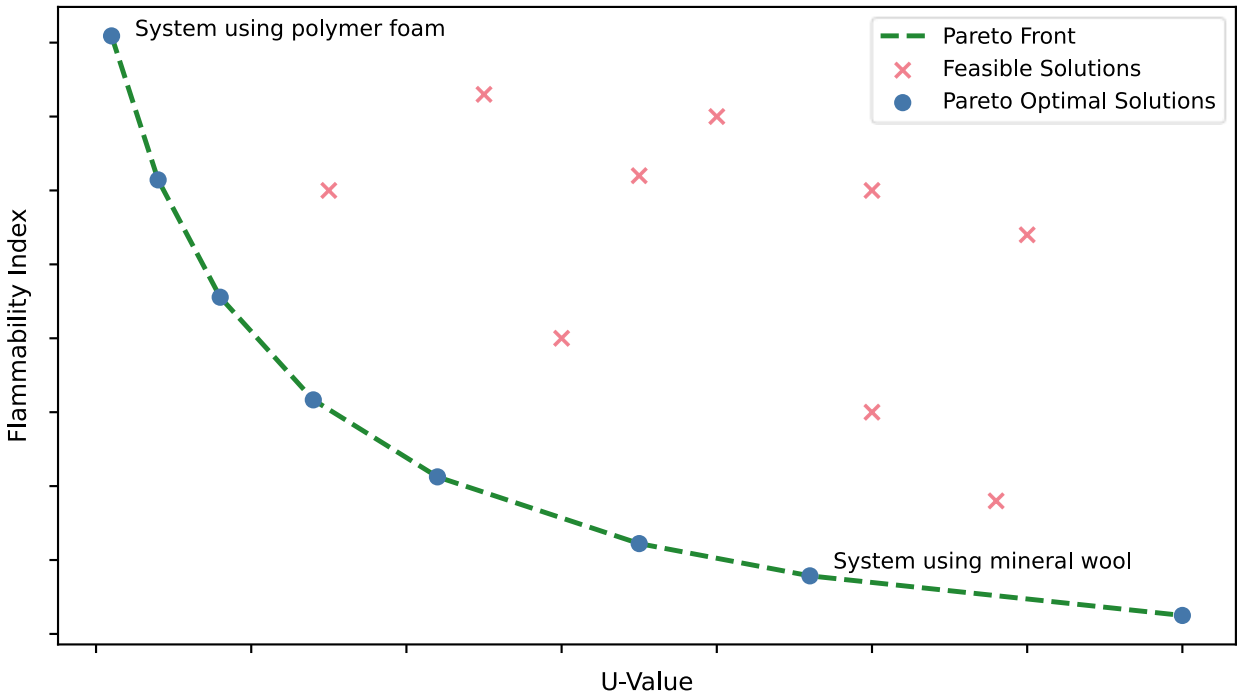

Figure 2.7: Example of a Pareto front, minimizing flammability vs. U-Value. Each solution represents a particular facade system design. Crosses represent solutions that are feasible, but not optimal. Labels show where hypothetical systems using polymer foam or mineral wool insulation might fall.

2.6 Conclusions

With an increasing number of facade fires occurring worldwide, understanding the flammability of high-rise facades has never been more important. The complexities of facade design, where many different objectives need to be considered, require a balanced design approach. By looking at the flammability of common facade systems, it is clear that as these systems have become more complex over time so too has their flammability

increased. Unfortunately, the increased complexity of the problem has not, until recently, been followed with an increased body of research, and there are many key aspects of facade flammability that are not well understood. This is particularly true in regard to the additional complexities of constructing a real facade – how these systems behave when they are damaged or include additional fixings and openings.

The lack of understanding of the overall flammability of facade systems containing flammable components has meant that many countries have developed national standardised fire tests to assess whether these facades will promote flame spread or not (one key aspect of flammability). While the effectiveness of using a single pass or fail test to assess facade safety is debatable, the data recorded during these tests should be connected to the flammability of the facade (at least in the sense of ease of ignition and flame spread). There are many different national test standards that use a range of different fire sources, meaning that data from across these standards would give examples of facade behaviour in different kinds of fire. By structuring this data and combining it with AI, it could be possible to predict the performance in these tests of different facades across different national standards. As the outputs of these standards relate to the flammability of the facade, this could be a path to quantifying the flammability of facades by proxy. At least until the state-of-the-art can reach this point from fundamental physics and chemistry.

The rest of this thesis takes steps towards transforming these tests into a potential tool for quantifying facade flammability. While the state-of-the-art may be a long way from being able to quantify the flammability of facade systems from fundamental principles, the advantages of being able to do so are clear. By quantifying flammability alongside other facade design objectives, a new approach using multi-objective optimization can be taken to facade design. Taking such an approach would not only guarantee near optimal design solutions but would also ensure that fire safety was considered as an integral part of the design process.

Chapter 3

KRESNIK: A top-down statistical approach to understanding the performance of building facades through standard test data

Summary[2]

The previous chapter discussed how the current body of bottom-up facade fire research is insufficient to reliably predict the fire behaviour of entire facade systems. This chapter presents a complementary, top-down approach to this problem that focuses on identifying trends in large numbers of tests on full-scale systems. We present a unique database, named KRESNIK, containing 252 commercial facade fire tests, the first time these commercial fire tests have been collected and analysed in this way. We found that the outputs from these tests were correlated, which could be used to gain more information on facade performance than only a pass or fail, and that different layers of a facade can have a significant effect, particularly the addition of a cavity. Rainscreen facades performed worst in these tests (45% failed), whereas none of the ETICS or sandwich panel facades in KRESNIK failed. We found that the choice of cladding material was the most important factor in predicting the fire performance of these rainscreen facades, but that neither its total fuel load nor its thermal transmittance could be correlated.

3.1 Introduction

In the previous chapter I mentioned the importance of being able to quantify a facade's flammability. This would not only support fire engineers with an explicit measure of the impact of any changes in a facade's design but would also open the way to advanced optimisation methods to support modern facade design. I also mentioned

[2] This chapter is based on the published paper: M. Bonner, W. Wegrzynski, B. K. Papis, and G. Rein, KRESNIK: A top-down, statistical approach to understand the fire performance of building facades using standard test data, Building and Environment, 169, https://doi.org/10.1016/j.buildenv.2019.106540.

how much of the available literature on facade fires tends to focus on individual components of the facade (the insulation for example) but not how the system interacts as a whole. The impact of each component on the system does not necessarily add together in a linear way, and so any approach to quantifying the flammability of a facade must take into account the entire system.

One way to approach this problem would be to study the fundamental science governing the fire behaviour of facades and slowly build up explanatory models of increasing complexity until such behaviour could be predicted with sufficient accuracy from first principles. I refer to this procedure as the *bottom-up* approach to understanding facade flammability. This approach is crucial to ensuring the fire safety of buildings in the long-term, however, as seen in the previous chapter, we are still a long way from succeeding in such an approach, and facade fires are an immediate threat.

In contrast, we could also take a *top-down* approach to quantifying the flammability of building facades. In both the bottom-up and top-down cases, a composite variable accounting for the different factors making up flammability (ease of ignition, rate of fire growth, etc.) would need to be identified. However, whereas the bottom-up approach would calculate this variable from fundamental principles, the top-down approach would try to collect large quantities of existing data on the performance of different facades in fire and store them in such a way that they could be compared easily. By finding empirical trends across this data, it would be possible to quantify how different factors affect facade flammability, without a full understanding of the fundamental behaviour controlling these trends. This approach, whether in the form of statistical analysis, machine learning, or artificial intelligence, is common in other research fields with complex behaviour, such as a medicine, and has also been used in the field of fire safety (see Chapter 2 [86]–[89]).

The data needed for this kind of approach would have to come from experiments involving complete facade systems in order to capture representative behaviour. Most statistical or AI methods require large amounts of data (in the hundreds or thousands) and performing enough experiments at the intermediate or large scale would be prohibitively expensive for any research group – remembering that a large-scale facade fire test can cost more than £10,000. However, as mentioned in Chapter 2, in most countries a facade must pass a standardised fire test before being allowed to be used on a building. Every year, thousands of these tests are performed around the world, but the data collected from them remains unused.

By collaborating with Instytut Techniki Budowlanej (ITB), a testing and research institute in Poland, I was allowed access to the data from 252 such facade fire tests. In this chapter, I will explain how I transformed the data from loosely structured test reports into a relational database, allowing the data to be compared easily using a computer. This database was named KRESNIK[3], after the Slavic god of fire. I then go on to show the results of my initial analysis of this database, demonstrating the kind of information that can be learned from collecting such data.

3.2 Methodology

3.2.1 PN-B-02867 Test Standard

KRESNIK is a unique database containing data on 252 tests that were recorded at ITB (a research and testing institute in Poland), according to the PN-B-02867 test standard [94]. This standard is an intermediate scale test originating in Poland, though it shares some similarities with ISO 13785-1 [95]. This test standard was analysed in [96] to demonstrate the effectiveness of the PN-B-02867 test method, however, it is only one of many national tests used worldwide. Reviews of these different standards can be found in [29]–[31], and 2 more test standards are discussed in detail in Chapter 6 of this thesis. Details of PN-B-02867 are shown in Figure 3.1. The standard involves igniting a 600 x 300 mm, 20 kg wood crib 50 mm from the facade at its centreline, and then removing the crib after 15 min. The facade is then observed for an additional 15 min for continued fire behaviour. The surface of the facade facing the wood crib must be as close to 1.8 x 2.3 m as any panel dimensions will allow and must be constructed as it would be on a building.

[3] **K**nown **R**ecords of **E**xternal wall tests, **S**toring **N**ovel **I**nformative **K**nowledge

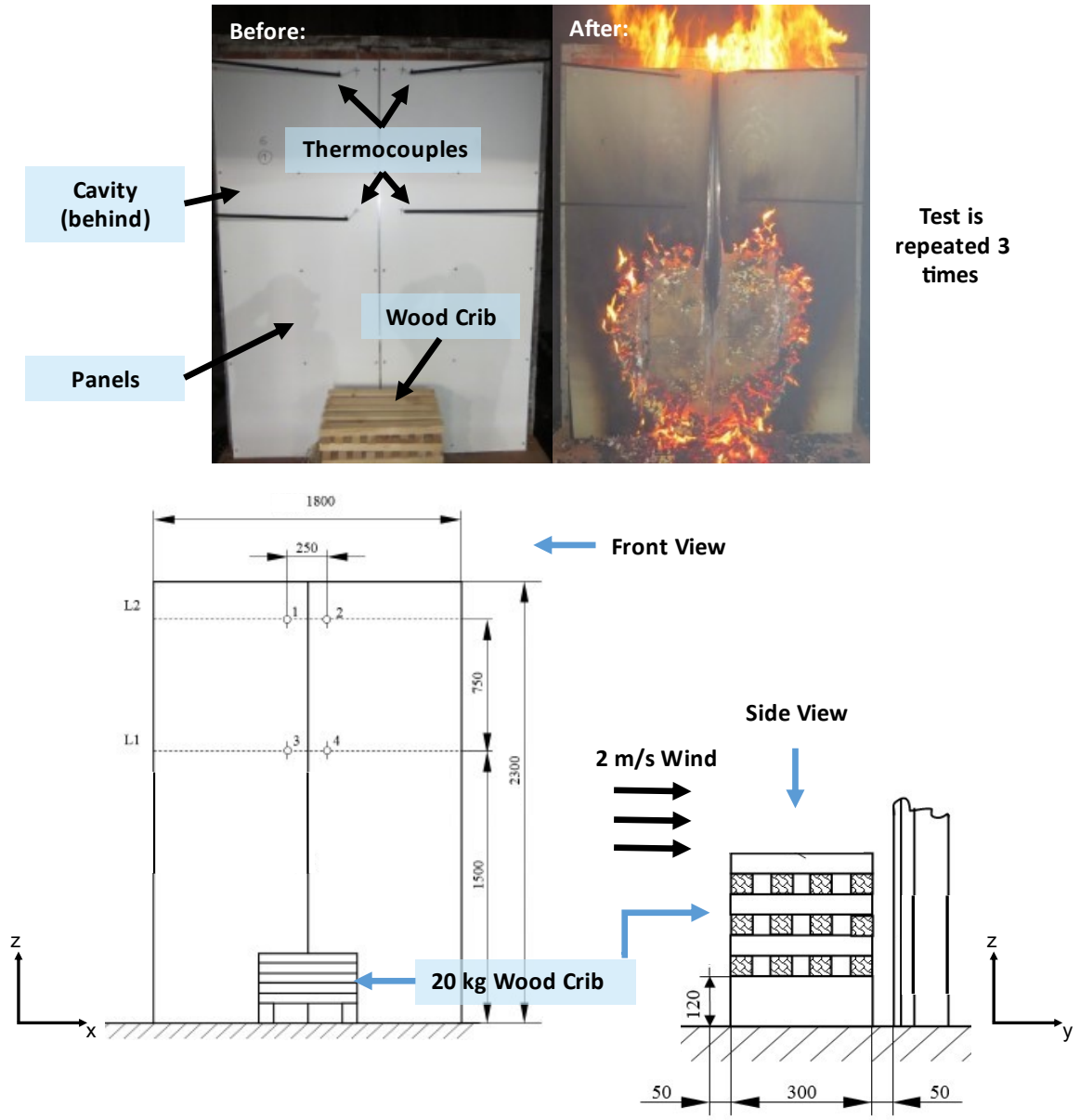

Figure 3.1: Photos and schematic diagrams of the PN-B-02867 intermediate scale facade test. The length units are in mm. To be approved, a facade must pass this test 3 times. Pass / fail criteria are shown in Table 3.1.

Throughout the test, a fan applies an average 2 m/s air flow towards the facade; this is in contrast to other similar test standards, where no wind is included, provides a worse-case condition that will increase the incident heat flux on the facade. Also, unlike other test standards that require a facade to pass only once, the test must be repeated 3 times on identical facades, and all 3 tests must pass for a facade to be approved.

To pass the test, thermocouple data and qualitative observations from the technician running the test are recorded. The thermocouples are placed 125 mm either side of the centreline at heights of 1.5 and 2.25 m. These temperature data and observations are

then recorded in a test report and checked against the pass/fail criteria for the standard. These criteria are shown in Table 3.1. Nearly all of these criteria are related to the flammability of the facade. The observations of continued burning or visible flames above a certain height identify whether the facade promotes flame spread in the relatively short timeframe of the test or if the facade could sustain this spread past the duration of the test. The temperature criteria also relate specifically to detecting flames at that height and are complementary to the visual observations made by the technician overseeing the test.

Table 3.1: Pass / fail criteria for PN-B-02867 [94]

Pass / Fail Criteria	**Explanation**
Temperature at 1.5 m	Thermocouples at a height of 1.5 m must not exceed a temperature of 450 ℃ for more than 30 s
Temperature at 2.25 m	Thermocouples at a height of 2.25 m must not exceed a temperature of 350 ℃ for more than 30 s
Flaming above 1.5 m after 15 min	No flaming *or smouldering* should be observed on the facade above 1.5 m, after the wood crib is removed (15 min into test)
Flaming above 2.25 m after 15 min	No flaming *or smouldering* should be observed on the facade above 2.25 m, after the wood crib is removed (15 min into test)
Continued burning after 30 min	No flaming *or smouldering* should be observed *anywhere* on the facade after 30 min
Falling droplets, solid residue, or large parts	No flaming debris or large parts must fall from the facade for the duration of the test

3.2.2 KRESNIK Database Design

Data from the PN-B-02867 standard are recorded in written test reports. These reports record similar information from the tests each time, however these written documents do not allow for data to be processed and analysed in a structured way. By transferring the information in these test reports into a database it can be combined and compared in a way that allows new knowledge to emerge. However, to achieve this I could only select

information that was common across the vast majority of reports, and structure this data in a way that could be easily built upon.

To achieve this, I created a relational database. As opposed to a simple spreadsheet, a relational database allows different test standards or facade types to be stored in the same database by representing each standard as a separate table (also referred to as an *entity*) containing only the observations that are relevant to that particular standard [97]. Each table is made up of columns that represent different features of the entity being represented (for instance, a column for the peak temperature recorded in a test). Similarly, different types of facades (such as those shown in Figure 2.5) can be represented as separate entities, allowing me to capture different details for different types of facades. For instance, not all facades contain a cavity but if one does then it is crucial to include this feature when studying its fire behaviour (in this case by including a column for cavity width). Storing data in this way meant the database could be built upon in the future, including new types of facades or test standards that recorded different information.

Data stored in a relational database can be visualised using an Entity Relationship Diagram (ERD). The ERD for KRESNIK is shown in Figure 3.2. Each box in the diagram represents a different entity / table. The names inside each box represent features / columns that are recorded in that table. The lines connecting tables represent the relationships between entities – in other words how tables can be joined together to connect information. A one-to-one relationship will connect one row of a table to one row of another table. A one-to-many relationship will connect one row of a table to many rows of another table. The features / columns that contain "id" in the name are used as "keys" to connect these databases, a standard feature of database design and usage. More information on how to read this diagram can be found in [98].

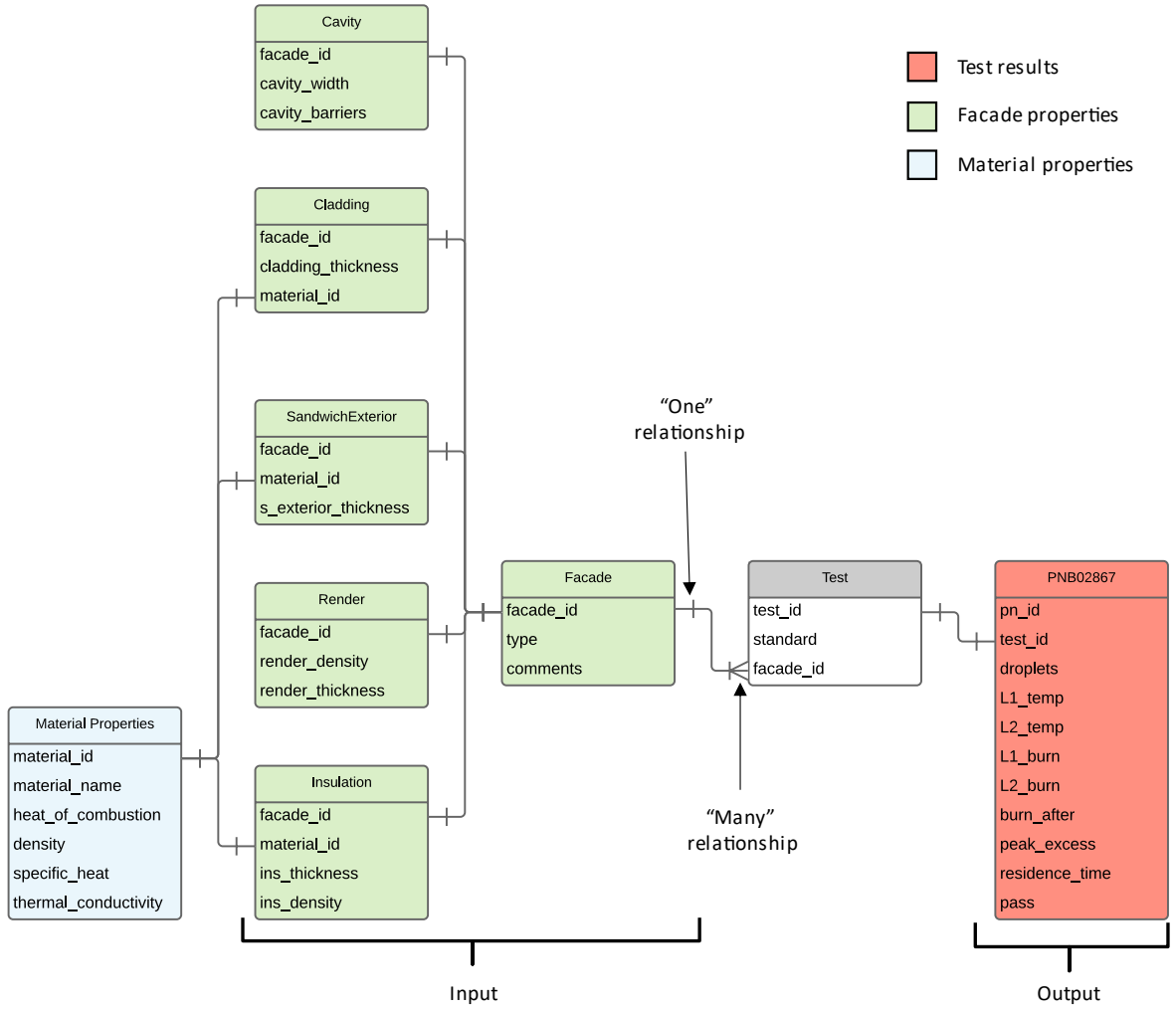

Figure 3.2: An entity-relationship diagram for the KRESNIK database. Descriptions of each feature / column can be found in the Appendix.

The data recorded in the test reports fell into two categories: input and output. The input data for each test was the design of the facade. Such designs are often complex and recording every detail would include a lot of information which would not be present across all facades, harming the ability to compare facades within the database. The data I recorded was also commercial, and so I had to ensure that it was not detailed enough to reveal any individual product or manufacturer (in other words, the data had to be anonymous). Therefore, the facades were represented as multiple layers of generic materials - for instance, the cladding could be recorded as 4 mm of terracotta but could not include the precise make of terracotta. This created a degree of uncertainty in my results, as different brands of these materials can be significantly different from a chemical point of view [72]. However, this is an uncertainty that is often present in practical fire engineering, where the exact chemical makeup of a product is often

unavailable. A large number of examples is therefore required to capture the variation within each category, as well as between categories.

The type of facade was recorded according to the categories shown mentioned in the previous chapter and shown in Figure 2.5. There are no strict definitions of these categories, and so some bias was introduced by the authors here. However, because the majority of facades that are tested tend to follow standard designs, almost every entry in the database fell neatly into one of the three types: ETICS, sandwich panel, or rainscreen. Those that did not were labelled as "other" (for instance, one test was simply a polycarbonate cladding panel with no other facade components).

The output data for each test was the results from that test. This consisted of the thermocouple measurements (time-averaged over every 30 s) and a recording of which of the failure criteria in Table 3.1 was met during the test. The 30 s time-averaging period was chosen based on the failure criteria of the BS 8414 standard [11], which only consider a temperature rise as failure after 30 s. I wanted to analyse the temperature measurements independently of the effects from the wood crib. Therefore, 3 additional tests using only a wood crib against a masonry wall were performed, with the thermocouple measurements recorded in the same way as the other tests. The results of these additional tests are shown in Figure 3.3. I then fitted curves to the data from the three tests and used these to represent the effect of the wood crib. The curves were fitted in four parts, representing the ignition, growth, steady-state, and decay phases of a well-ventilated fire [99]. The decay phase was an instantaneous drop, as the wood crib is removed after 15 min. The other phases were represented by a mean temperature, or by a quadratic fit in the growth phase. I then used this curve to calculate two new variables related to the temperature.

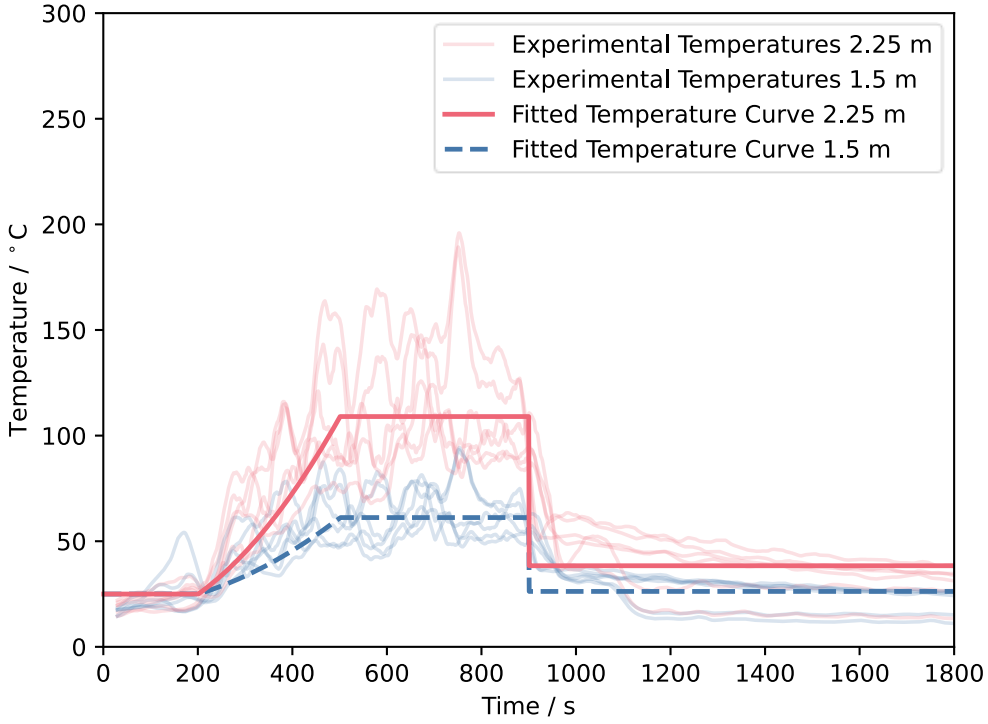

Figure 3.3: Temperature vs. time curves for 3 PN-B-02867 tests performed against an inert wall. These show the effects of the wood crib alone, without the fire contribution of the facade.

The first new output variable was named *peak excess temperature*. This is the maximum difference between the temperatures from a particular test and the fitted temperature curve from the 3 wood-crib-only tests. This is similar to the definition of excess temperature above ambient conditions used in other areas of fire science but relating to the conditions of the wood crib alone. This variable represents the most severe increase in temperature caused by the facade alone and is related to the maximum heat release rate of the fire – one factor determining flammability. The second output variable was named *residence time*. This was defined as the amount of time that at least one of the thermocouples in a test was 100 ℃ higher than the fitted wood crib temperature curve. This is because the maximum variation from the fitted curve in the wood-crib-only tests was approximately 100 ℃. The *residence time* represents how long a severe temperature condition, well above the effect of the wood crib, is maintained on the facade; this relates to the period of time the facade is in theory ignited and contributing to the fire, another factor determining flammability.

The final output variable created for KRESNIK was a *flammability index*. This was a variable created from the pass / failure criteria in Table 3.1. The variable can take a value from 1-4 ($i = \{1,2,3,4\}$) based on how many of the pass / failure criteria were

observed during a test. The variable is ordinal in nature, as the pass / failure criteria in the test were such that they always occurred in a particular order, with each increasing value representing a worse performance than the one before. For example, there were no tests in the dataset where flaming was observed above 1.5 m and the facade did not continue burning after 30 min. There were also no tests where flaming was observed above 2.25 m that did not also produce falling droplets or residue, and vice versa, so these criteria were combined. This means that the flammability index is directly connected to the ignition and flame spread on the facade, hence its name. This is shown in Table 3.2. With these 3 output variables combined, we can get as close to representing the flammability of a facade in each test as possible.

Table 3.2: Corresponding values of flammability index in KRESNIK, based on the failure criteria observed in an individual PN-B-02867 test. Flaming above 2.25 m and falling droplets also always occur together, hence them sharing a value.

Pass / Fail Criteria Observed	Flammability Index Value
No failure criteria observed	1
Continued burning after 30 min	2
Flaming above 1.5 m after 15 min	3
Flaming above 2.25 m after 15 min	4
Falling droplets, solid residue, or large parts	

For the analysis done in this chapter, KRESNIK contained data from 90 different facades and 252 tests. Not all facades were tested three times, as some tests were stopped after the first failure. Of these 90 facades, 38 were rainscreens, 24 were ETICS, 21 were sandwich panels, and 7 fell into the "other" category. These "other" facades were mostly testing individual components of a facade, such as the fixings. The materials used in the facades were not evenly distributed. In particular, insulation varied very little between facades of each type. All the ETICS contained either EPS or mineral wool, all the sandwich panels contained either EPS, PUR, or PIR foam, and all but 5 of the rainscreen facades contained mineral wool. Therefore, I could not analyse the effect of varying insulation materials in this chapter.

A final remark on KRESNIK is that using these commercial tests introduced a certain amount of bias into the data. The data here were representative of the population of commercial facades tested in Poland but may not have been completely representative of these facades once they were used on a building, or of the kinds of facades tested in other countries. However, this does not mean that the results are not at all representative of other facades, and the uniquely large number of tests in KRESNIK means that any conclusions drawn from the data should be more generalisable than a very small sample of more varied data, as a larger sample size should better capture the variation and uncertainty in such data, while a small sample could fail to capture certain trends or the uncertainty in those trends.

3.3 Results

Each facade test in KRESNIK included 3 variables representing the performance of the facade during that test: *peak excess temperature*, *residence time*, and *flammability index*. These variables are connected, but they represent different aspects of flammability during a test. The relationship between these three variables is shown in Figure 3.4. In these plots, each point represents the median value of each output for a facade, as the standard is normally repeated 3 times on identical facades. The error bars are then the maximum and minimum from the other repeats. Occasionally, facades were tested only once or twice, as the manufacturer stopped any additional testing after the first failure. For flammability index, the worst case performance across repeated tests was taken.

Figure 3.4 shows that there is a positive trend between residence time and peak excess temperature. This might be expected, as if a severe temperature is maintained for a long period of time (residence time) because of the fire, then it might be expected to reach a higher peak temperature overall. The trend is also stronger as flammability index increases. This might also be expected, as if there is definite flaming going on, then the connection between the maximum temperature and the length of time at high temperatures would be stronger as more of the available fuel has time to contribute to the fire. However, at the maximum value for flammability index of 4, the trend seems to fall apart. The cause of this is unknown, but it could also be that because the flames have spread so high in this case (2.25 m, see Table 3.2) that enough of the facade is burning to quickly consume all of the fuel fast enough that the temperature does not remain high for long periods of time. This is supported by photos taken before and after

these tests (with $i = 4$), as the tests with shorter residence times had much larger areas of the facade consumed than the tests with longer residence times.

The R^2 values between residence time and peak excess temperature in Figure 3.4 increase with flammability index up to $i = 3$. R^2 values represent how much of the variation in the data is explained by the trend line. As this kind of analysis had not been done before in the literature, there were no similar values to compare these fits to. However, this tells us that residence time can explain more of the variation in peak excess when the flammability index is higher, suggesting that the connection between the two values is stronger in the case of a more severe fire.

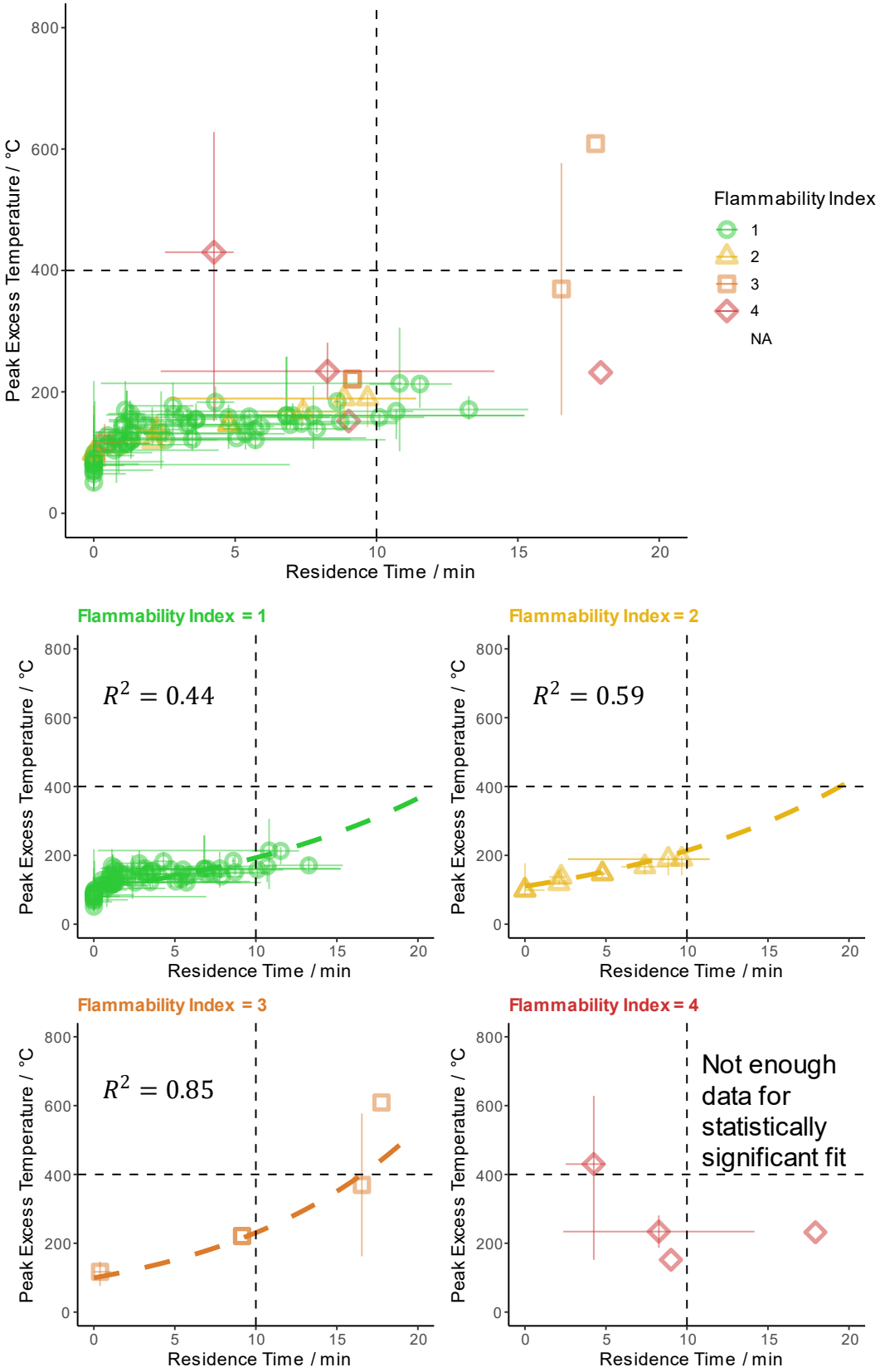

Figure 3.4: Plots showing the relationship between output variables in KRESNIK. Error bars represent the range of values for one facade over 3 repeated tests, with the median test as the central point.

A comparison of the performance of the different facade types is shown in Figure 3.5. The plot shows the percentage of tested facades of each type that achieved different flammability indexes in the test. It is clear that in this dataset, rainscreen facades performed significantly worse than the other facade types, with 45% of the tested facades achieving a flammability index greater than 1 (i.e., failing the test). This could be due to the difference in materials used in the rainscreen facades, or the presence of a cavity, which is known to increase the severity of fire conditions in a facade [60], [62], [63], [100].

There were 7 facades in the database (of a total of 90) that were significantly different to all the other facades tested. These facades were different enough from one another that they were impossible to analyse in aggregate, we therefore did not include them in Figure 3.5. They all achieved a flammability index of 1, with the exception of a facade of polycarbonate panels with a cavity, which achieved a flammability index of 4. This means that all of the facades that failed the test in our database contained a cavity.

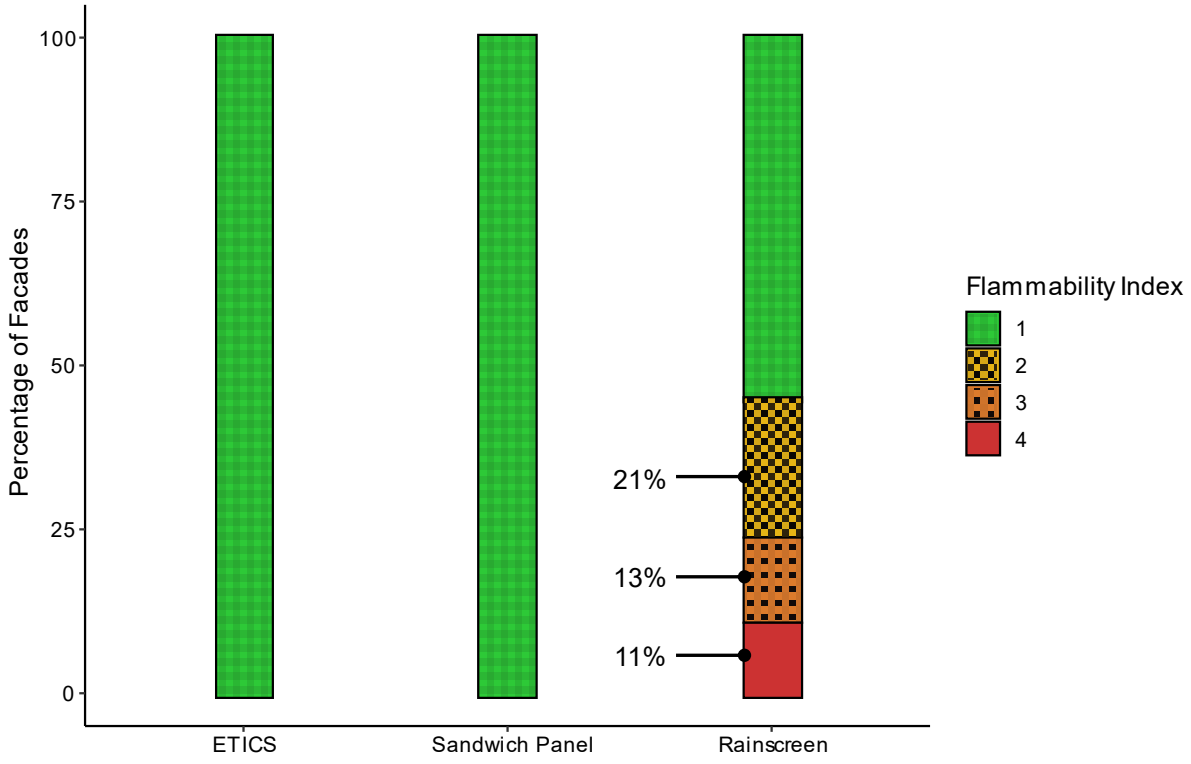

Figure 3.5: Bar plot of the percentage of facades that fail for different facade types. There was a total of 24 ETICS, 21 Sandwich Panels, and 38 Rainscreen facades in KRESNIK.

To check whether the materials in the different types of facades were the reason for their relative performances, I analysed whether facades with particular materials were

the ones that failed. None of the Sandwich Panels and ETICS facades in KRESNIK failed the test, meaning it would only be possible to analyse variations in thermocouple measurements, making it difficult to draw conclusions about the materials in these types of facades. For instance, it may be that the reason that no ETICS facades failed the test is because the test method does not consider flame spread behind the render unless it breaks through during the test. This is a limitation in considering only this test method.

For the rainscreens however, there was a large variation in the type of cladding used. Figure 3.6 shows the frequency distribution of the cladding materials used, and the flammability index achieved by rainscreens with those cladding materials. The majority of rainscreens in KRESNIK had mineral wool insulation, with the exception of 5 facades that had phenolic foam insulation. These included both of the rainscreens with terracotta and compressed basalt cladding, one of the rainscreens with wood polymer composite (WPC) cladding, and one of the rainscreens with cement board cladding. This was the only facade with cement board cladding that failed the test.

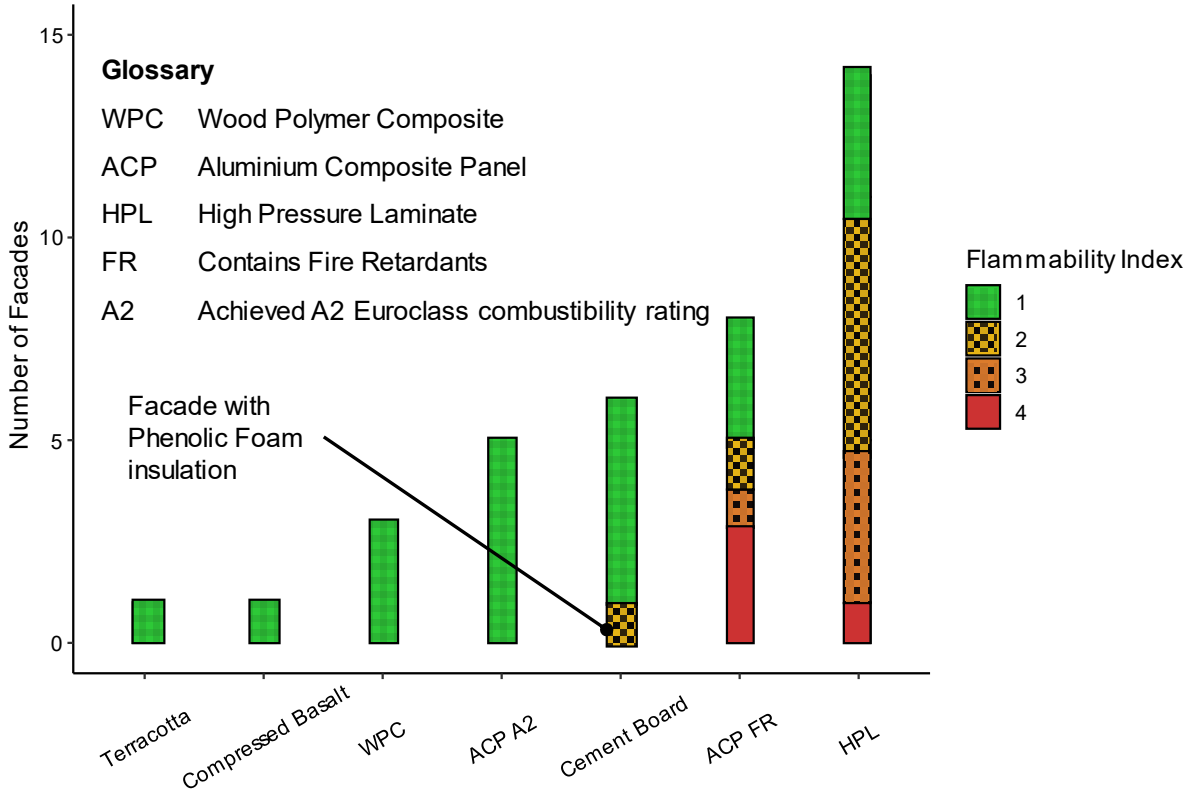

Figure 3.6: Bar plot showing the number of rainscreen facades in KRESNIK with different cladding materials, and their distribution in flammability index. Rainscreens with ACP FR or HPL performed the worst.

From Figure 3.6 it is clear that only the rainscreens with combustible cladding achieved a flammability index greater than 1 in this test. Rainscreens with high pressure laminate (HPL) cladding and aluminium composite panels with added fire retardants (ACP FR) in particular performed poorly, with approximately 80% of the HPL and 60% of the ACP FR achieving a flammability index greater than 1. This aligns with a similar prediction of issues with HPL cladding from a recent study [70]. With this test setup therefore, it seems that the inclusion of a combustible cladding material drives the facade performance in the test, a finding that is supported by [67]. While it may seem obvious that combustible cladding would decrease a facade's fire performance in a fire test – this has been hypothesised by other fire experts [9], [67], [101] – this is the first time that this claim has been supported by such a large set of data at the system level. It should also be pointed out that not every facade containing combustible insulation achieved a bad performance in this test, suggesting that it is not the combustibility of the material alone that is driving the facade fire behaviour. The only non-combustible cladding that achieved a flammability index greater than 1 in KRESNIK also contained phenolic foam, suggesting the insulation also plays a role. However, only one of the 5 facades containing phenolic insulation failed this test, so this is something to be investigated in future research.

Although there is clearly a difference in facade performance based on the materials present, it is not certain what aspect of the materials is driving this behaviour. Figure 3.7 shows our attempt to predict each output using simple regression models and 2 different design variables of a facade, *fuel load* and *U-value*. The fuel load was calculated as the mass per unit length multiplied by the heat of combustion for the insulation and cladding summed together. The U-value was calculated as the inverse of the summed thermal resistance of each layer of the facade. These variables represent the maximum amount of fuel that could be burned on a facade and the ease of heat transfer through a facade (under steady state conditions), respectively. These variables were chosen as they are variables that consider the entire facade system and are often implied as some of the most important in driving fire behaviour in a facade (representing combustibility and heat transfer).

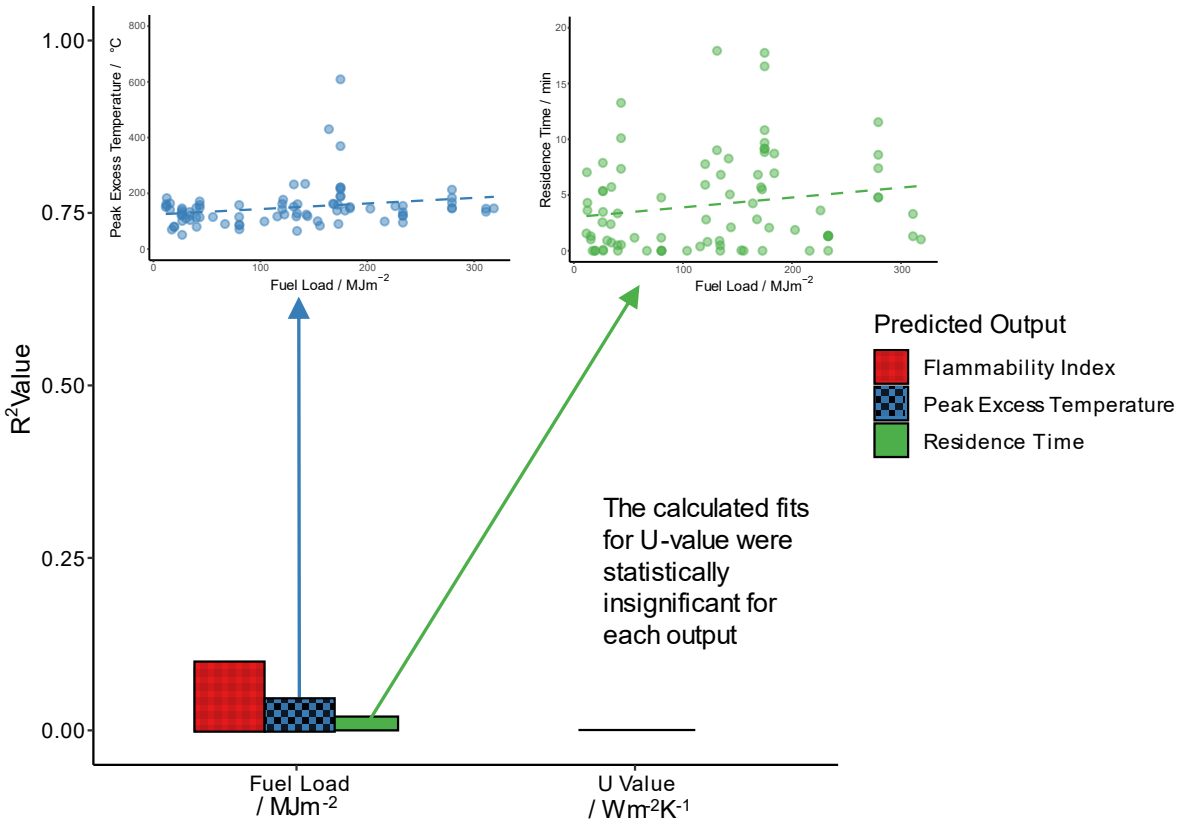

Figure 3.7: Bar plot showing the R^2 values achieved by trying to predict each output variable in KRESNIK using the Fuel Load and U Value of the facade, and a simple linear / logistic regression model (logistic in the case of flammability index as it is a categorical variable, rather than a numerical variable). The R^2 method chosen for the logistic regression models was McFadden's Pseudo R^2 [102].

Figure 3.7 shows the R^2 values for 3 simple regression models fit for each output and predictor variable. For peak excess temperature and residence time a simple linear regression was used, but because flammability index is an ordinal variable, a logistic regression model was used instead (which predicts probabilities of being in different categories). Logistic regression models have more than one way of calculating an R^2 value. In this case, McFadden's Pseudo R^2 [102] was used, which is the simplest. These R^2 values represent the amount of variation in the outputs that can be explained by each predictor variable.

It is clear that neither fuel load nor U-value can fully explain the output results. With a simple linear fit, fuel load only manages to explain about 10% of the variation in output. This is very low, but the relationship is statistically significant. This means that if you take a simple linear regression:

$$y = \beta_0 + \beta_1 x \qquad 3.1$$

And then test the null hypothesis that $\beta_1 = 0$ (i.e., that x and y are unrelated) then fuel load's effect has a p value < 0.05. This suggest that fuel load does have some explanatory power, but that it cannot predict the output of these tests on its own. U-value has no explanatory power, however, which may be expected given the dynamic conditions of a fire, while U-value is defined under steady-state. The sub-plots in Figure 3.7 suggest that there is no obvious function that can explain the shape in the data, so exploring other variables and fits should be a subject for future work.

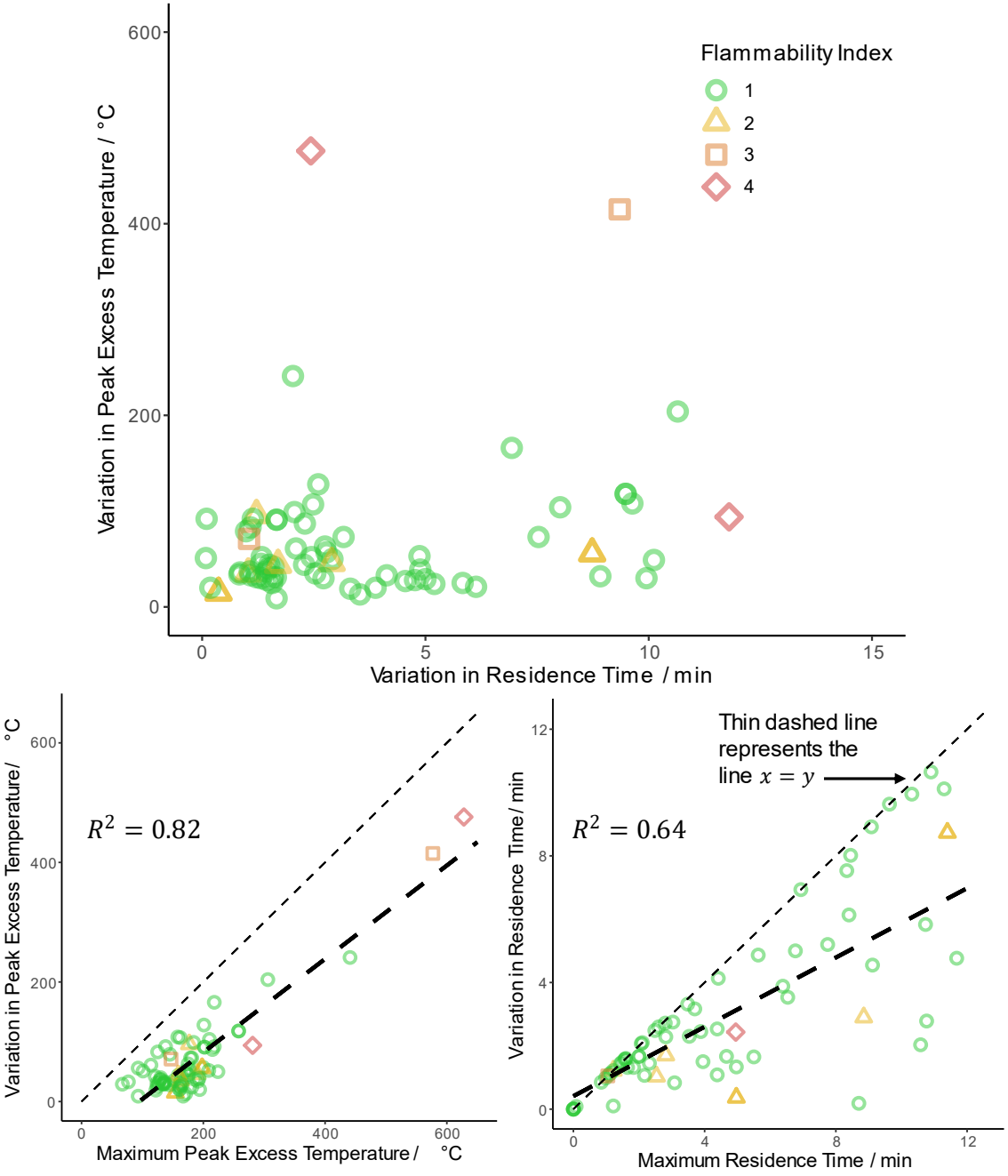

Figure 3.8: The upper plot shows the variation over repeated tests of an identical facade. The bottom plots show how the variation across repeats increases as the severity of the output increases, implying the tests that varied the most are also the ones that performed the worst.

Part of the difficulty in explaining trends in the data is the large amount of variation, even in the repeated tests of identical facades. Figure 3.8 shows the variation in each output across 3 tests of each facade in KRESNIK. It is clear that the variation in both of the numerical outputs can be huge, as much as 500℃ in peak excess temperature or 12 minutes in residence time. Interestingly though, there seems to be no correlation

between the variation of the different outputs (i.e., a large variation in peak excess temperature does not guarantee a large variation in residence time).

It does seem that the facades with the highest variation in temperature readings were the ones with a higher flammability index. The bottom plots in Figure 3.8 show that a lot of the variation in output can be explained by the maximum value of that output measured across the 3 repeats. This suggests that the minimum values of each output tend to stay pretty similar in the case of peak excess, although there is more variation in residence time.

Despite this large variation, there were only 4 facades (out of 90) in the database that varied in flammability index across repeats. All 4 shift from a pass to a failure. This suggests that the ignition behaviour of these facades is relatively consistent, however this result may also be because facades that fail the first test are not always repeated again but are simply deemed to have failed.

Future work will focus on expanding this approach across multiple test standards, to see whether these results are generalisable beyond PN-B-02867, although finding organisations that are willing or able to share this kind of commercial test data is difficult. It would also be useful to investigate the effect of different insulation types more, as this dataset does not have the required variation in insulation materials to see any effects.

3.4 Conclusions

A unique database of 252 commercial facade tests, named KRESNIK, was created and analysed, taking a top-down approach to understanding facade performance in fire. The tests in KRESNIK were performed according to the Polish PN-B-02867 standard [94]. It was found that the outputs from this test, which each related in part to the flammability of the facade, were correlated, which could be used to gain a deeper understanding of facade performance in a test than a simple pass or fail, for instance, by combining these output parameters into a single variable correlated with facade flammability. It was found that the type of facade had a significant effect on fire performance, with ETICS facades performing best and rainscreen facades performing worst (over a third of rainscreens failed the test), which seemed to be driven by the cladding materials, though the positive performance of ETICS facades may be due to the nature of the test's failure criteria, which does not consider flame spread that might

occur behind the render in ETICS facades. We also found that there was huge variation in the temperature performance of an identical facade across repeated tests, but whether the facade ignited or not remained relatively consistent.

These results show the power of a data driven, top-down approach to fire research. Although each of these commercial tests has only a small amount of information recorded, by combining large numbers of tests together and extracting as much information as possible from test reports, novel evidence of facade performance in fire can be gained. For instance, with a larger dataset, it could be possible to estimate how the probability of a facade having a flammability index > 2 changes when changing the cladding material (by plotting a probability density histogram). This could help engineers quantitatively assess the impact of their design choices.

Future test standards could capitalise on this approach by recording more detailed information and allowing it to become accessible for scientific research. Precise knowledge of material properties of products used in a facade, combined with less coarse thermocouple measurements, video recordings, and even heat flux measurements (or if possible, measuring the most important parameter for fire, the heat release rate) could allow for much more advanced prediction capability, either by passing the results from many tests through a regression model, or through a more advanced machine learning model. The output from such a model could be used to find which design parameters are sensitive to help guide future research or be used as an indicative model prior to large-scale testing.

This kind of evidence can also be used to critically assess the engineering judgements made to extend the application of facade tests (so called “desktop studies”) by correlating changes in different design inputs to outputs related to facade flammability, and thus providing quantitative evidence for such judgements. As researchers, it is not for us to tell architects or engineers how to design buildings. However, by providing empirical evidence of the performance of different facades and materials in these tests, we can better inform engineering decisions and allow for the creation of tall buildings with safe facades.

Chapter 4

Visual Fire Power: Method and Algorithm for Measuring Heat Released Through Visible Flames in Regular Camera Footage

Summary[4]

Chapter 3 mentioned the value of improving the range of the measurements taken during standard facade tests. By taking more measurements related to facade flammability, such as the heat release rate, rate of flame spread, or time to ignition, these tests could be used to assess the flammability of facade systems more clearly, rather than produce a simple pass or fail. This chapter presents a methodology that could be used to easily extend the measurements taken during such tests. This methodology can be used to estimate the heat released by through visible flaming in a turbulent fire, referred to as *visual fire power*. This value, measured in kW, is closely related to the heat release rate of a fire, but does not capture flames that cannot be seen. This chapter discusses how volumetric heat release rate should be approximately constant for a turbulent, diffusion fire, and explains a step by step method for estimating flame volume from camera footage. This methodology is then calibrated, first using virtual objects with known volume in the software Blender, then using experiments with propane sand burners fixed at different flow rates. The outcome of this work represents a powerful tool for fire safety research and was applied to the experiments discussed in Chapter 5.

4.1 Introduction

Chapter 3 mentioned the value of improving the range of the measurements taken during standard facade tests. By taking more measurements related to facade flammability, such as the heat release rate, rate of flame spread, or time to ignition,

[4] This chapter is based on the paper in progress: M. Bonner and G. Rein, A Novel Method for Measuring Heat Released Through Visible Flaming in Regular Camera Footage (to be submitted).

these tests could be used to assess the flammability of facade systems more clearly, rather than produce a simple pass or fail. One key aspect of flammability is the rate of fire growth, captured in the heat release rate of a fire. Traditional methods of measuring heat release rate require collecting all the emissions released by a fire, a task which becomes more expensive the larger the fire is. This would make it a more challenging variable to add to current facade fire tests. However, most of these tests are filmed to assist the technician making qualitative observations. This chapter presents a novel method for estimating the heat release by a turbulent fire through visible flaming, referred to as *visual fire power*, by estimating the flame volume from regular camera footage taken at different angles. Such a methodology could be easily included in current standard tests to improve their ability to assess facade flammability.

To the best of the author's knowledge, the observation that the volume of a flame is proportional to its heat release rate was first made by De Ris and Orloff [103], who found that up to a heat release rate of 250 kW, fires of methane, propene, and PMMA had a constant volumetric heat release rate of $\dot{Q}''' = 1200$ kW/m^3. Other work has found volumetric heat release rates of 1100 kW/m^3 for fires between parallel plates [104] and 800 kW/m^3 for furniture fires [105]. A figure of 500 kW/m^3 was also cited by [106]. Theoretical justification for a constant value for $\dot{Q}'''$ is given by Xin in [107]. For a buoyant, turbulent diffusion flame, the molecular mixing time should be approximately constant. By assuming that the heat released by combustion is transferred entirely to the surrounding gases, which then behave ideally, and that the heat released per mole of oxygen is approximately constant, the heat released per unit volume of the flame should also be constant. If this is true, then it should be possible to estimate the heat release rate of a fire based on videos taken at different angles, provided the shape and size flames in the video can be measured.

The idea of detecting fire in camera footage using computer vision techniques is not new [105], [108], [117], [109]–[116]. Attempts to detect flames focus on taking colour information from individual pixels in the image, sometimes taking into account the dynamic nature of fires by comparing changes between frames of a video. More detailed reviews of this topic can be found in [118], [119]. Most of this research was intended to detect early fires in order to raise an alarm [109]–[111], [114] and so did not necessarily focus on accurately finding the shape of the flame. However, [108] used the intermittency of a pool fire to estimate its centreline temperature, [116] used video processing as an estimate for flame height, and [117] used the flame height and

diameter of an axisymmetric pool fire to estimate its heat release rate based on traditional plume correlations.

In contrast, this work is trying to find the heat release rate of a fire based on its volume, by using multiple 2D images from different angles to recreate a 3D representation of a flame. This problem has been studied before in [105], [112], [120]. These studies identified that traditional approaches to tomography (3D reconstruction from 2D images) are difficult to apply to fire, firstly because a fire is a dynamic process with unclear boundaries, and secondly because it produces its own light, making it impossible to take into account reflections from the flame surface. The solution from these studies was to produce a cloud of points where the fire could be and to use knowledge of each camera's position and intrinsic properties (lens shape and sensor size and position) to estimate where each point would fall in the 2D images, then identify whether those pixels detected fire. This work initially tried a similar approach; however, the final method was somewhat different due to issues with accuracy, which will be explained in the next section.

4.2 3D Reconstruction of Fire from 2D Images

Let us consider a scenario with multiple videos of the same fire, taken by similar cameras in different positions. The objective is to convert the 2D images from these videos into a 3D representation of the fire. To do that, we need to know how a camera converts 3D coordinates in the real world ($X \quad Y \quad Z$) into 2D coordinates in the image plane ($u \quad v$).

The relationship between an image taken by a camera and its coordinates in the real world can be represented using a pinhole camera model [121], shown in Figure 4.1. The line along which the pinhole is located is called the *axis of projection*. All light rays coming from objects in the real world will pass through the pinhole, also known as the *centre of projection*, and travel to the image plane located 1 focal-length f away (the focal length is an intrinsic property of the camera, representing the distance from the lens to the imager). Using similar triangles, this means that an object with height X from the axis of projection and distance Z from the centre of projection in the real world will have height $x = \frac{-Xf}{Z}$ on the image plane. Repeating this logic for the Y-axis, you can show that the relationship between a point in the real world ($X \quad Y \quad Z$) and a point in 2D coordinates ($u \quad v$) is:

$$\begin{pmatrix} u \\ v \end{pmatrix} = -\frac{f}{Z}\begin{pmatrix} X \\ Y \end{pmatrix} \quad 4.1$$

Notice that multiple real world coordinates will map to the same coordinate in the image plane. This is because it is impossible to distinguish between points along the same ray in this projective mapping.

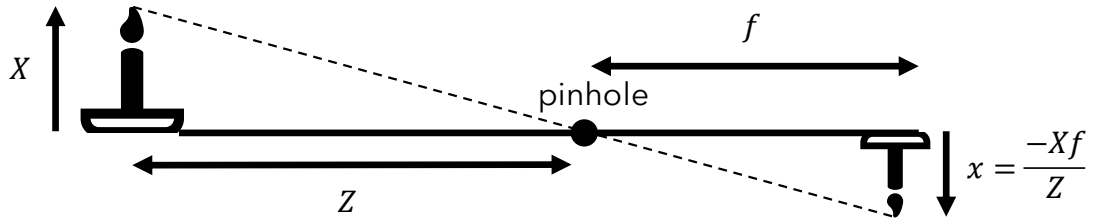

Figure 4.1 - Visual representation of a pinhole camera model and projective geometry. The lens of the camera is represented by a single point, through which all rays the camera sees must pass. This simplifies the geometry for estimating how these rays will then appear on the camera's sensor, or image plane.

What this means in practice is that each pixel in an image can be mapped to a ray projecting from the cameras centre of projection into the real world. The first opaque object that each ray hits would in theory be the object imaged in that pixel (obviously with different degrees of transparency, this becomes more complicated). This is the basis of the method for 3D reconstruction of a fire presented by [105], [112], [120]. These studies take the following steps:

1. Create an array of 3D pixels (voxels) in real-world coordinates (as opposed to image coordinates) in an area where the fire could be located.
2. Find the projective mapping of each voxel onto the image plane of your camera. This would create an M x N matrix that relates M voxels in world coordinates to N pixels in image coordinates. Remember that multiple voxels can map to a single pixel if they lie along the same ray.
3. Identify which pixels in your image do not contain fire. Any voxel that maps onto these pixels must not contain fire.
4. Remove voxels that do not contain fire from your voxel grid.
5. Repeat for multiple cameras. Each repetition will remove more voxels not associated with fire and get closer to an accurate representation of the real world.

With enough cameras, this method should provide an accurate reconstruction of the fire, regardless of its shape. However, this method is very computationally expensive. Most images taken today contain at least 10^6 pixels, and to create a grid of 1 mm^3 voxels covering a volume of 1 m^3 would require 10^9 voxels. This would mean the associated M x N matrix would contain 10^{15} elements, and the number of computational operations would be even higher. The calculations also need to be repeated for each camera being considered. For this reason, these approaches need to use coarse grids and efficient computational tricks to be computable in a reasonable time.

This approach was not used in this work, as we found it produced inaccurate results for our experiments. This was due to error arising from areas behind the fire that cannot be seen by other cameras, highlighted in grey in Figure 4.2. Each pixel in an image will only map the first opaque object hit by its associated ray. This means that any one camera will assume that the entire region behind any fire it detects will also contain fire. Adding additional cameras will reduce this error, as they can see more areas around the fire. However, this error was significant for our four camera setup (overestimating by more than 1 m^3 in some cases).

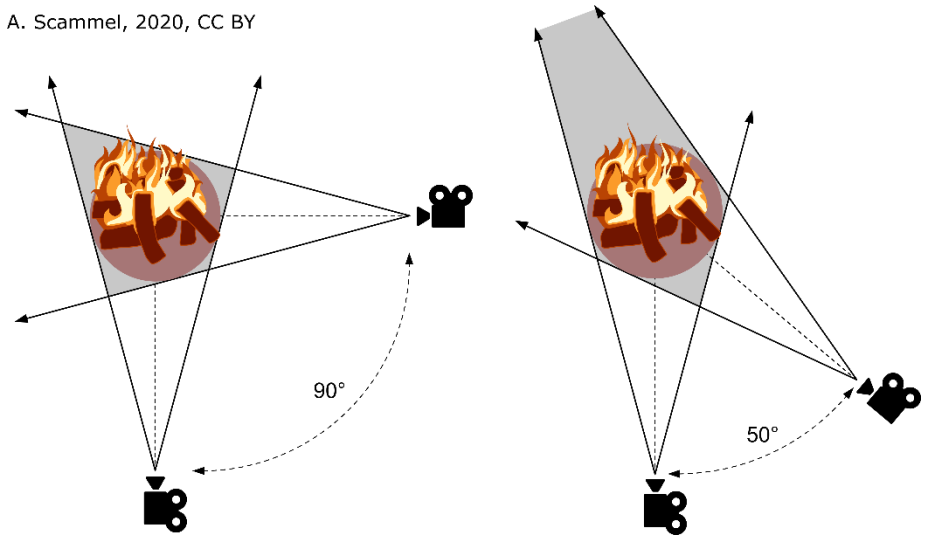

Figure 4.2 – Sketch demonstrating how errors arise from the ray tracing approach with too few cameras. Each ray projected from the camera is associated with a single pixel and will only record the first opaque object it hits. Therefore, if a camera detects a point along a ray as fire, then it will detect the entire region behind it as fire as well. Inspired by work from [122].

The original method of reconstruction used here will be referred to as *planar volume reconstruction*. As the name suggests, this method assumes that all relevant pixels in an image fall into the same 2D plane in real coordinates. This assumption becomes more

valid the further the distance from the camera to the objects of interest vs. the distance between the objects of interest along the axis of projection. The full methodology is demonstrated in Figure 4.3, and was implanted in Python using the open-source computer vision library OpenCV [123]. It consists of the following steps:

Step 1: Take an image of the xz plane

This method uses two cameras at approximate right angles to each other. To make the explanations clearer, I will refer to the specific example of the experiments in Chapter 4. In this case, I will take the x axis to be located along the width of the facade, the y axis to be located through the facade's build-up, and the z axis to be located along the height of the facade, as indicated in Figure 4.3. The origin of the coordinate system is located at the centre of the wood crib. In this case then, an image of the xz plane would be a photo taken towards the front face of the facade (from the same direction as the 2 m/s wind condition).

Step 2: Remove lens distortion

The pinhole camera model represents an idealisation of reality. In a real camera, imperfections in the sensor array and lens will lead the image to be distorted. This can be corrected by calibrating the cameras to find a transformation that maps each pixel in the image to where it would be located in a "perfect" image. The cameras were calibrated using the built in camera calibration toolbox in OpenCV. Full details can be found in [124], but this essentially involves taking many images of a flat object – in this case a chess board – and calculating the deviations from the pinhole model by recording how the corners of each square of the chess board move between images.

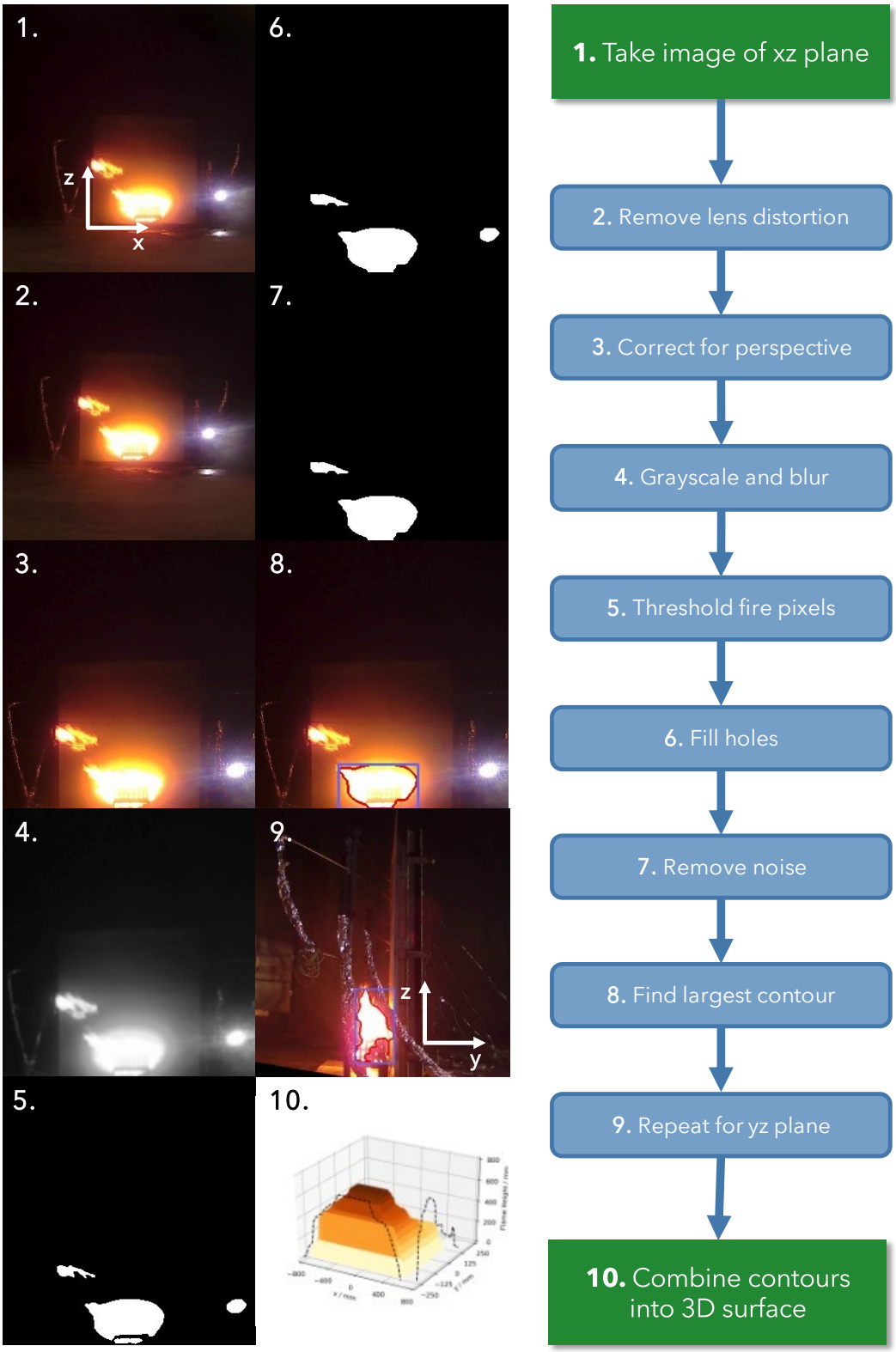

Figure 4.3 - 10 step explanation of the planar volume reconstruction methodology. A sketch of the experimental setup in these images is shown in Figure 5.1.

Step 3: Correct for Perspective

It is unlikely that the camera taking the image is completely aligned with the plane origin. To correct for perspective and calculate the relationship between image coordinates and world coordinates we need to select points that fall on a plane in the real world with known dimensions. In this case, the facade's cladding is perfect. We want the image to be centred on the front face of facade, with margins of fixed length around each edge.

We select each of the bottom-left, bottom-right, top-left, and top-right corners of the facade in pixel coordinates P_{bl}, P_{br}, P_{tl}, and P_{tr}, respectively. The width of the facade in pixels is:

$$\max\left(\sqrt{(P_{br} - P_{bl})^2}, \sqrt{(P_{tr} - P_{tl})^2}\right) \quad 4.2$$

The height of the facade in pixels is similarly:

$$\max\left(\sqrt{(P_{tl} - P_{bl})^2}, \sqrt{(P_{tr} - P_{br})^2}\right) \quad 4.3$$

Using these dimensions in pixels, we can calculate the width and height of each individual pixel in real world units (in this case mm) by dividing the width / height of the facade in pixels by the width / height of the facade in mm. We can also use the dimensions of the facade to calculate the "ideal" position of the four corners in an image where the camera was perfectly aligned. This transformation would represent a shift in perspective and is part of a category of transforms called *perspective transforms* or *homographies*, which are illustrated in Figure 4.4.

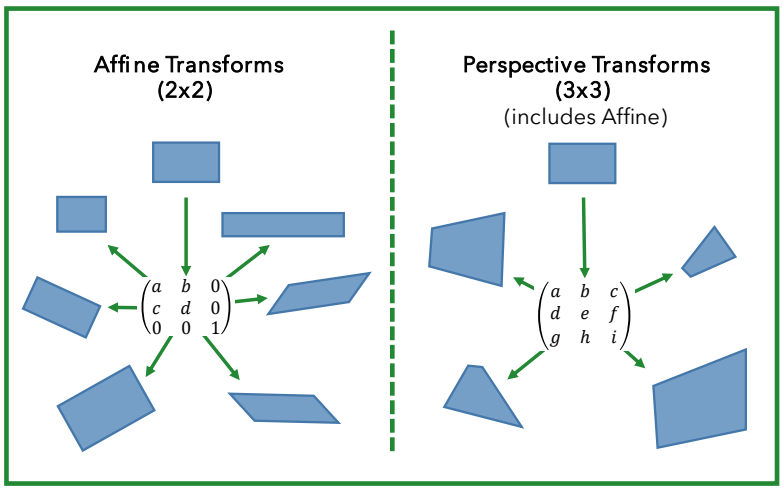

Figure 4.4 - Affine vs Perspective transforms of quadrilaterals. Affine transforms preserve parallel lines. Inspiration for figure taken from [121].

Combining this information, we can calculate a fixed margin around each edge of the facade in mm and convert this into pixels. We can then centre the perspective-corrected image on the centre of the facade (which is our chosen origin in world coordinates) and produce a direct mapping from our image coordinates to coordinates in our plane of interest in the real world.

Step 4: Grayscale and Blur

Images in OpenCV are represented as M x N x 3 arrays of pixel intensities, with values between 0 and 255, with the third dimension representing the individual red, green, and blue colour channels for the image. This can be converted to a single M x N array by combining the three colour channels into a single array of intensities, based on how the human eye detects different colours in real life (the eye is more sensitive to green, so the channel is weighted more heavily). The formula used in OpenCV is:

$$Y = 0.299R + 0.587G + 0.114B \tag{4.4}$$

Where R, G, B are the pixel intensities of the red, green, and blue channel, respectively. This single channel array is then blurred/smoothed using a Gaussian smoothing function. Smoothing or blurring an image is achieved by considering each

pixel in an image individually and then applying some function to that pixel based on the surrounding pixels. The specific shape and size of the window used to select which surrounding pixels to take into account is called a *kernel*. The most basic smoothing function would be setting a pixel to the mean of itself and the surrounding 9 pixels. A Gaussian smoothing function is similar, except it weights pixels further from the central pixel less in the average based on a normal distribution. Here, I used the built-in GaussianBlur() function in OpenCV. The reason for this step was to improve the quality of the thresholding done in step 5.

Step 5: Threshold Fire Pixels

A binary image is an image where every pixel has an intensity of either 0 or a fixed non-zero value, usually the maximum intensity possible (in this case 255). To transform an image into a binary image, we can apply a thresholding function. This is a set of logical rules that will set each pixel to either 1 or 0. Most commonly, a thresholding function will transform a grayscale image into a binary image based on some threshold value of intensity, hence the name.

In this instance, we want to select rules that will distinguish between pixels that do or do not contain flames. Previous fire detection methods have often used rules based on the red colour intensity and pixel saturation to detect fire. For instance, [113] uses the following rules:

$$R > 180 \tag{4.5}$$

$$R > G > B \tag{4.6}$$

$$(100 - 0.39B) > S > (-2.01 + 90.59e^{-\frac{B}{77.6}}) \tag{4.7}$$

Where S is the pixel's saturation. However, these rules did not detect fire well in our experiments. The experiments were done throughout the day in natural light, meaning the lighting conditions were different in each video. This affected the colours significantly.

A simpler approach, taken in [108], is to use the grayscale intensity to identify pixels containing flame. A value between 0 and 255 is selected as the threshold value, and all pixels above or below this are set to 1 or 0. We found this was effective at detecting fire, but that using a single threshold value got different results in different lighting conditions. We solved this by using an approach inspired by Otsu's binary threshold [125], which tries to separate an image based on peaks in the frequency histogram of pixel intensities in a grayscale image, like the one shown in Figure 4.5. Knowing that flames would always be on the upper end of grayscale intensity, we disregarded all pixels with < 200 intensity. We then selected a threshold based on the maximum pixel intensity, above which 80% of the pixels in this region were located. In other words, I take a cumulative sum of the values of the individual bars in Figure 4.5 from right to left until it is greater than or equal to the sum of all the bars in the highlighted region from 200-255.

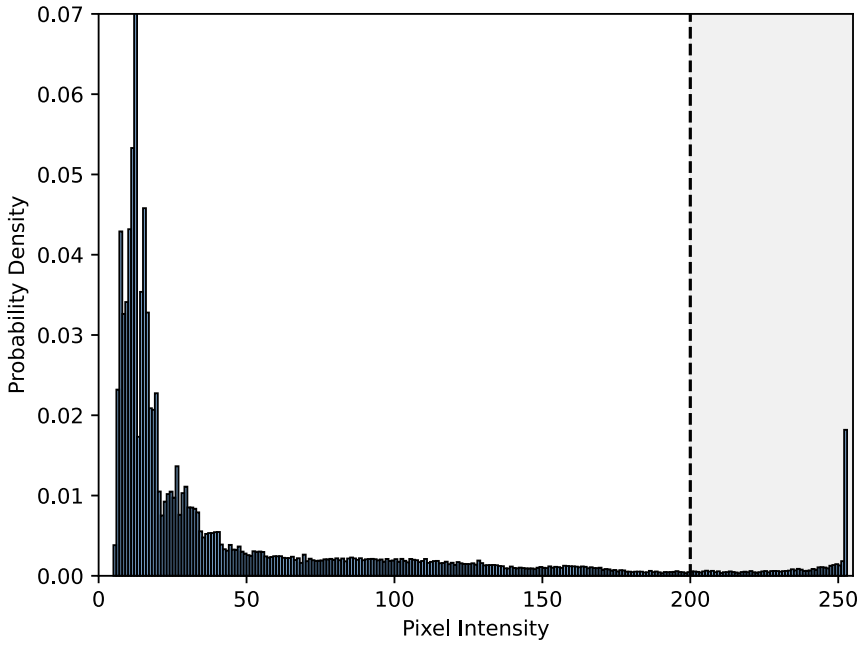

Figure 4.5 - A histogram of the pixel intensities in the image in step 4 of Figure 4.3. The area considered by the variable threshold is highlighted in gray.

Step 6: Fill Holes

As thresholding is done on a pixel by pixel basis, it is quite common for small holes to appear in a binary image, made up of small regions of pixels that did not meet the threshold (black pixels) surrounded by large regions of pixels that did (white pixels). This can interfere with contour finding algorithms. The problem can be alleviated

somewhat by smoothing the image prior to thresholding, but some holes may still remain. To deal with this, we can use a *morphology function* which essentially deals with the boundaries between white and black pixels in a binary image. One such function is a *hole filling function* that fills small regions of white pixels while leaving large regions the same size.

Step 7: Remove Noise

The issue with thresholding based on grayscale intensity is that the algorithm may also pick up other bright objects, like the spotlight in Figure 4.3. To remove this kind of background noise, we can apply the threshold algorithm to a frame of the video from before each experiment started. This would pick up all bright objects that weren't fire. These regions are then removed from the binary image.

Step 8: Find Largest Contour

The contours of a binary image are the outside edges of regions of white pixels. OpenCV has a built-in algorithm for finding contours in binary images. This was used to find a list of all contours in the frame. The largest contour was selected as the fire region. Due to the blurring and hole closing steps, this would include detached flames close to the main body of the fire but would not include small regions of flame casting far away from the main body. This is something to improve upon in future versions of this method.

Step 9: Repeat for the yz plane

The previous steps were repeated for a camera at 90° to the original camera. In the case of these experiments, that would be facing the facade side-on with the y axis going in the direction of the masonry wall from the centre of the wood crib.

Step 10: Combine Contours into a 3D Surface

By following the previous steps, we are left with two contours representing the largest region of fire in each image. To combine these into a 3D shape, we need to find a shared point between them. In practice, the relative z coordinates of the two images were usually slightly different from each other due to the accumulation of small errors in the previous steps. To solve this, we calculated the difference between the maximum

and minimum z value for each pixel in the contours to give the "flame height" at that point in the contour, producing two arrays containing the variation in flame height with the variation in x and with y. These arrays are then combined into a 3D surface by creating a 2D mesh grid over each combination of x and y in the two contours and then taking the minimum flame height at each position.

$$z_f(x,y) = \min\left(z_f(x), z_f(y)\right) \tag{4.8}$$

The reasoning behind this relates to the discussion of camera rays from before. Taking our assumption that the image represents a plane in the real world, then any ray coming from the camera should be perpendicular to the plane it is imaging. Because the pixel takes an image of the first opaque object it sees, the pixels at the edge of the flames will represent the maximum height along the y axis. Similarly, the pixels at the edge of the fire in the yz plane will represent the maximum height along the x axis. Therefore, for any point (x, y) on our surface, the flame height must be *at most* the smaller of the two values seen by the two cameras. It is possible of course that some of the points on the surface could have even lower flame heights, but this would be undetectable using this method (a similar problem to the issue in Figure 4.2). Figure 4.6 shows what the surface produced from these two images looks like. To find the volume we then integrate over the surface.

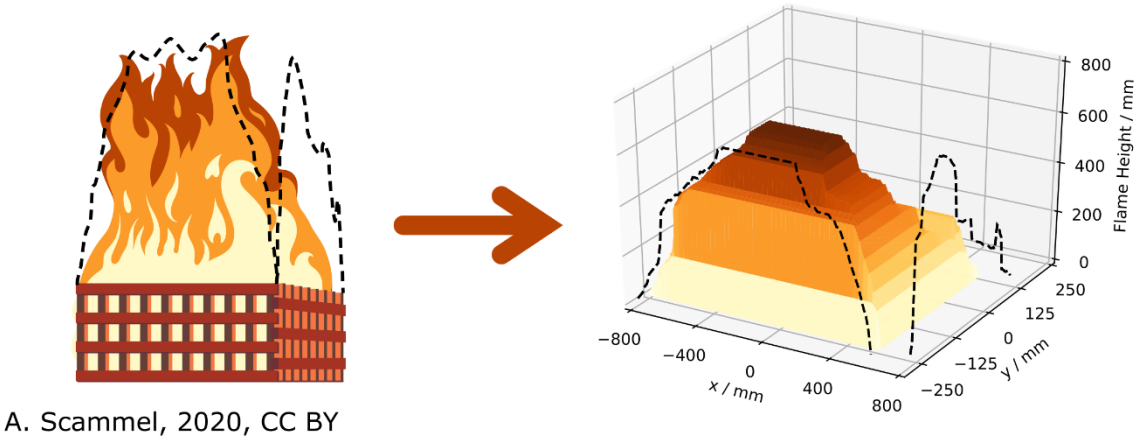

A. Scammel, 2020, CC BY

Figure 4.6 - Demonstrating a 3D surface formed from 2 2D line plots of flame height varying with x and y. The colour of the surface varies with height for clarity.

4.3 Method Calibration

4.3.1 Calibration using a virtual scene

As this is a novel method, it is important to test its efficacy by using it to analyse an object with a known volume. Unfortunately, there isn't a consistent way to measure the volume of fire precisely. However, it would be ideal to calibrate the method against something similar to its end use. With this in mind, we created a virtual scene of a simulated burner against a wall inside the virtual imaging software Blender [126]. Blender is a computer graphics software that can create virtual 3D scenes, which can then be photographed or filmed using virtual cameras in the generated scene. This allows us to test the planar volume reconstruction method in a scenario with ideal cameras and thresholding, ensuring that any residual error comes from the volume reconstruction method itself, rather than imperfections in the cameras or in detecting the boundaries of a fire.

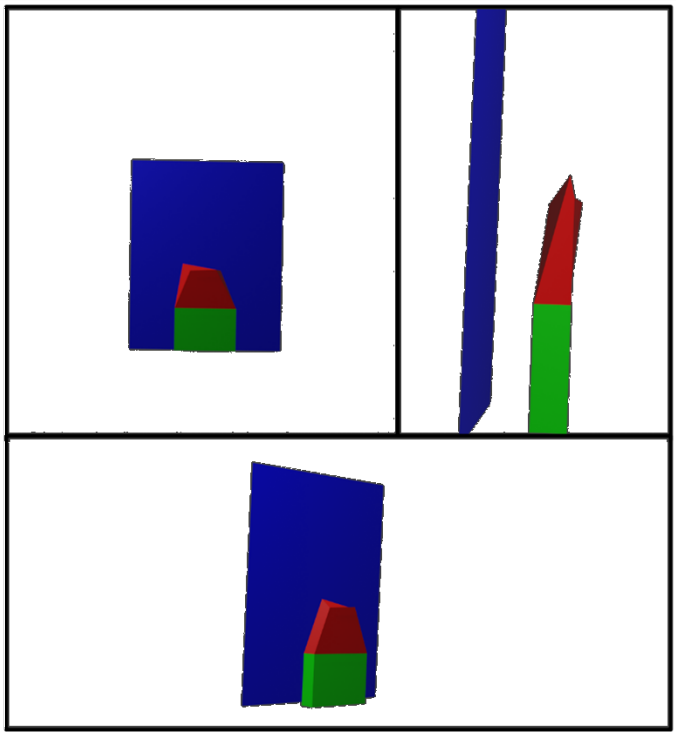

Figure 4.7 - A virtual scene of a simulated burner against a facade. Bright colours are chosen to allow for simple and precise thresholding rules. The top two views are equivalent to the xz and yz planes used in planar volume reconstruction. The bottom view is to give additional context to the scene.

Figure 4.7 shows images of a virtual scene created in blender, taken using virtual cameras in the space, imitating a burner against a facade with an irregular flame

surface. Using red, green, and blue shading for the flame, burner, and facade, respectively, allowed for perfect thresholding and identification of both the flame boundaries in step 5, and the corners of the facade and the burner that are required for the perspective transform in step 3. The virtual cameras were set to have no lens distortion, meaning the calibration step was unnecessary in this case. Any remaining error in estimating the volume of the red "flame" object (which had a volume of 0.044 m^3) would therefore only arise from the fundamental assumption that the objects in the image lie in a plane in the real world, or from the potential over-estimation of flame height at certain coordinates that was mentioned in step 10 of the method.

The computational efficiency of planar volume reconstruction depends on the number of pixels (the resolution) of each image. For this reason, we chose to test whether reducing the resolution of the image would have any effect on the accuracy of the method. We introduced a *scale factor* into the algorithm, which shrunk the image to $1 \times$ scale factor of its original size. The results of the calibration and the effect of changing the resolution are shown in Figure 4.8. While shrinking the image by a large amount will have a large effect on the size of the estimated volume, this volume tends to flatten out above a scale factor of around 0.25. The overall error in estimating the volume using this method was around 0.006 m^3, or 14% of the true volume. As we will see, this is much smaller than the variability in the volume of a flame with a constant heat release rate, and so the method would seem to be useful for our purposes.

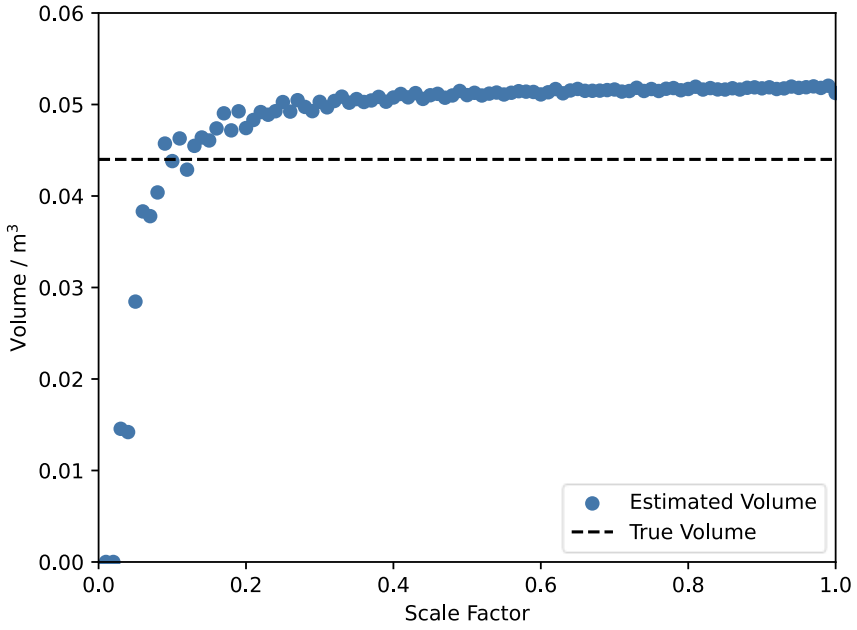

Figure 4.8 - Estimated volume of the red surface in the virtual scene shown in Figure 4.7, for images at (1 × scale factor) of their original resolution. The true volume of the surface is given by the dashed line.

4.3.2 Calibration using real experiments

To explore the relationship between the heat release rate of a fire and the estimated flame volume using planar volume reconstruction, we performed a series of experiments, using propane sand burners with known flow rates against a masonry wall (similar to the virtual scene in Figure 4.7). Pictures of the experiments are shown in Figure 4.9. The sand burners were 800 x 160 x 550 mm and were place 250 mm from the wall. Experiments were performed with both a single burner and 2 burners side by side, and with and without the 2 m/s wind condition used in the experiments in Chapter 4. The flow rates used for the different burner configurations are given in Table 4.1. The fuel was a mixture of 95% propane and 5% butane, as this was easily available in the lab. We converted the flow rates to heat release rates by approximating the mol / l of fuel to be that of an ideal gas with the same molecular weight, and using values for the chemical heat release rate of the two fuels burned in air given in [127]. This gave a value of 80.21 kJ/l for the fuel. Comparing this to calculations using the lower heating value of the two fuels using a bomb calorimeter, the value of 80.21 kJ/l represents a combustion efficiency of 94%.

Table 4.1 – Flow rates of a mixture of 95% propane and 5% butane gas, for experiments with a single sand burner and two sand burners side by side. Experiments were performed with and without a 2 m/s wind.

	Flow Rate / l/s					
Single Burner:	0.5	1.0	1.5	2.0	2.5	3.0
Dual Burners	0.5	1.0	1.5	2.0	2.5	5.0

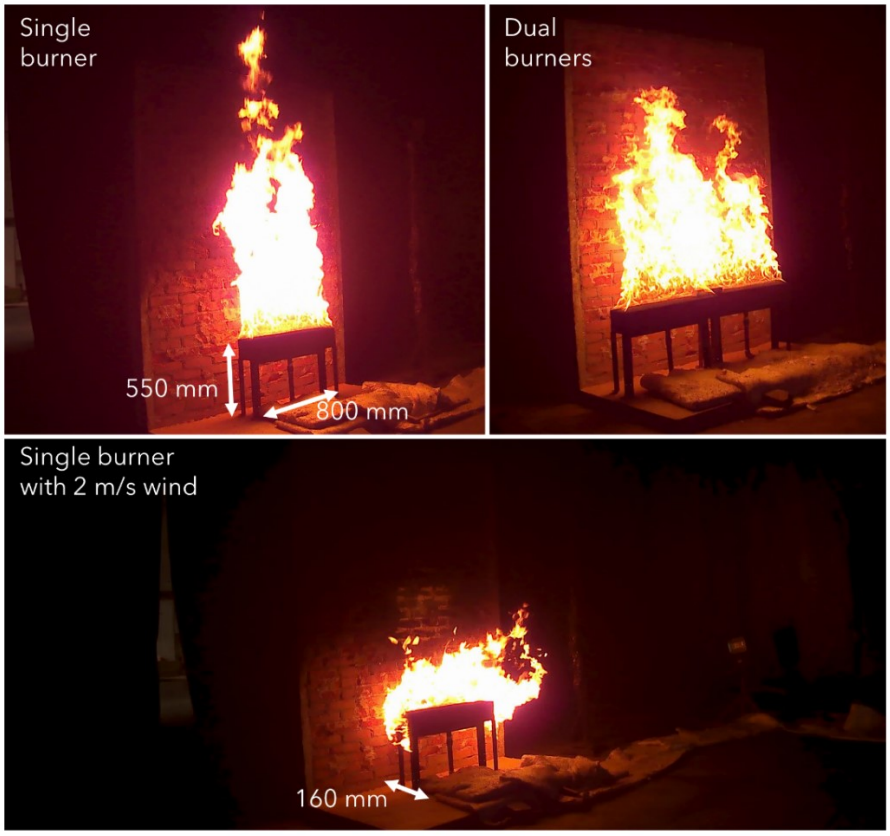

Figure 4.9 - Photos of the calibration experiments with sand burners against a masonry wall

The results of these experiments are shown in Figure 4.10. Estimated volumes are plotted against the heat release rate for each flow condition by taking the mean volume over a 90 s period at this flow rate. The σ error bars represent the standard deviation over this same 90 s period. The errors bars are plotted for each flow rate and burner condition separately, but the values given in the legend are the average across all wind / no wind experiments. The black lines show the constant volumetric heat release rates measured by Orloff and De Ris [103], Stratton [105], and fitted to this data using least

squares. Looking at the plot, it seems that the volumetric heat release rate increases for higher flow rates. However, this was likely due to an issue in thresholding the fire in these experiments. Using the simple thresholding rules explained in step 5, reflections of the flame from the surface of the wall were also detected. This effect is shown in Figure 4.11. This gave an over-estimation of the volume of the flame, particularly for lower heat release rates where less of the flame had reached the wall in these reflections. Reflections were also picked up more during experiments with wind. This may explain the larger volumes for smaller heat release rates. In the future, we hope to repeat these experiments without the presence of a wall to test this hypothesis.

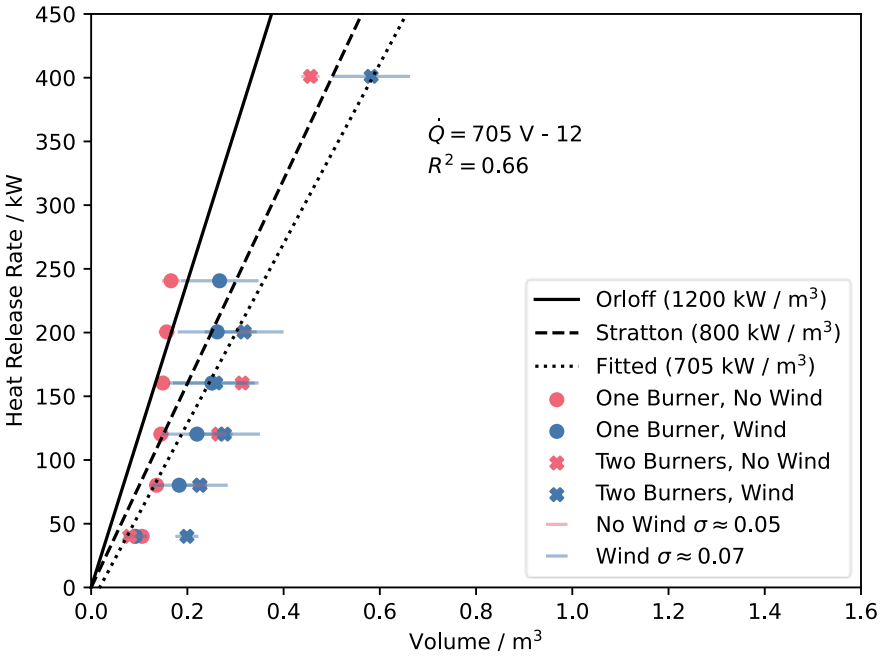

Figure 4.10 - Volume vs Heat Release Rate for single and dual sand burners, with and without a 2 m/s wind condition. Lines of the volumetric heat release rates found by Orloff and De Ris [103] and Stratton [105] are plotted, alongside a line fitted to the experimental data using least squares.

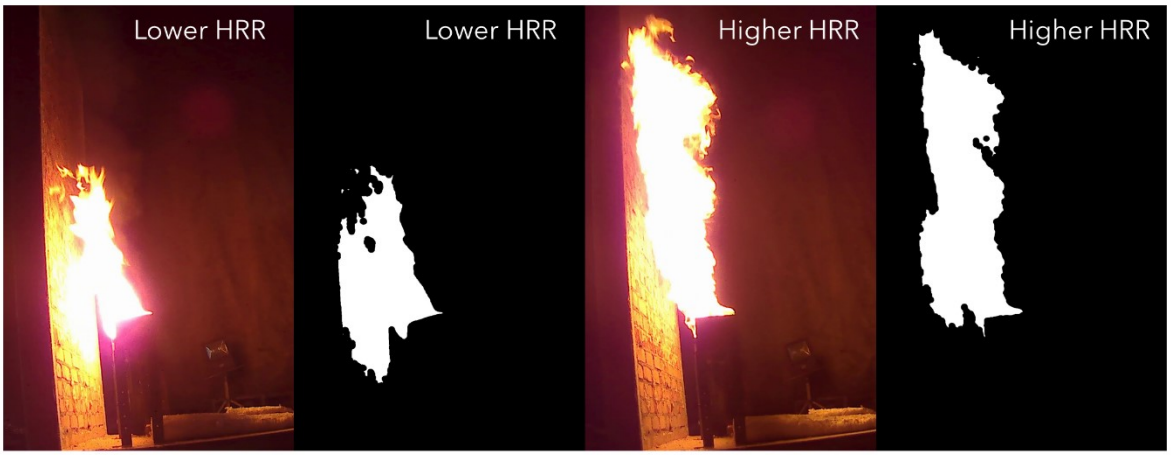

Figure 4.11 - Demonstration of the effect of reflections in the calibration experiments. The thresholding technique cannot distinguish between reflections from the fire and the fire itself in either case, but for higher heat release rates, the reflections represent a smaller proportion of the flame, so produce less error.

Given that the results from these calibration experiments were likely overestimating the volume, and by extension the heat release rate, we also studied the results from the first experiment in Chapter 5, where a 20 kg wood crib was burned against a non-combustible facade. In the experiments in Chapter 5, the facades did not produce reflections on the same magnitude as these calibration experiments, and so using the volumetric heat release rate from these calibrations would probably underestimate the true heat release. To test this, we plotted the visual fire power across time for this first experiment (essentially burning a wood crib against an inert wall) using the volumetric heat release rates taken from Orloff and De Ris [103] and from the fit to the calibration experiments. Using the value of 1200 kW / m^3 gave a peak heat release rate much closer to the expected value of 500 kW, estimated by the chief technician at ITB. For this reason, I used a value of $\dot{Q}''' = 1200$ kW/m^3 in my analysis in Chapter 5. The value of this constant should be revisited in future work and compared across different scales, along with a more in-depth study of the sensitivity of this method to different camera parameters.

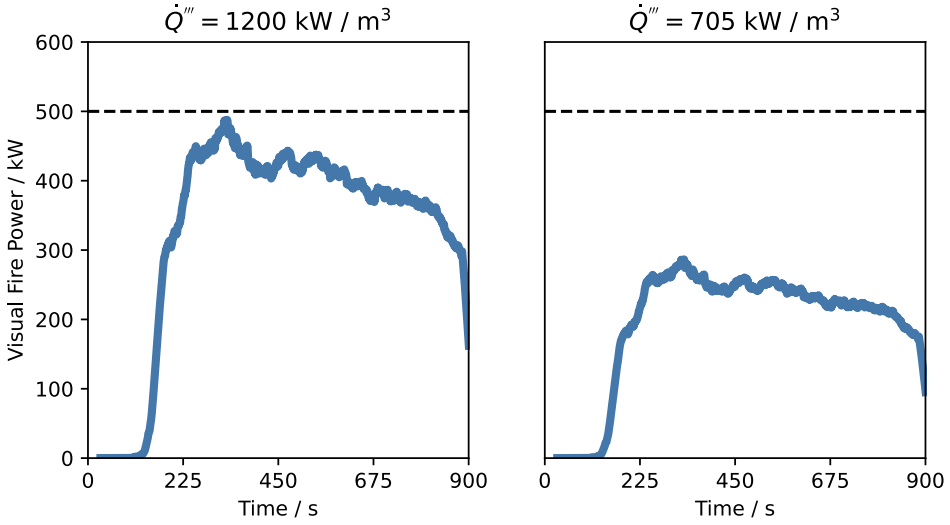

Figure 4.12 - Plots of Visual Fire Power with time using the volumetric heat release rate from Orloff and De Ris [103] and from the fit to the calibration experiments shown in Figure 4.10. The 500 kW line, which is the expected peak heat release rate of the wood crib, is marked on each plot.

4.4 Conclusions

This chapter showcases a novel method to measure the visual fire power of a turbulent diffusion fire using regular video footage taken by cameras at right-angles to each other. This method relies on the fact that the volumetric heat release rate of such fires should be relatively constant. By assuming that relevant objects in the videos from each camera fall along a plane in real-world coordinates, it is possible to use the planar volume reconstruction method to create a 3D surface and estimate its volume. This method was calibrated against both virtual objects with known volume, and real experiments using sand burners. We found that it could accurately recreate the volume of a well-defined object, but that defining the edges of the flames in our calibration experiments was tricky.

Although further experiments without reflections would be needed to properly calculate an appropriate volumetric heat release rate for this method, it is important to mention that this should not affect the results of the visual fire power analysis in Chapter 5. This is because any change in the volumetric heat release rate would be constant across all experiments, meaning only the relative size of the effects would change.

This work could be expanded upon with further calibration experiments and a more general methodology to allow it to be used as a cheap and effective tool for measuring visual fire power in fire tests and experiments. Currently, the code can only be used in the specific case of a fire against a wall, with videos taken at right angles to each other. It has also only been validated for this condition. By performing experiments at a range of scales and conditions, it could become a much more general tool. As it is, it is a proof of concept of a powerful and novel method, which could have wide-ranging practical applications in the future.

Chapter 5

Parametric Study of Intermediate-Scale Facade Experiments Containing Combustible Components

Summary[5]

In contrast to the coarse data of the commercial tests in Chapter 3, this chapter presents a parametric series of 20 intermediate-scale facade experiments, based on the PN-B-02867 standard. This represents the largest series of experiments at this scale in the literature. The experiments varied the material of the cladding panels and insulation in rainscreen facades, as well as the presence and location of a ventilated cavity, in order to investigate the impact of each parameter on facade flammability. Four times as many thermocouples are used compared to the original test standard, and video recordings were taken from four different angles to give more information – including an estimate of the heat release rate of the fire through visible flames, referred to as *visual fire power* (explained in the previous chapter). The experiments revealed that each varied parameter affected different aspects of the fire behaviour of the test. The cladding material seemed to affect the overall size of the fire in all conditions, whereas the insulation behaviour was more dependent on whether or not a cavity was present. The presence of a cavity seemed to have the largest effects, producing dramatic changes in the fire scenario, particularly in increasing the rate of flame spread on the facade. The results of these experiments reveal for the first time the impact of each of these parameters at this scale and can provide fire safety engineers with useful knowledge to help design fire safe facades in tall buildings.

[5] This chapter is based on a paper in progress: M. Bonner, W. Wegrzynski, B. K. Papis, B. Khoo, F. Lugaresi, and G. Rein, Fires in the Walls of Tall Buildings: A Parametric Study and 3D Reconstruction of Intermediate-Scale Facade Experiments Containing Combustible Components (To be submitted)

5.1 Introduction

Chapter 3 discussed the power of a top-down approach to assessing fire safety in facades and demonstrated this using data from the Polish national facade fire test, PN-B-02867. This approach used a large amount of coarse data – the specific products used in each test were not known and we could only study variables recorded in the test reports. This chapter explores the possibility of using a top-down approach to learn from a smaller number of whole system experiments where more details were recorded, both in terms of knowledge of the products used in the facade, and in measurements taken during the experiment.

The analysis of KRESNIK in Chapter 3 identified some key results in the data. Firstly, tests of rainscreen facades recorded consistently higher flammability index, peak temperatures, and residence times than the ETICS or sandwich panel facades in the database. Looking at the facades that did not fall into any of these categories, the ones that failed also had a ventilated cavity. In other words, all of the facades that failed a test in KRESNIK had a cavity. Secondly, the cladding material was clearly important in predicting a facade's flammability index, but there was no obvious quantitative trend that could explain the variation in the data. Finally, the variation between repeats was significant for the temperature measurements, but 95% of the facades had a consistent flammability index between repeats.

There were also limitations in the data available. All of the rainscreen facades in the database had non-combustible, mineral wool insulation, so the effect of insulation on fire performance could not be investigated. It was also impossible to know the specific products used in each facade, so some of the unexplained variation in output may have been due to the variation in material properties within each category of cladding material (not all fire retardant panels may have been equally fire retardant for instance). In addition, the test reports only recorded temperatures from 4 locations on the surface of the facade, and a table of failure criteria observed during the test (converted to the flammability index).

To address these limitations, this chapter presents parametric series of 22 experiments, varying the type of cladding material by its Euroclass reaction-to-fire rank [128], the type of insulation material by its Euroclass reaction-to-fire rank, and whether or not the facade had a ventilated cavity, as well as two experiments including a

ventilated cavity between the masonry wall and the insulation, rather than the insulation and the cladding (in Table 5.1, these experiments' cavity widths are labelled as "50 (reverse)"). In wet countries, like the UK, a ventilated cavity would be located between the insulation and the cladding to control moisture from the outside, but in dry countries the position is reversed, which is why we included this scenario. A cavity width of 50 mm was chosen for comparison with other experiments performed following the Grenfell Tower fire (which had a 50 mm cavity). The full list of experiments is shown in Table 5.1. It is worth noting that, in reality, a rainscreen facade would always include a ventilated cavity, but by testing facades with no cavity in some of the experiments, we could examine the effect of that cavity. When discussing the materials in this chapter, I will refer to their Euroclass rank in brackets, e.g., Phenolic Foam (C).

A similar series of experiments was performed previously by Guillaume et al [67]. This work involved 9 different facades containing different combinations of Aluminium Composite Panel (ACP) cladding and an insulation material, all with a 50 mm ventilated cavity. Here, we have some overlap with these tests, but have also included facades without ventilated cavities and with High Pressure Laminate (HPL) cladding, which has come under scrutiny recently [69], [70]. While the experiments in [67] measured the heat release rate (HRR) directly using oxygen consumption calorimetry, this was not possible in our lab. Therefore, the visual fire power of the different experiments was estimated instead using the camera footage (see Chapter 4).

Table 5.1 - Planned parametric series of facade experiments.

Experiment (*not completed)	**Cladding (Euroclass Rating)**	**Insulation (Euroclass Rating)**	**Cavity Width / mm**	**Cladding Height / mm**
1	Cement Board (A2)	Glasswool (A2)	50	3050
2	Cement Board (A2)	Phenolic Foam (C)	50	3050
3*[6]	Cement Board (A2)	Glasswool (A2)	0	-
4*	Cement Board (A2)	Phenolic Foam (C)	0	-
5	ACP FR (B)	Glasswool (A2)	50	2500

[6] * refers to experiments that were not completed by time of writing

6*	ACP FR (B)	Phenolic Foam (C)	50	-
7	ACP FR (B)	Glasswool (A2)	0	2500
8*	ACP FR (B)	Phenolic Foam (C)	0	-
9	10 mm HPL (C)	Glasswool (A2)	50	2300
10	10 mm HPL (C)	Phenolic Foam (C)	50	2300
11	10 mm HPL (C)	Glasswool (A2)	0	2300
12	10 mm HPL (C)	Phenolic Foam (C)	0	2300
13	6 mm HPL (D)	Glasswool (A2)	50	2800
14	6 mm HPL (D)	Phenolic Foam (C)	50	2800
15	6 mm HPL (D)	Glasswool (A2)	0	2800
16	6 mm HPL (D)	Phenolic Foam (C)	0	2300
17	ACP PE (E)	Glasswool (A2)	50	2550
18*	ACP PE (E)	Phenolic Foam (C)	50	-
19	ACP PE (E)	Glasswool (A2)	0	2550
20*	ACP PE (E)	Phenolic Foam (C)	0	-
21	6 mm HPL (D)	Glasswool (A2)	50 (reverse)	2300
22	6 mm HPL (D)	Phenolic Foam (C)	50 (reverse)	2300

5.2 Methodology

The experiments were performed in collaboration with Instytut Techniki Budowlanej (ITB) at their laboratory in Pionki, Poland. The experimental setup is shown in Figure 5.1. The experiments were based on the PN-B-02867 fire test standard [94]. In the standard, a mock-up of a facade is attached to a 2 m wide x 2.5 m tall masonry wall. A 20 kg wood crib, placed 50 mm from the facade, is then ignited and allowed to burn for 15 min while being subjected to a 2 m/s air flow into the front of the facade. After 15 min the crib is removed, and the facade is observed for a further 15 min before being extinguished (if it has ignited). The facade is also extinguished if it has failed all the observation criteria of the test. Alongside these observation criteria, temperature measurements are taken on the surface of the facade at heights of 1.5 and 2.25 m, $\pm$125 mm from the centreline of the facade.

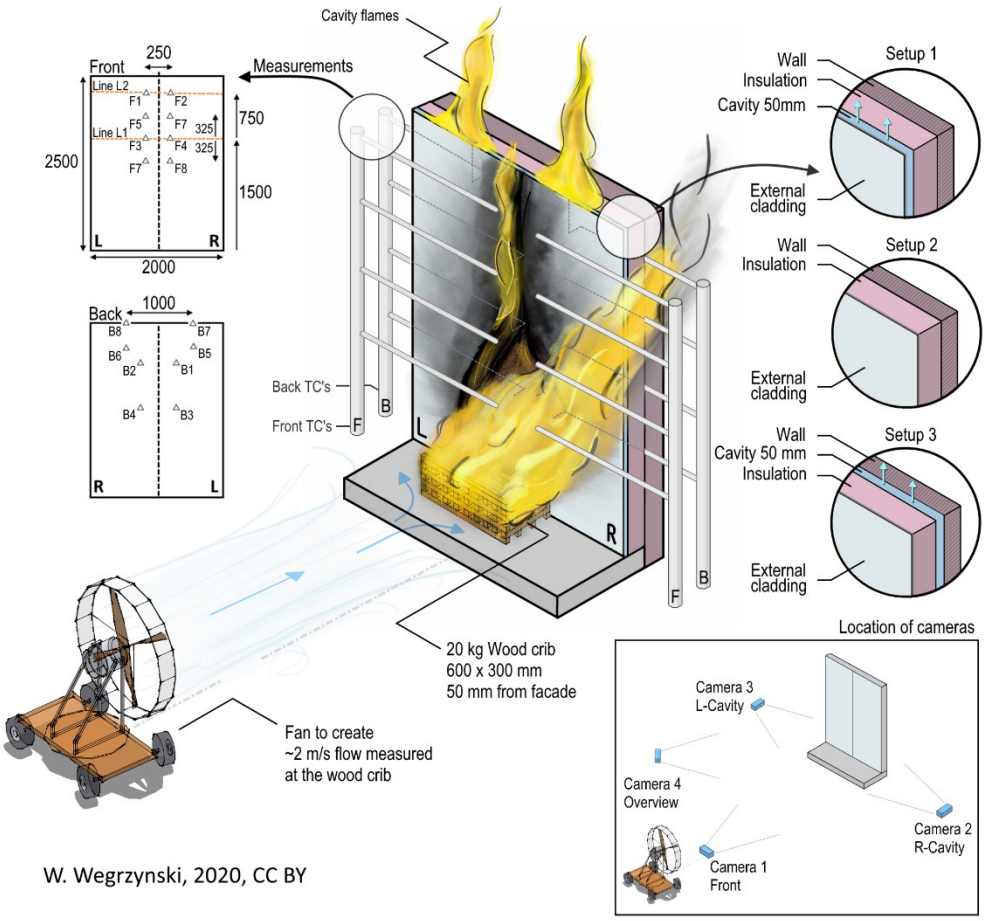

Figure 5.1 - Experimental setups for the 3 different cavity scenarios. Setup 1 is similar to a ventilated facade in wet countries, setup 2 has no ventilated cavity and is for experimental purposes, setup 3 is similar to ventilated facades in dry countries.

These experiments differed from the PN-B-02867 standard, firstly by allowing the facade to continue to burn for as long as possible. This was usually at least the expected 15 min after the crib was removed, though some experiments were extinguished early due to safety concerns. Additional temperature measurements were taken compared to the standard. 12 K-type, NiCr-NiAl thermocouples (as opposed to 4 in the original standard) were used at heights of 1.125, 1.5, 1.875, and 2.25 m on the surface of the facade at ±125 mm from the centreline of the facade, as well as in the same position at heights of 1.5 and 2.25 m but at a distance 25 mm from the inside edge of the cladding – either in the centre of the ventilated cavity, if it was present, or at the same depth in the insulation if not. There were also 4 thermocouples placed in the cavity at heights of 2.3 and 2.5 m but ±250 mm from the centre of the facade. These thermocouples were 1.5 mm in diameter, which can affect the response time and radiation errors in temperature

measurements [129]. The purpose of these extra thermocouples was to be able to track temperature changes in the cavity, and to try and increase the spatial resolution of the measurements on the surface of the facade. 4 Vmotal GSV 8580 action cameras were also set up in a semi-circular radius around the facade to record the experiments at a capture rate of 2 Hz. These cameras were protected with aluminium tape to shield them from radiation.

Including these cameras gave us a lot of additional information versus only the temperature measurements from the commercial tests in KRESNIK. As well as allowing a qualitative analysis of the experiments "by eye", features of the fire could be extracted using techniques from computer vision. This allowed us to measure the height and area of flames on the surface of the facade, as well as estimate the rate of heat release through visible flames during the experiments. The method used to do this is explained in Chapter 4. This value is related to the total heat release rate of the fire; however, it cannot capture the heat released from smouldering or from fire in the cavity (which cannot be seen by the cameras). In order to distinguish it from the true heat release rate, this value is referred to as *visual fire power*, measured in kW.

There were some challenges with completing the experimental series exactly as planned. The fire during the experiment with ACP PE (E) cladding, glass wool, and a cavity was large enough that the experiment was extinguished early for safety. The facades with HPL (C) and HPL (D) cladding with phenolic foam and a cavity were also cooled slightly by spraying water into the smoke plume above the facade intermittently, again to manage the size of the fire. In the experiments with HPL (C) and HPL (D) cladding, glass wool, and a cavity, one or both of the facade panels came off onto the crib during the experiment, preventing the wood crib from being extinguished and hitting the thermocouples. In one experiment with HPL and glass wool, one of the cameras used to calculate visual fire power also cut out part way through but, because this test was a repeat, recordings of visual fire power still exist for this setup.

There were also some challenges with communication, given that the experiments were constructed by a different team to those that designed it. Not all of the cladding was a consistent height (shown in Table 5.1). The wood crib was also sometimes removed slightly earlier or later than the 15 minutes desired. This was not intended, but it was accounted for in the analysis of "excess" temperature and visual fire power by comparing the difference between the measured temperature and the expected

temperature time curve from the wood crib only for times when the wood crib was still burning. The material budget for the experiments also ran out before completing the experimental series meaning only 20 experiments were completed (including some repeats) covering 16 of the planned combinations. The experiments missing are also marked in Table 5.1.

5.3 Results and Discussion

5.3.1 Qualitative Observations

Before trying to quantify any of the effects we saw in the experiments I will first discuss my observations from the camera footage. One observation across all of the experiments was that the fire near the crib always managed to break through the cladding into the cavity, and in most of the experiments the insulation nearest the crib was entirely burned away, leaving the masonry wall exposed. This is indicated for the Cement Board (A2) in Figure 5.2. This suggests that even for this relatively small fire source, the cladding was insufficient to prevent flames entering the cavity. This is important as it suggests that for lightweight cladding, simply sealing the cavity with cavity barriers may not prevent a fire from breaking inside.

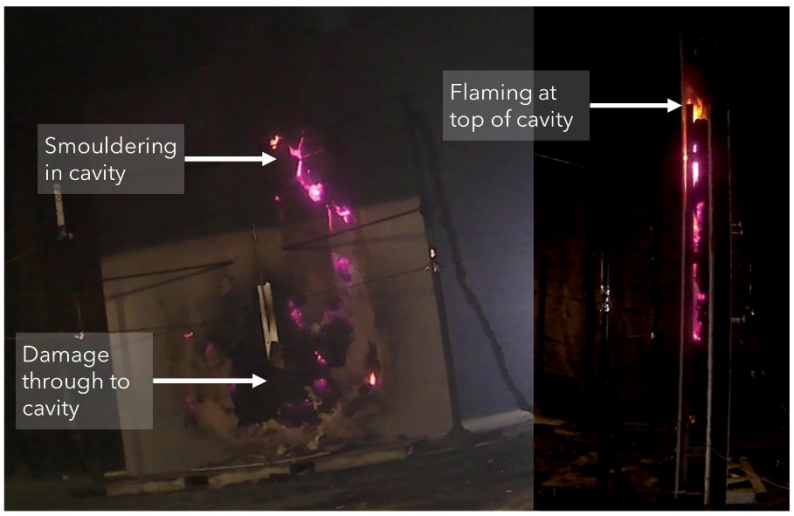

Figure 5.2 - Photos of an experiment with Cement Board (A2) cladding, phenolic foam insulation, and a cavity. Key features from the discussion are labelled.

Observing the effect of the different cladding materials, the materials with a worse reaction-to-fire performance, produced much larger fires than ones with better reaction-to-fire performance. The HPL (D) and ACP PE (E) ignited very quickly and the whole of

the facade was consumed or melted away. The ACP FR (B) meanwhile self-extinguished after the crib was removed in both experiments. Interestingly, the HPL (C)'s behaviour seemed more dependent on the presence of a cavity and choice of insulation. When a cavity was present the maximum fire size was larger and the rate of fire growth was faster, but without a cavity the fire spread much more slowly (see Figure 5.3). In the case with glass wool and no cavity, the HPL (C) cladding even self-extinguished. This implies that one effect of the cavity is reducing the threshold at which a material becomes likely to self-sustain a fire on a facade. It is also worth mentioning that the Cement Board (A2) produced a significant amount of debris due to spalling, particularly with Phenolic Foam (C) insulation.

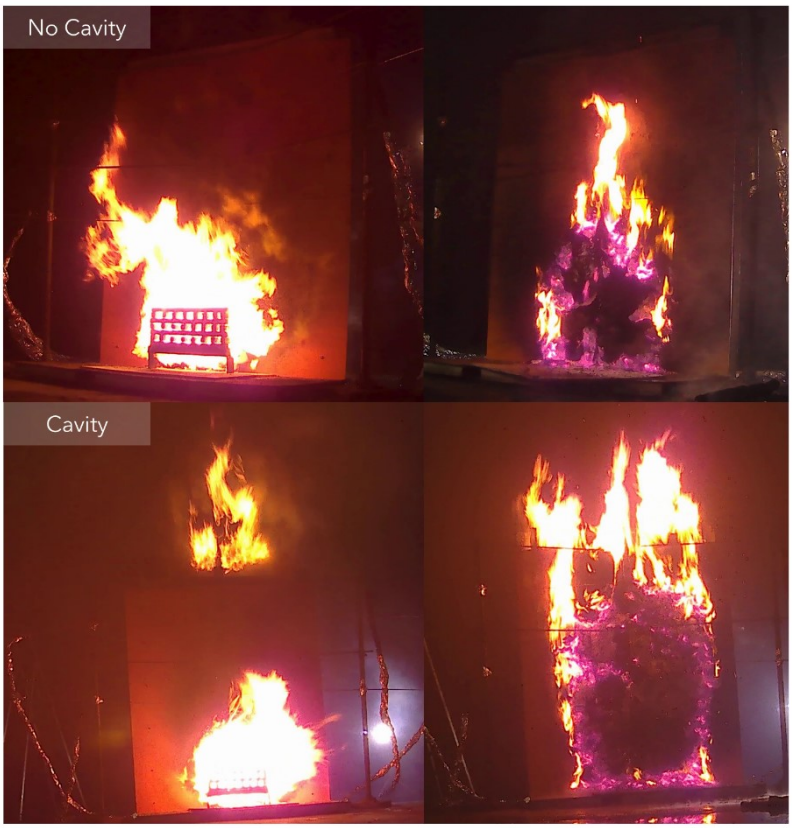

Figure 5.3 – Photos of two experiments with HPL (C) cladding and Phenolic Foam (C) insulation, with (below) and without (above) a cavity. The left column shows the facades at 12 minutes into the experiments with the wood crib still burning. The right column shows the facades at 18 minutes into the experiments, 3 minutes after the crib was removed.

The effect of insulation was more nuanced. Although the Phenolic Foam (C) could definitely be observed burning and contributing to the fire, the size of the fire for both HPL claddings when a cavity was present was not very different for the two insulation

materials. The main difference was that, because the Glass Wool (A2) melted away, most of the flaming occurred behind the cladding in this case, whereas the Phenolic Foam (C) seemed to keep some of its structure and so more flaming occurred above the facade (similar to the bottom right photo of Figure 5.3). Because of this, in the experiments with either of the HPL claddings, glass wool insulation, and a cavity, the cladding actually detached from the rest of the facade after the insulation melted away. This can be seen in Figure 5.4. This was not an issue in the case of the ACP PE (E) because it burned away so quickly that there was no cladding panel to detach. The phenolic foam also introduced an additional hazard of smouldering in the cavity in the case of the cement board cladding, as can be seen in Figure 5.2.

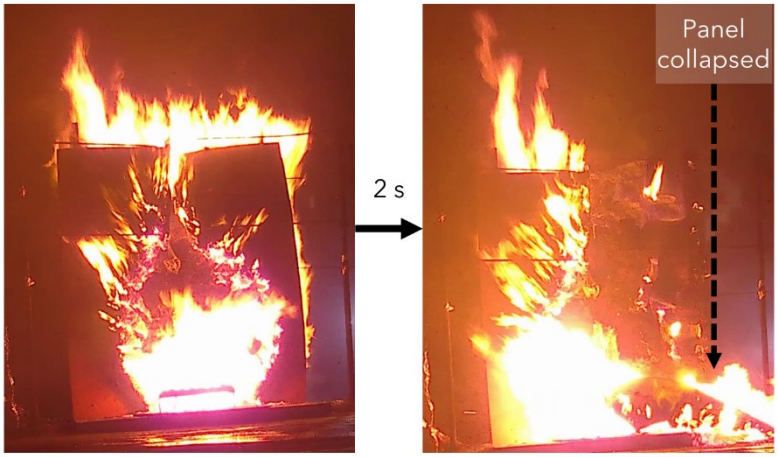

Figure 5.4 - Photos of an experiment with HPL (C) cladding, Glass Wool (A2) insulation, and a cavity before and after the right cladding panel detached and fell onto the crib.

The most complex effects came from the presence of a cavity between the insulation and the cladding. Figure 5.3 clearly demonstrates the dramatic difference in the size of the fire with and without a cavity. It was already mentioned that the cavity seemed to reduce the threshold of how much combustible material was needed to sustain a fire on the facade. In addition, flames appeared at the top of the cavity much faster than they spread on the surface. The flaming at the top of the facade in the bottom left photo of Figure 5.3 would occur before the crib was removed, long before the flames on the cladding surface reached the top of the facade. The reason for this may have been that the cavity was under-ventilated, and so the hot pyrolyzates would have had to reach the top of the cladding before igniting. This is supported by Figure 5.2, where the Phenolic Foam (C) is smouldering in the cavity, but flames only occur at the top of the cavity; smouldering combustion requires less oxygen, and so this suggests that the cavity was

under-ventilated. Flames also tended to appear from the gap between panels at the centre of the facade, as shown in Figure 5.5, supporting this under-ventilation hypothesis.

It is also worth noting that even in experiments without a cavity, sometimes the flame would ignite the cladding in a channel formed between the cladding and the masonry wall at the left and right of the facade. This channel was formed due to imperfections in the installation of the facade system, such that the insulation and cladding were not completely flush with the masonry wall, as shown in Figure 5.6.. In the experiments with HPL and no cavity, the flames from the wood crib ignited the insulation in this side channel and then would spread rapidly along this channel, perhaps in a manner related to the trench effect [130], by which flame spread along an inclined surface is increased when constrained in two directions.

In the two experiments where the cavity was located between the masonry wall and the insulation, rather than the insulation and the cavity, the facade behaved almost identically to the cases with no cavity.

Figure 5.5 - Photo of an experiment with ACP FR (B), Glass Wool (A2) insulation, and a cavity. Flames can be seen ejecting from the small gap between the two panels along the centreline of the facade.

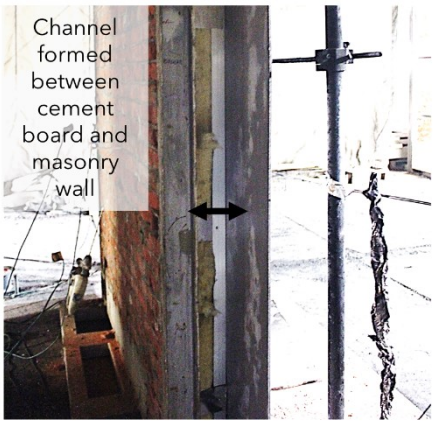

Figure 5.6 – Photo demonstrating the how a channel was formed between the cladding and the masonry wall, due to the insulation and cladding not being installed completely flush to each other.

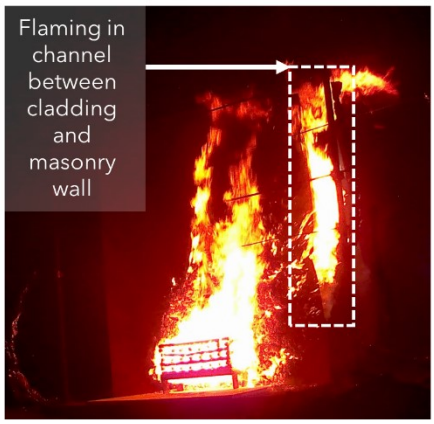

Figure 5.7 – Photo of an experiment with HPL (C), Phenolic Foam (C) insulation, and no cavity. Flames have rapidly spread along the channel between the cladding and the masonry wall formed by the insulation not being flush with the cladding.

5.3.2 Quantitative Analysis

Having discussed some of the effects from varying the cladding material, insulation material, and presence of a cavity I will now try and quantify some of these aspects. The first quantity of interest is the rate of fire spread on the surface of the facade. I have considered this separately to flaming in the cavity, which would be impossible to see, if there were any flames at all. To calculate the surface spread rate, I had to consider the flaming only after the wood crib was removed. This was because the cameras could not distinguish between flames from the wood crib and flames from the facade. This meant that I was unable to calculate surface spread rate for the Cement Board (A2) or ACP FR (B) facades, which did not support flames after the crib was removed, or for the ACP PE (E) facades, which had already burned completely before the crib was removed. I could also not calculate the spread rate for the experiments with HPL (C) cladding and Glass Wool (A2) insulation with a cavity, as the panel fell off before the wood crib was extinguished (see Figure 5.4).

Detecting flames on the facade was difficult when the fire was small, as the technique only tracked the largest area of connected flame. Therefore, the spread rate was calculated by assuming it was constant over as long a period of time as possible, using both graphs of the flame height detected by the thresholding algorithm (see Chapter 5) and my own judgement using the original video. This is illustrated in Figure 5.8. I

mainly used the trailing edge of the flame contours, as the flames would reach the top of the facade before the crib was removed (particularly for the HPL (D) cladding). I used a similar method to calculate the growth in flame area on the surface of the facade. For some of the facades this was 0, even if the vertical spread rate was positive. This meant that the flame was only spreading upwards on the facade, and not spreading horizontally.

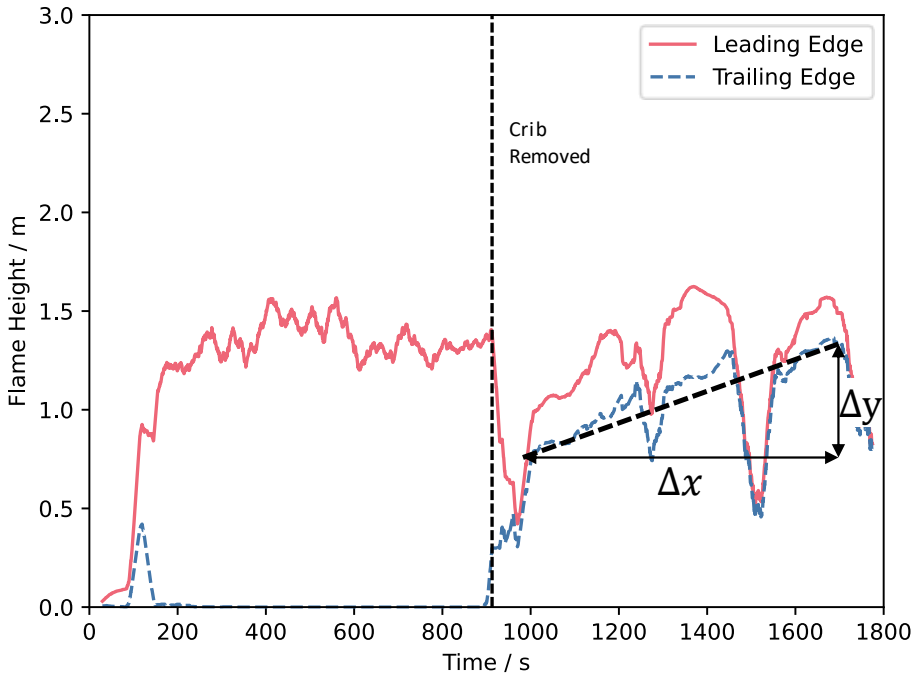

Figure 5.8 - Plot of flame height above the wood crib on the cladding surface with time for an experiment with HPL (C) cladding, Glass Wool (A2) insulation, and no cavity. The leading edge represents the highest point of the flame contour, and the trailing edge the lowest. I estimate the rate of flame spread by drawing a line manually over the data, based on whether the video supported a constant flame spread.

The calculated surface spread rates are shown in Figure 5.9 for tests with HPL cladding. In general, the more combustible HPL tended to have a faster vertical and area spread rate, with the exception of when there was a cavity and phenolic foam, where the spread rate was slightly smaller. The insulation material seems to have a more significant effect, with only the facades with phenolic foam insulation promoting spread horizontally across the surface of the facade (having an area spread rate > 0). Interestingly, in the case without a cavity the insulation does not seem to affect the vertical spread rate. The biggest effect comes from the cavity, which increases both the vertical and horizontal spread rate significantly.

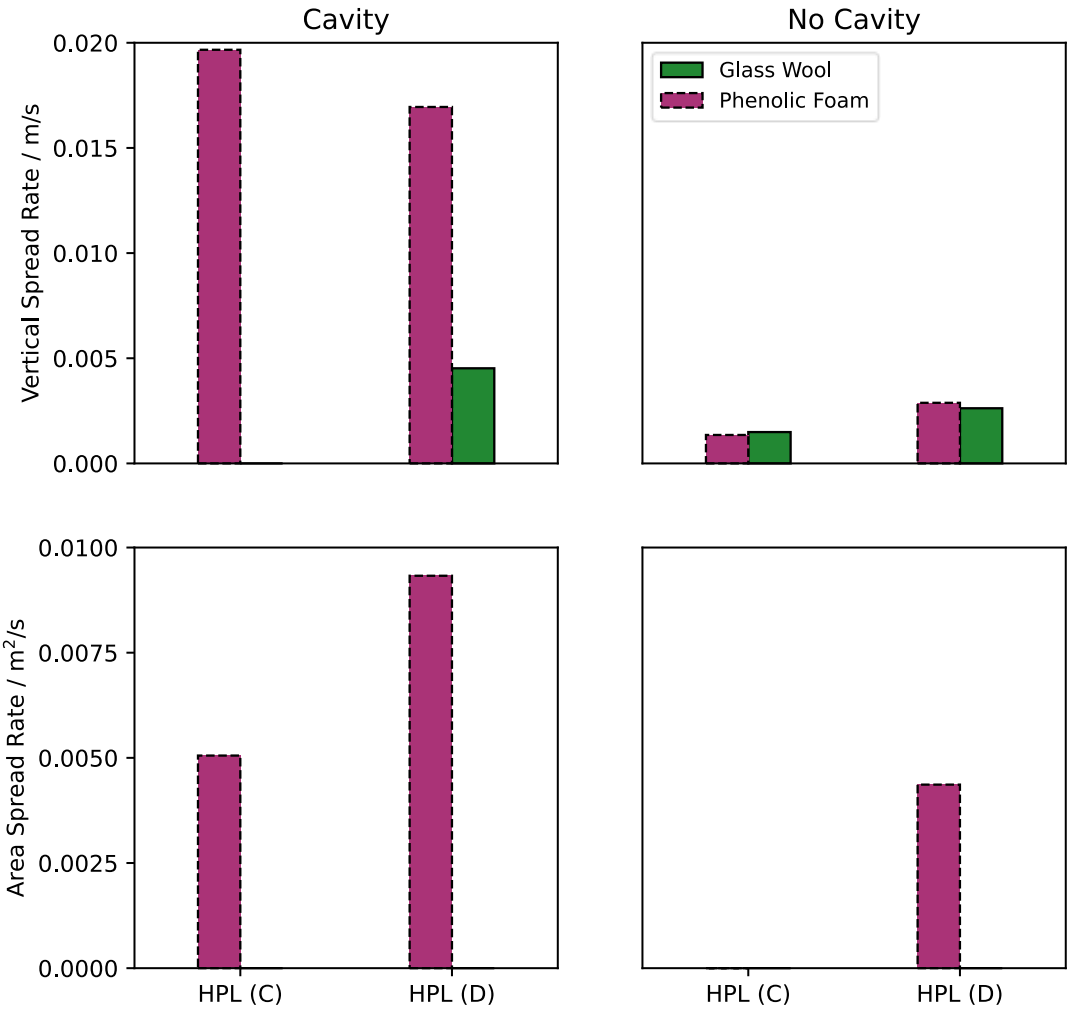

Figure 5.9 - Vertical and area flame spread rates on the surface of the cladding for different combinations of cladding material, insulation material, and cavity.

To analyse the flaming above the facade, coming from the cavity (as seen in the bottom left of Figure 5.3) camera thresholding was used to detect the time flames first appeared above the cavity (See Chapter 4), and the maximum area of flaming seen above the cavity (from the front of the facade). The time that flames first appeared above the cavity may have been dependent on the height of the cladding, as the cladding was sometimes taller than the cavity (as seen in Figure 5.1). To take account of this, the facade height was divided by the time that flames first appeared to get a "cavity flame speed". The variation of the cavity flame speed and maximum flame area with different cladding and insulation materials is shown in Figure 5.10.

The results show a trend of increasing speed for flames to start appearing at the top of the cavity with an increasing Euroclass rank of the cladding material, with the exception of the HPL (D) panels. The Euroclass rank of the insulation did not seem to

affect the speed at which flames started to appear. However, the maximum size of the flames above the cavity was highly dependent on the insulation material, which makes sense, as the more material there was to produce flammable gases in the cavity, the larger the area over which you would expect that gas to ignite. The trend of maximum flame area with cladding is not as clear, as many of the maximum flame areas are quite small. However, this is slightly misleading, as the HPL panels with Glass Wool (A2) collapsed before a large region of flame could be established, and the ACP PE (E) experiment was extinguished early before the flames above the cavity became too large.

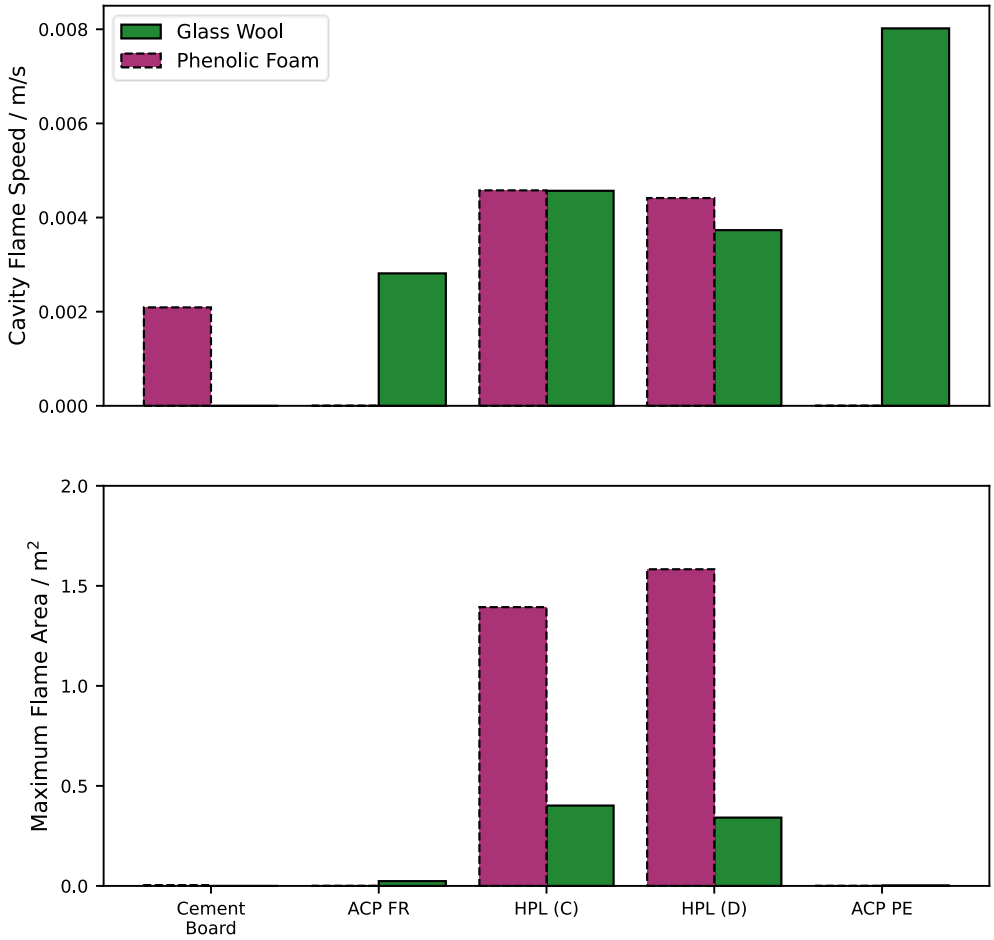

Figure 5.10 – Plots of the height of the cladding divided by the time for flame to appear (top), and the maximum area of flaming above the cavity (bottom) for different combinations of cladding and insulation material. ACP PE (E) has a misleadingly small maximum flame area, as the test was extinguished before they had a chance to grow.

The other quantities of interest were the temperature measurements on the surface and in the cavity, and the visual fire power measurements from the cameras. As in the analysis of KRESNIK in Chapter 3, the influence of the wood crib was accounted for in

this analysis. In Chapter 3 the excess temperature was calculated by subtracting a temperature-time curve fitted to experiments with the wood crib alone (see Figure 3.3). Here, a similar approach was taken to calculate an excess visual fire power, by fitting a simplified curve to the first experiment with a non-combustible facade containing Cement Board (A2) and Glass Wool (A2), meaning the heat release from flaming should have come from the wood crib alone. The growth phase was represented as a t^2 growth over the first 300 s of the fire, with the peak being the mean value over the next 600 s. After 900 s the crib was removed, giving an instantaneous decay phase. This curve was subtracted from the visual fire power measurements from each experiment, averaged over a 30 s window, to give excess visual fire power with time. Earlier, it was mentioned that the crib was sometimes removed slightly earlier or later than 900 s. To take this into account, the decay phase of this curve was located at the time the crib was removed for each test, rather than always at 900 s. The excess temperature was calculated in the same way as Chapter 3 (see Figure 3.3).

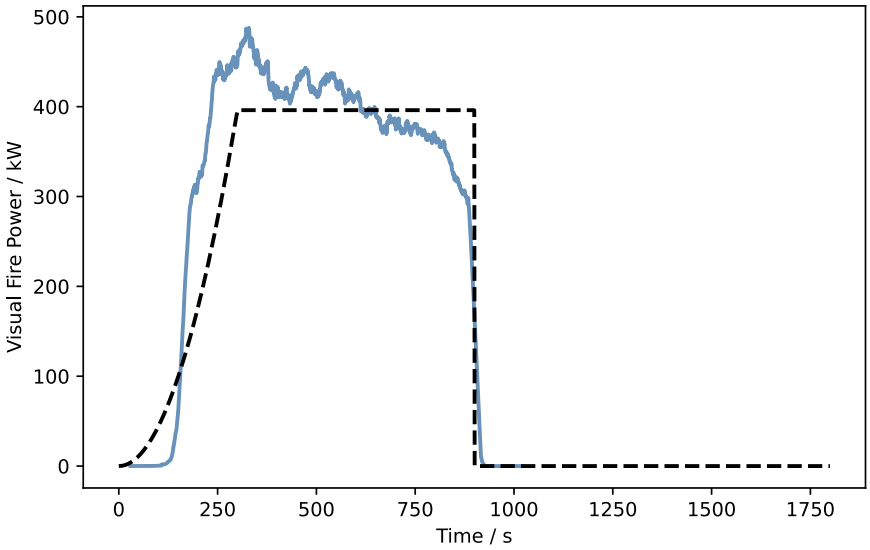

Figure 5.11 – Curve fitted to the visual fire power measurements from the experiment with cement board cladding, glass wool insulation, and a cavity. The curve represents the growth, peak, and decay of the fire.

To allow for comparison between different facades, the excess temperature vs. time and excess visual fire power vs. time curves for each experiment were collapsed into single values (or norms) that represented key characteristics of these curves. In particular, the peak values, and the mean values of these excess variables were studied. The peak values represent the worst case temperature condition on the facade, or the maximum fire size during the experiment. The mean excess values represent the

facade's average contribution to the temperature or heat released in the fire was over the entire experiment. The standard deviation around these mean values was also recorded, to show the degree of variation over the course of the experiment.

Peak and mean excess visual fire powers are plotted in Figure 5.12. The base case on which the curve in Figure 5.11 was based is marked in blue. The bars from this base case would indicate the variation in this test from the ideal fitted curve in Figure 5.11. From these plots there seems to be a large correlation between the combustibility of the cladding material and the peak and mean excess visual fire powers. The mean excess fire power for ACP PE (E) seems to break this trend, however this is likely because the flaming occurred entirely within the first 15 minutes of the test, before the crib was removed; because the effect of the wood crib is only subtracted within these first 15 minutes, claddings that burned outside this time would have higher excess values. The case of ACP PE (E) with a cavity was also extinguished before it grew to its full size. The visual fire power for ACP FR (B) may also have been slightly overestimated, as it was more reflective than the other claddings and this caused issues with detecting the flames clearly (see Chapter 4 for details).

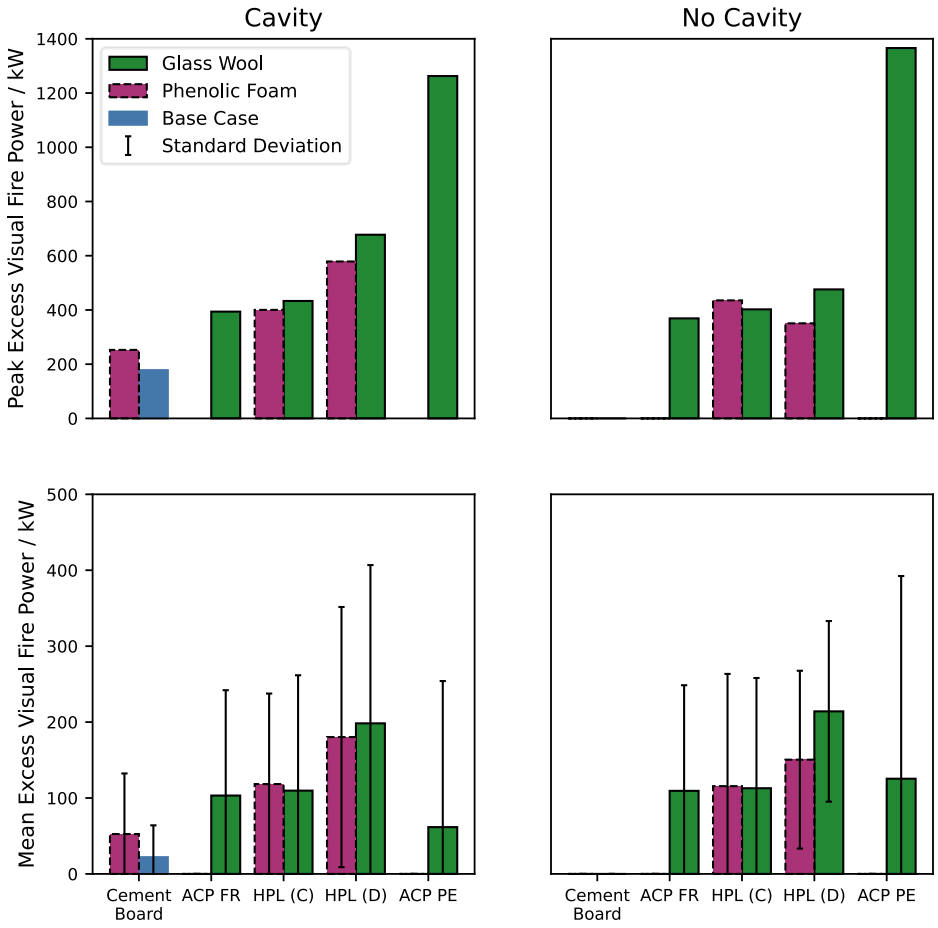

Figure 5.12 - Plots of peak and mean excess visual fire power, including the standard deviation around the mean during each experiment, for different combinations of cladding material, insulation material, and cavity.

Peak and mean temperatures on the surface of the facade are plotted in Figure 5.13. Peak excess temperature seemed to increase with cladding combustibility up to a point, but then level off. The ACP PE (E) did not follow this trend, though it is unclear why this was the case. In the case with a cavity, the experiment was extinguished early, meaning the fire may not have had a chance to grow to its full potential, but for the case without a cavity the facade was allowed to burn. Perhaps because the ACP PE (E) was consumed before the wood crib was extinguished, the excess temperature is lower even though the peak temperature was similar to the HPL (D) facade. The phenolic foam seemed to increase the peak and mean temperatures when there was a cavity present but have no determinable effect when no cavity was present. In general, temperatures when the facade had a cavity were higher. These trends were also similar for the temperatures in the cavity shown in Figure 5.14, however the cavity temperatures were generally lower. This is likely due to the cavity being under-ventilated.

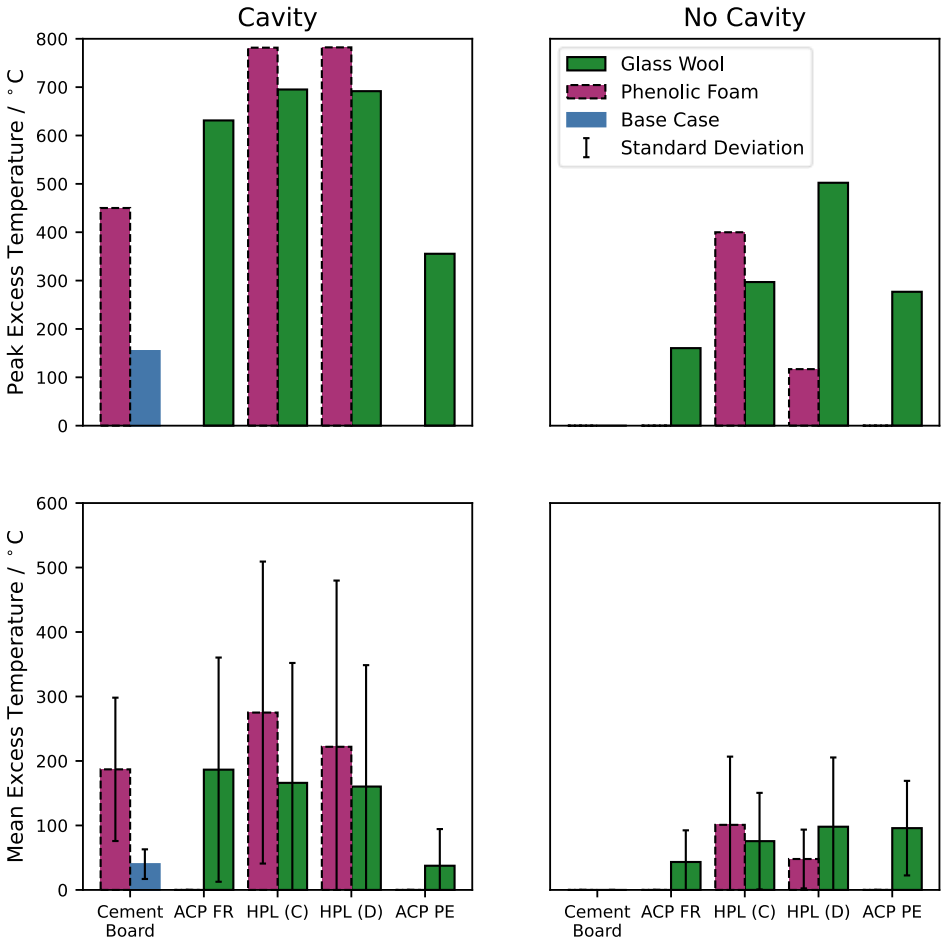

Figure 5.13 - Plots of peak and mean excess temperature across the thermocouples on the surface of the facade, including the standard deviation around the mean during each experiment, for different combinations of cladding material, insulation material, and cavity.

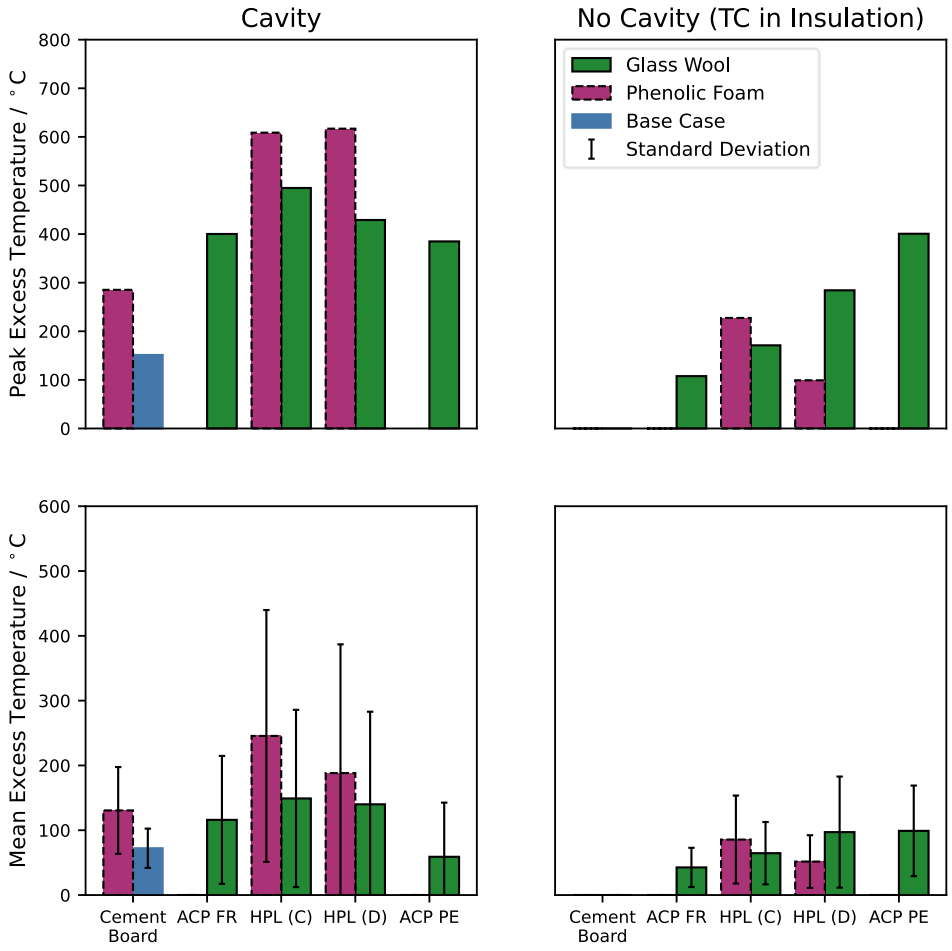

Figure 5.14 - Plots of peak and mean excess temperature across the thermocouples either in the ventilated cavity or in the insulation if no cavity was present, including the standard deviation around the mean during each experiment, for different combinations of cladding material, insulation material, and cavity.

To quantify the effect of each facade parameter more concretely, a series of simple linear regression models were fit to the measured output variables. For each output Y (for instance peak excess visual fire power) a model of the form:

$$Y = \beta_0 + \beta_1 x_1 + \beta_2 x_2 + \beta_3 x_3 \qquad 5.1$$

Was fit to the data, where x_1 was a value between 1 and 5, representing the Euroclass rank of the cladding (1 for rank A2, 5 for rank E); x_2 was either 1 or 3, representing the Euroclass rank of the insulation; and x_3 was either 0 or 1, representing whether or not a cavity was present. This kind of model assumes that these variables affect the output in a linear way, which may not be the case. However, using an assumption of linearity as a first approximation is a common way to also test whether

an independent variable has a monotonic relationship with each dependent variable (it always increases/decreases with an increase/decrease of that variable) [131]. The relative values of β_i in each fitted model would represent the size of the effect of that parameter on the size of the output Y. These are given for each output in Table 5.2, alongside the adjusted R^2 and p-values for each fit. The R^2 value is a value between 0 and 1 that represents how much of the variation in output is explained by the linear model, 0 meaning the model explains none of the variation and 1 meaning it explains 100% of the variation. The p-value comes from testing the null hypothesis:

$$\beta_1 = \beta_2 = \beta_3 = 0 \qquad 5.2$$

i.e., that the model is no better than random.

Table 5.2 – Size of the effects (β_i) of each parameter in the linear models, fitted to the different variables analysed in this section, alongside the R^2 and significance values of each model. A negative value of β_i means the effect reduced the size of that particular output variable. Cavity effects (β_3) labelled as N/A mean that the cavity was not included in estimating this output variable, because those variables only apply for facades with a cavity.

Output Variable	β_1 (cladding)	β_2 (insulation)	β_3 (cavity)	R^2	p-value
Vertical Flame Spread Rate	-1.7×10^{-3}	2.6×10^{-3}	11.3×10^{-3}	0.72	0.025
Flame Area Spread Rate	1.9×10^{-3}	2.2×10^{-3}	2.8×10^{-3}	0.62	0.052
Cavity Flame Speed	10.4×10^{-4}	-0.4×10^{-4}	N/A	0.44	0.073
Maximum Flame Area Above Cavity	0.28	0.54	N/A	0.62	0.023
Peak Excess Visual Fire Power	218	−85	98	0.61	0.006
Mean Excess Visual Fire Power	22	6	−19	0.18	0.189
Peak Excess Temperature on Surface	54	43	306	0.31	0.086

Mean Excess Temperature on Surface	4	32	82	0.33	0.074
Peak Excess Temperature in Cavity	71	78	N/A	0.47	0.088
Mean Excess Temperature in Cavity	8	42	N/A	0.33	0.161

This table demonstrates that for different variables, different aspects of the facade are more important. The presence of a cavity has a dramatic effect on the vertical flame spread rate (5 times more pronounced than that of the insulation), but not so much on the horizontal spread rate on the surface of the facade. Comparing this with Chapter 3, it also shows that precise knowledge of the materials did not help to explain much more of the variation in peak excess temperature than before, suggesting that either a simple model is inappropriate, or that the natural variation in these kinds of experiments will be inherently large. Interestingly, the Euroclass rank of the cladding had a negative correlation with vertical flame spread, which contradicts the results expected from Chapter 3. However, this may be due to the limited sample of only the experiments with HPL cladding, due to the limited ability to measure spread rate while the wood crib was still burning. The general message to take away from this table is that different parameters are important for predicting different variables, and a lot of variation is still left unexplained by a simple linear addition of these parameters. This supports the argument that the fire behaviour of a facade is more than a simple sum of the behaviour of its individual components.

After completing this work, I was made aware of a series of intermediate-scale experiments performed at the University of Queensland in 2018 [132], [133]. These experiments varied the cladding and insulation materials of a system with fixed cavity width (considering 2 types of ACP and 3 types of insulation) and looked at fire behaviour within the cavity plus overall heat release rate. The work found that the type of insulation used had a large impact on performance in the case of the less flammable ACP, but not in the case of the more flammable panels. This suggests that if the missing experiments here with ACP PE (E), ACP FR (B) and Phenolic Foam (C) were to be performed then there would be little difference from the glass wool case for the ACP PE (E) but may be a large difference in the case of the ACP FR (B). For instance, it may not self-extinguish.

5.4 Conclusions

This chapter shows the results from 20 experiments, covering 16 out of 22 combinations in a parametric series of experiments varying the cladding and insulation material of rainscreen facades, and whether or not they had a cavity. This represents the largest series of intermediate scale facade experiments in the fire safety literature to date.

It was found that each of the 3 varied parameters had impacts of different aspects of the fire behaviour of the facade. The Euroclass rank of the cladding seemed most important in determining the overall size of the fire, while the Euroclass rank of the insulation affected the fire in different ways depending on whether there was or wasn't a cavity. The non-combustible glass wool also melted away quickly and provided less support to combustible cladding panels. The most dramatic changes seemed to come from the addition of a cavity, which made the fire scenarios generally worse, particularly with regard to the speed of vertical and horizontal flame spread, both in and outside of the cavity itself. The effect of the cavity of vertical flame spread was 5 times more pronounced than that of the insulation. However, temperatures in the cavity were still lower than on the surface, perhaps due to the cavity being under-ventilated.

In future work, it would be useful to complete the missing entries in the parametric series, particularly the combination of ACP FR and phenolic foam with a cavity, as this case lies between the self-extinguishing ACP FR and glass wool, and the self-sustaining HPL (C) and glass wool.

Overall, these experiments demonstrate the impact of using materials of different Euroclass rank in ventilated facades. They demonstrate the complexity of this fire scenario, and that the final performance is not simply a linear sum of the components. These results are the first of the size on an intermediate-scale and can provide fire safety engineers with useful information when helping to design fire safe facades in tall buildings.

Chapter 6

KRESNIK II – Comparing Data Across Different International Facade Fire Test Standards

Summary[7]

This thesis has so far only considered facades tested according to the Polish national facade test standard, PN-B-02867. This is only one of many international facade test standards, each of which vary in the heat release rate and geometry of the fire the facade is exposed to, the size of the facade tested, and the criteria used to assess whether a facade passed or failed. This chapter presents an updated version of the database in Chapter 3 containing an additional 168 tests from 3 different international test standards, named KRESNIK II for distinction. This database was used to evaluate a novel method for comparing the results of facades tested using different standards, by creating dimensionless forms of the peak temperature and flame heights that accounted for the heat release rate and geometry of the fire source of each standard. This method was inspired by correlations for predicting the temperatures and flame height of the buoyant convective plumes produced by pool fires. This method was found to be unable to remove the differences in flame height and peak temperature measurements for identical facades across the different standards, such that the standards did not even agree on how to rank facades consistently, suggesting that these standards may not give a consistent measure of flammability. Although differences in behaviour between standards could not be accounted for by using dimensionless parameters, the flame height and peak temperature measurements of a facade in different tests could be successfully predicted by using a neural network trained on the data in KRESNIK II. This demonstrates the power of using a top-down approach to learn from facade test data as a complement to traditional fire research.

[7] This chapter is based on a paper in progress: M. Bonner, W. Wegrzynski, B.K. Papis, and G. Rein, KRESNIK: Comparing the Performance of Similar Facades Across Different International Fire Test Standards. (to be submitted)

6.1 Introduction

Chapters 3 and 5 discussed tests and experiments based on the Polish national facade test standard PN-B-02867. While these tests and experiments were informative, the results may have been somewhat biased as this is not the only facade fire standard in use around the world. In fact, there are at least another 13 test standards across almost the same number of countries [29], [30]. These tests vary in the type and amount of fuel used to simulate a fire, as well as the size and geometry of the facade tested, and each measure different criteria to determine whether a facade has passed or failed a test; criteria such as vertical and horizontal flame spread, temperature at different locations, debris from the facade, or even continued smouldering after the test has finished. Although these standards may be different, each of these standards explicitly measures the maximum vertical flame spread during the test, and the other failure criteria relate in some way to aspects of facade flammability. Passing these tests almost always allows a particular facade system to be used on a real building, and some countries allow a choice between which test standard to use to qualify that a facade is safe. Underlying these decisions is an assumption that the flammability of a facade will remain relatively consistent under these different test standards, at least to the degree that a facade will still be safe to be used on a building.

This chapter discusses an updated version of the original KRESNIK database, referred to as KRESNIK II for distinction. In Chapter 3, KRESNIK contained 252 tests from Instytut Techniki Budowlanej (ITB), each performed according to the PN-B-02867 standard. KRESNIK II has been updated to include another 122 tests performed using the NFPA 285 standard [134] (used by Arup to verify the EFFECT tool [65]), 26 tests using the BS 8414 standard [11], [12] (taken from public reports and research papers), and the 20 experiments discussed in Chapter 5. This means that KRESNIK II contains 420 tests across 3 different test standards. These standards will be discussed in detail, but a summary of their different conditions and failure criteria are shown in Table 6.1 and Table 6.2.

Table 6.1 - Basic summary of the 3 test standards in KRESNIK II

Standard	Country	Fire Source	Geometry (width x height)	Wind Condition

PN-B-02867	Poland	20 kg wood crib directly against facade	Flat wall (2.0 x 2.3 m)	2 m/s
NFPA 285	USA	Gas burner inside combustion chamber + gas burner against facade	Flat Wall (4.1 x 5.3 m) against 2 storey compartments with ground floor window	None
BS 8414	UK	400 kg wood crib inside combustion chamber	Corner configuration with main wall (2.6 x 8.0 m) and side wall (1.5 x 8.0 m)	None

Table 6.2 - Comparison of the different measurements considered in the failure criteria of the 3 test standards in KRESNIK II

Failure Criteria	**PN-B-02867**	**NFPA 285**	**BS 8414**
Peak temperature at different locations	Yes	Yes	Yes
Vertical flame spread	Yes	Yes	Yes
Horizontal flame spread	No	Yes	Yes
Continued burning after test ends	Yes	No	No
Debris fallen from facade	Yes	No	No

These standards each have a different fire source, facade geometry, and failure criteria. This makes it challenging to aggregate and compare data across different tests in the same way as Chapter 3. However, it presents a unique opportunity to use the data in KRESNIK II to compare the differences in the standards themselves. Each of the 3 standards considers measurements of the peak temperature at particular locations and the vertical flame spread on the facade in their failure criteria. In this chapter, we present a methodology to remove the influence of the fire source of each test standard *when there is no facade present* from these measurements. Any remaining variation in the measurements should then be due only to differences in the facade systems being tested, or the natural variation of the individual tests themselves.

If this methodology were successful, it would be an invaluable tool for fire engineers and fire research. It costs at least 10 times more to perform a single BS 8414 test than a single PN-B-02867 test. If the performance in this smaller test could be compared to the performance in the large test, then it would allow more facade configurations to be tested and greater innovation in facade design. Being able to directly compare between the test standards would also make the conclusions from the kind of top-down analysis in Chapter 3 to be generalised across a wider range of countries. Ideally, these test standards could be compared directly by testing identical facades according to each one, similar to the parametric tests in Chapter 5, but performing so many large-scale tests would be incredibly expensive. The research in this chapter presents an alternative. If this methodology allows comparison between the different standards, then the benefits would be significant. If it cannot allow facades to be compared, it brings into question the underlying hypothesis of these tests: that there is a characteristic of the fire performance of each individual facade system that is independent of the standard it is tested to.

6.2 Methodology

6.2.1 Description of each test standard

I will begin by discussing each of the 3 standards in detail. The test setup for PN-B-02867 is shown in Fig. 1. A 2.0 x 2.3 m mock-up of a facade is attached onto a 2.0 x 2.5 m masonry wall in a way reminiscent of its end use on a building. A 20 kg wood crib of dimensions 0.6 x 0.46 x 0.3 m is then placed 50 mm from the front of the facade, ignited, and left to burn for 15 min with a 2 m/s wind blowing towards the front of the facade. After 15 min, the crib is removed, and the facade is observed for another 15 min. The standard measures vertical flame spread, temperature at fixed locations, and any debris or flaming droplets that fall from the facade. This test standard is repeated 3 times, and a facade passes the standard only if each of these repeats pass.

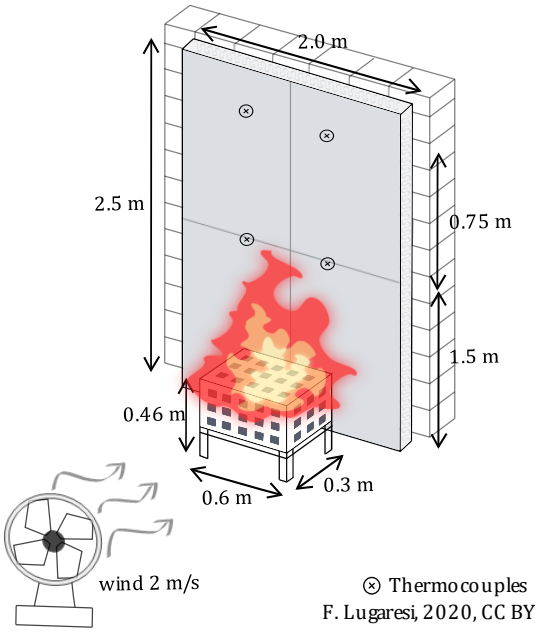

Figure 6.1 – Illustration of the test setup specified in the PN-B-02867 standard. The scenario is supposed to represent a fire from an object igniting next to a building, such as a car or bin fire.

The test setup for NFPA 285 is shown in Fig. 2. A two-storey, 4.8 m tall structure is built of compartments 3.05 x 3.05 x 2.13 m dimensions. A mock-up of a facade is constructed directly onto the test apparatus or attached to a 5.69 m movable metal frame that is then mounted onto the test apparatus. A 1.98 x 0.76 m “window” is made in the facade and test apparatus. Two gas burners are used during the test, one located inside the ground floor compartment, and one located at the top edge of the window. The flow rate of these burners is determined by a calibration procedure defined in the standard. The test lasts for 30 min, with the burners increasing in intensity every 5 min. After 30 min the burners are extinguished, and the facade is observed for an additional 10 min. The standard measures vertical and horizontal flame spread, temperature at fixed locations on the facade, and also temperatures within the second storey room.

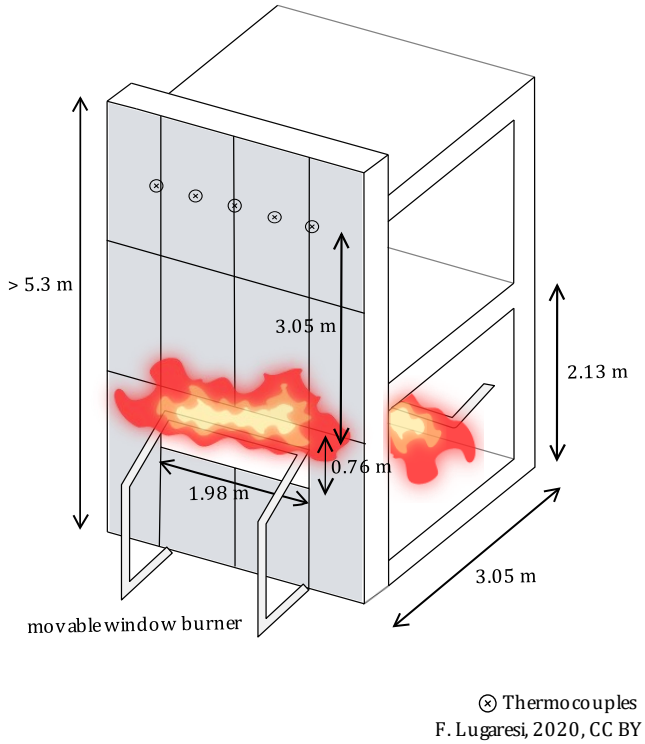

Figure 6.2 – Illustration of the test setup specified in the NFPA 285 standard. This scenario is supposed to represent flames ejecting from a window during a fully developed compartment fire.

The test setup for BS 8414 is shown in Fig. 3. A mock-up of a facade is constructed onto an 8 m high masonry wall, or steel frame structure depending on whether the BS 8414-1 or BS 8414-2 standard is used. The structure consists of a 2.6 m wide main wall and a 1.5 m wing wall, which together form a corner. A 2.0 x 2.0 x 1.0 m burn chamber is located at the bottom of the main wall. During the test, a 400 kg wood crib designed to output a peak heat release rate (HRR) of 3 MW is ignited and left to burn for 30 min. After 30 min, the wood crib is extinguished and the facade is then observed for another 30 min, or until it fails the standard. Failure in the standard is based on vertical and horizontal flame spread, or the temperature recorded at fixed locations, however, the report also records whether debris or flaming droplets fall from the facade during the test.

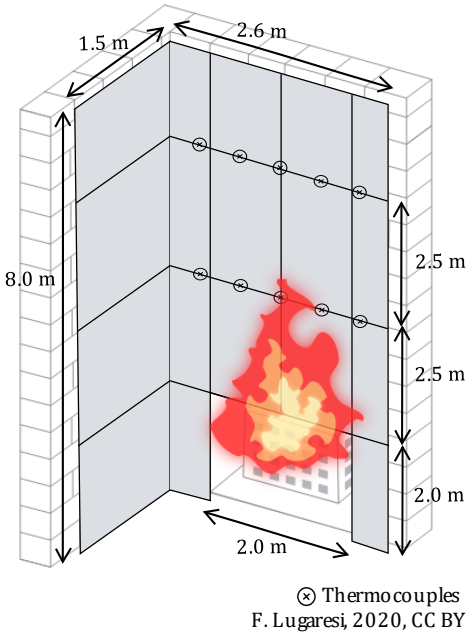

Figure 6.3 – Illustration of the test setup specified in the BS 8414 standard. This scenario is supposed to represent flames ejecting from a window during a fully developed compartment fire.

6.2.2 Removing the influence of each fire source

As mentioned in Table 6.2, each of the different standards in KRESNIK II measures the temperature at different locations and the vertical flame spread on the facade. To remove the influence of the different fire sources from these measurements, it is necessary to account for both the geometry and heat release rate of the fire source. This is not dissimilar to previous research done to find correlations for the flame height and plume temperatures above different pool fires [135]. In that study and others, the goal was to find how the temperatures at different locations in the buoyant plume and the height of the flame varied with different fuel types, pool shapes, and heat release rates. In general, studies have found that the temperature and flame height above an axisymmetric buoyant flame are proportional to a dimensionless heat release rate Q^* according to the following equations:

$$Q^* = \frac{\dot{Q}}{\rho_\infty c_p T_\infty g^{1/2} D^{5/2}} \tag{6.1}$$

$$\frac{\Delta T}{T_\infty} \propto \left(\frac{z}{Q^{*2/3}}\right)^\beta \tag{6.2}$$

$$\frac{L}{D} \propto Q^{*n} \qquad 6.3$$

where $\dot{Q}$ is the convective heat release rate of the fire, $\rho_\infty, c_p, T_\infty$ are the density, specific heat capacity, and temperature of the ambient atmosphere, g is the acceleration due to gravity, D is the diameter of the circular fire source, ΔT is the change in temperature above ambient, L is the flame height, and β and n are constants.

These correlations refer to circular pool fires in quiescent conditions, whereas the PN-B-02867 standard's fire source is a rectangular wood crib with a wind condition, and the NFPA 285 and BS 8414 standards fire sources are flames ejecting from a compartment (often referred to as externally venting flames or EVFs). Fortunately, work has been done to extend these correlations to other fire conditions. Work by Yokoi [136] tried to find similar correlations for externally venting flames by comparing the results of experiments to a buoyant plume from an equivalent circular fire source, related to the size of the window the flames were ejected from. These original correlations were with respect to a changing gas density with height. They were extended in [137] to relate to a fixed ambient density; this time by relating the correlations to a rectangular heat source located at the mid-height of the window. Work by Heskestad [138] also extended buoyant plume theory to conditions beyond liquid pool fires, including wood cribs. This suggests correlations could also be used for the PN-B-02867 standard. Unfortunately, no papers could be found that measured these correlations for a wood crib in wind. However, Ren et al [139] did extend the work of [136], [137] and investigate the effect of wind on the temperature profiles of externally venting flames, finding that a wind condition reduced the centreline plume temperatures by a factor dependent on wind speed.

Unfortunately, these correlations cannot be easily applied to the test standards in KRESNIK II. There are no correlations for the temperature profile or flame height above a wood crib when a 2 m/s wind condition is applied. The correlations for externally vented flames are based on the heat release rate at the window, however only the peak heat release rate within the compartment is given in the NFPA 285 and BS 8414 standards – not accounting for heat losses from other walls. The NFPA 285 standard also includes an additional burner at the top edge of the window that diverges from previously studied conditions. Therefore, a more empirical approach was taken.

In Chapter 3 the influence of the wood crib on the temperature measurements in the PN-B-02867 standard was reduced by taking an excess temperature based on fitting a curve to the temperature measurements from 3 experiments performed with only the wood crib against a masonry wall. The peak temperature from this fitted curve at 2.3 m was about 61℃ (see Figure 3.3). This is the same as the minimum peak temperature measured across all the PN-B-02867 tests in KRESNIK II. By following this logic, the peak temperature of the fire source (independent of the influence of the facade) for the other two standards was estimated to be the minimum peak temperature measured across all the tests in KRESNIK II performed according to that standard. These values were 271℃ for the NFPA 285 standard, and 325℃ for the BS 8414 standard. I will refer to these minimum peak temperatures across all the data from a particular standard as the standard's fire source temperature T_s.

In buoyant plume analysis, the plume temperatures are often analysed using the *excess temperature* above ambient conditions. This is defined as:

$$\theta_{\infty}^{*} = \frac{T(z) - T_{\infty}}{T_f - T_{\infty}} \qquad 6.4$$

Where T_f is the flame temperature. This is a dimensionless quantity, represented by the asterisk. This quantity represents the temperature rise above ambient conditions as a proportion of the maximum possible temperature rise and can have values between 0 and 1. Using the source temperatures, it is possible to define a similar dimensionless quantity for the excess temperature above the source:

$$\theta_{s}^{*} = \frac{T_p - T_s}{T_f - T_s} \qquad 6.5$$

Where T_p is the peak temperature measured in a test. Between different standards, both T_s and T_p would be a function of height, however, in this analysis the value of these quantities was fixed, as the temperatures recorded in these test reports were recorded at a fixed height defined by the failure criteria of the standard. This equation is the value we will use to investigate the peak temperatures of the tests independent of the influence of the different fire sources. T_f has had different values in different experiments. In [135] T_f is given as 800℃, while in [140] T_f is given as 1000℃. As the

excess temperature above ambient is usually a proportion of the maximum possible temperature rise, T_f was taken as the maximum temperature measured across all tests of a particular standard. This means that this method is equivalent to normalising the peak temperature data from each standard to fit between 0 and 1 using the minimum and maximum values for that standard, a common practice in statistics and machine learning.

Applying the same logic to the flame height, it is possible to scale the maximum flame heights measured in the tests by the heat release rate and diameter of the source. Equation 6.3 shows that these would be proportional to the flame height of the source. Therefore, in a similar way to scaling the peak temperature measured in the tests T_p by the peak temperature of the fire source alone T_s, it is possible to scale the maximum flame height measured in the tests L by the maximum flame height of the fire source alone, referred to as L_s. A different approach was taken to estimate L_s for each test standard. The BS 8414 standard was referenced as having a source flame height of 2.5 m in [31]. We contacted an engineer at the Thomas Bell-Wright testing lab in UAE to ask what the source flame height was in the NFPA 285 standard, and were told that it was 1300 $\pm$ 50 mm. Finally, for the PN-B-02867 standard we used the average flame height between 300 and 600 seconds in the standard, taken using the same thresholding techniques explained in Chapter 4. This gave us a value for L_s of 1.23 m.

Using these values, an *excess flame height* can be defined as follows:

$$\Delta L^* = \frac{L - L_s}{D_s} = \frac{L}{D_s} - \frac{L_s}{D_s} = \frac{L}{D_s} - \gamma {Q_s^*}^n \qquad 6.6$$

Where D_s is the characteristic length of the fire source and γ is an arbitrary constant. The equation has been written in different ways to explicitly show the relationship to the heat release rate of the source, derived from Equation 6.3. Note that the value of the maximum flame height L was estimated in different ways based on the information recorded in each standard. In the NFPA 285 and BS 8414 standards, the maximum flame height is recorded in the test report based on observations by an engineer during the test. In the PN-B-02867 standard, observations are only made about whether the flame height reached above 1.5 or 2.25 m. Therefore, L was estimated from the damage done to the facade based on pictures taken before and after each test. In some tests, no

visible damage was done to the facade, so the flame height was recorded as 0, even though there would have been a flame from the source during the test. Therefore, for some of the tests in KRESNIK II the maximum flame height measured in the test L was less than the maximum flame height of the source L_s. This would give a negative value of ΔL^*. These negative values intuitively do not make sense when comparing to the observations made during the test in the NFPA 285 and BS 8414 standards. For this reason, all negative values of ΔL^* were set to 0.

The characteristic length of each fire source also varies depending on the standard. For rectangular sources, the characteristic length is the longer axis. For the externally venting flames in the NFPA 285 and BS 8414 standards, the concept of a rectangular source at the mid-height of the window was taken from [137]. This paper defined the characteristic length of this source as:

$$D_s = \left(WH^{3/2}\right)^{2/5} \tag{6.7}$$

Where W is the width of the window the flames are spilling from and H is the height of the window. The different values used in the non-dimensionalisation of these measurements are given in Table 6.3.

Table 6.3 – Summary of values used in the non-dimensionalisation of the peak temperature and flame height measurements in KRESNIK II. T_s is the ambient temperature of each fire source, estimated by the minimum peak temperature measured across each standard. T_f is the flame temperature, estimated by the maximum peak temperature measured across each standard. L_s is an estimate of the peak flame height reached by the fire source alone in each standard. D_s is the characteristic length of the fire source in each standard.

Standard	T_s	T_f	L_s	D_s
PN-B-02867	61℃	790℃	1.23 m	0.60 m
NFPA 285	271℃	760℃	1.30 m	1.12 m
BS 8414	325℃	939℃	2.50 m	2.00 m

Chapter 3 introduced a flammability index $i = \{1,2,3,4\}$ to measure the performance of the facades in each test, which was based on observations made by an engineer during the test. The choice of which observations to record was based on the specific

observations recorded by technicians during the PN-B-02867 test standard, and so this same index cannot be used for the other 2 standards in KRESNIK II. However, the ranks of the flammability index above 2 are related only to the maximum flame height seen on the surface of the facade. Therefore, it is possible to convert the flame height measurements taken from the before and after images into a new flammability index, to allow for comparison with Chapter 3. This index would be 4 for flame heights greater than 2.25 m, 3 for flame heights greater than 1.5 m, and 1 otherwise. However, this new flammability index will not perfectly align with the old one, partly because it does not have a rank 2 index, and partly because the new values of flame height have been estimated from the pictures of the facade before and after the test, rather than from observations taken by a technician. This presents a source of uncertainty in these estimated flame heights, however 75% of the PN-B-02867 tests in KRESNIK II measured the same result in both flammability indexes, and 89% of the tests differed by 1 or less. This suggests that the analysis of flame height and excess flame height in this chapter can be compared with the analysis of the flammability index in Chapter 3.

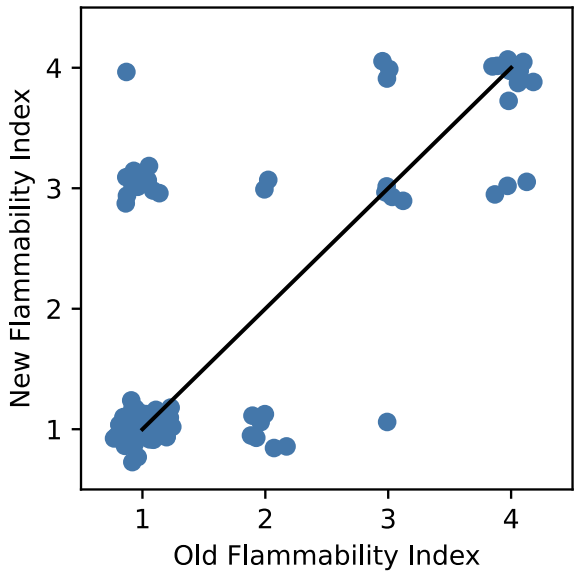

Figure 6.4 – Plot comparing the flammability index used in Chapter 3, based on the failure criteria of the PN-B-02867 standard, with a new flammability index, based on the maximum flame height in the test, estimated from images of the facade damage after the test. Individual points have been shifted randomly within the range ±0.1 to make the number of points visible.

6.3 Results and Discussion

Figure 6.5 shows the frequency distributions of both the dimensional outputs T_p and L, and the non-dimensional outputs θ_s^* and ΔL^* taken from all the tests in KRESNIK II. In the case of the repeated tests of identical facades in the PN-B-02867 standard, the mean value across the repeats was taken. For the dimensional outputs, the distributions from the different standards are generally distinct, with the exception of the flame heights measured in the PN-B-02867 and NFPA 285 standards. In particular, the BS 8414 distribution tends to have a higher frequency of tests with both large peak temperatures (> 500℃) and large flame heights (> 3 m). This is to be expected, as the fire source and scale of the test is much larger than for the other 2 standards. By non-dimensionalising the outputs and removing the influence of the source, we would expect to bring the distributions much closer together.

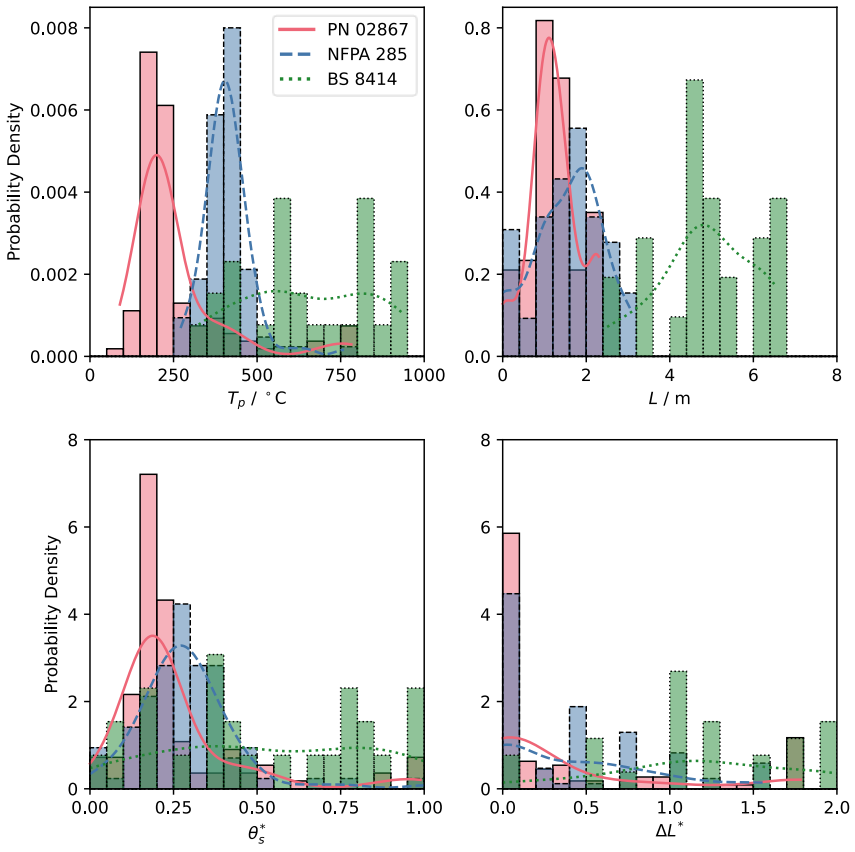

Figure 6.5 - Frequency distributions of T_p, θ_s^*, L, and ΔL^* for all the facades in KRESNIK II. If our methodology was successful, then the distributions of the dimensionless variables should be much more similar than the distributions for the dimensional variables. Remaining variation may be due to differences in the types of facades tested by each standard, or due to fundamental differences in facade behaviour between tests.

This seems to be the case in the bottom row of plots in Figure 6.5. The BS 8414 distribution overlaps much more with the other distributions in both θ_s^* and ΔL^*. However, the overlap between the NFPA 285 and PN-B-02867 distributions is still not perfect, and the shape of the BS 8414 distribution is still quite different to both of them. This could be for a few reasons. Firstly, the size of the BS 8414 population (the number of facades tested) is about a quarter of the size of the populations of the other standards. Most statistical distributions only take shape with a large number of observations. This is because a smaller sample size may not include a wide range of different facades. In other words, if the types of facades in the populations of each standard were different to each other, then the output distributions would also look different. Secondly, the BS 8414 tests come from a different kind of source to the other standards. The NFPA 285 and PN-B-02867 test data came from commercial test houses, meaning most of the facades being tested were intended to pass these standards. In contrast to this, the BS 8414 tests came from a mixture of publicly available tests. Some were commercial tests performed by Kingspan [141], some were tests performed by DCLG in the wake of the Grenfell tower fire [142], and some came from research papers [73], [143]. This suggests that the facades in the BS 8414 population may be skewed towards facades that would be more likely to fail the test, which may explain why there is a greater frequency of higher values for each output.

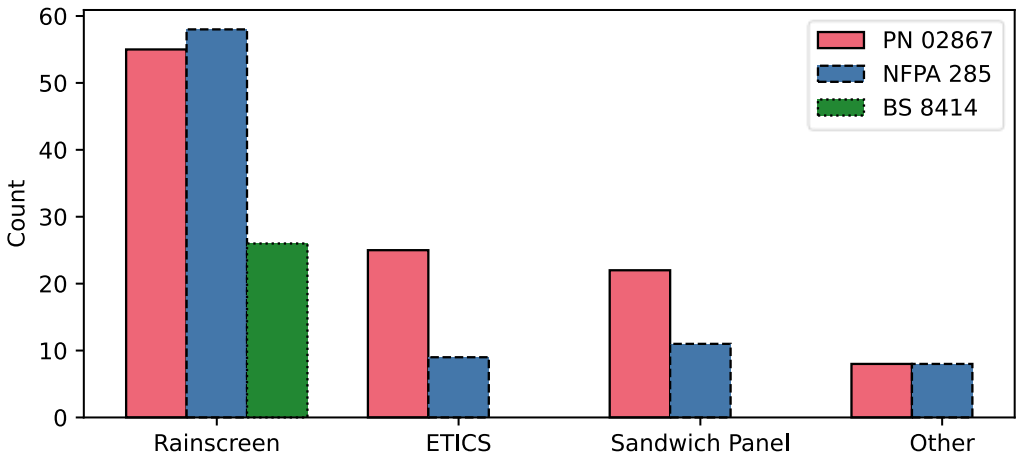

Figure 6.6 - Frequency distributions of the different types of facades in KRESNIK II, separated by test standard.

Figure 6.6 supports the idea that the populations of facades from each standard are quite different. The BS 8414 population only contains rainscreen facades, which seem to

generally perform worse in these tests based on the analysis in Chapter 3 and Chapter 4. The NFPA 285 and PN-B-02867 populations seem to be quite similar, though the PN-B-02867 population contains a higher proportion of ETICS and sandwich panel facades. Figure 6.7 goes into further detail, showing the frequency distribution of the materials used in the cladding and insulation of the rainscreen facades in each population. It is clear from these plots that the materials used in the facades in each population are quite different. The BS 8414 population seems to have a much higher proportion of combustible insulation materials, which are likely to change the outputs of the test. Similarly, the most common cladding material in the PN-B-02867 population is HPL, which doesn't appear in the rainscreen facades tested to the other 2 standards. This suggests that the remaining differences in the frequency distributions of the dimensionless outputs in Figure 6.5 could be due to differences in the facades tested, rather than differences from the test standards themselves.

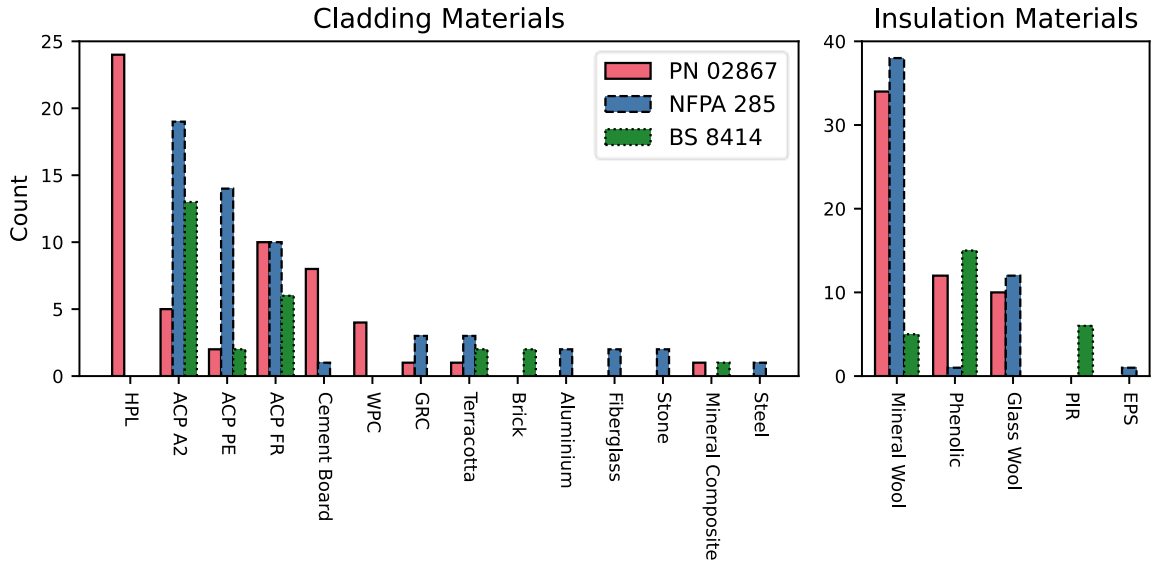

Figure 6.7 - Frequency distributions of the different types of cladding and insulation materials used in the rainscreen facades in KRESNIK II, separated by test standard

To confirm whether the differences in Figure 6.5 were due to differences in the facades being tested or due to differences in the standards themselves, the results from tests involving rainscreen facades with identical cladding and insulation materials were compared across the different standards. The results are shown in Figure 6.8 and Figure 6.9. These plots show comparisons of temperature and flame height measured for rainscreen facades with identical cladding and insulation materials across the different

test standards. If 2 standards agreed then the datapoints in Figures 8 and 9 would fall on, or close to, the 45° line. Of course, there will also be natural variation in output within identical tests. This variation was estimated by taking the average difference between the maximum and minimum values for a particular output across identical tests within the same standard. This is represented by the shaded area on the plots.

These figures seem to show that there is no agreement between the different test standards, even after we tried to take into account the influence of the source. Not only do the datapoints not fall close to the 45° line, but the standards do not even agree on the rank order of which facades performed worse. If the ranks did agree, then the datapoints would increase monotonically (they would never decrease). A parallel can be drawn here with the work of Emmons on evaluating test standards for material combustibility [144]. This paper showed that materials ranked in combustibility by different labs and standards across the world showed no better agreement than random data. The paper led to a review of the combustibility test standards at the time. More research should be done to assess whether there is a similar disagreement in ranking facade flammability from current facade test standards. The analysis here suggests there may be.

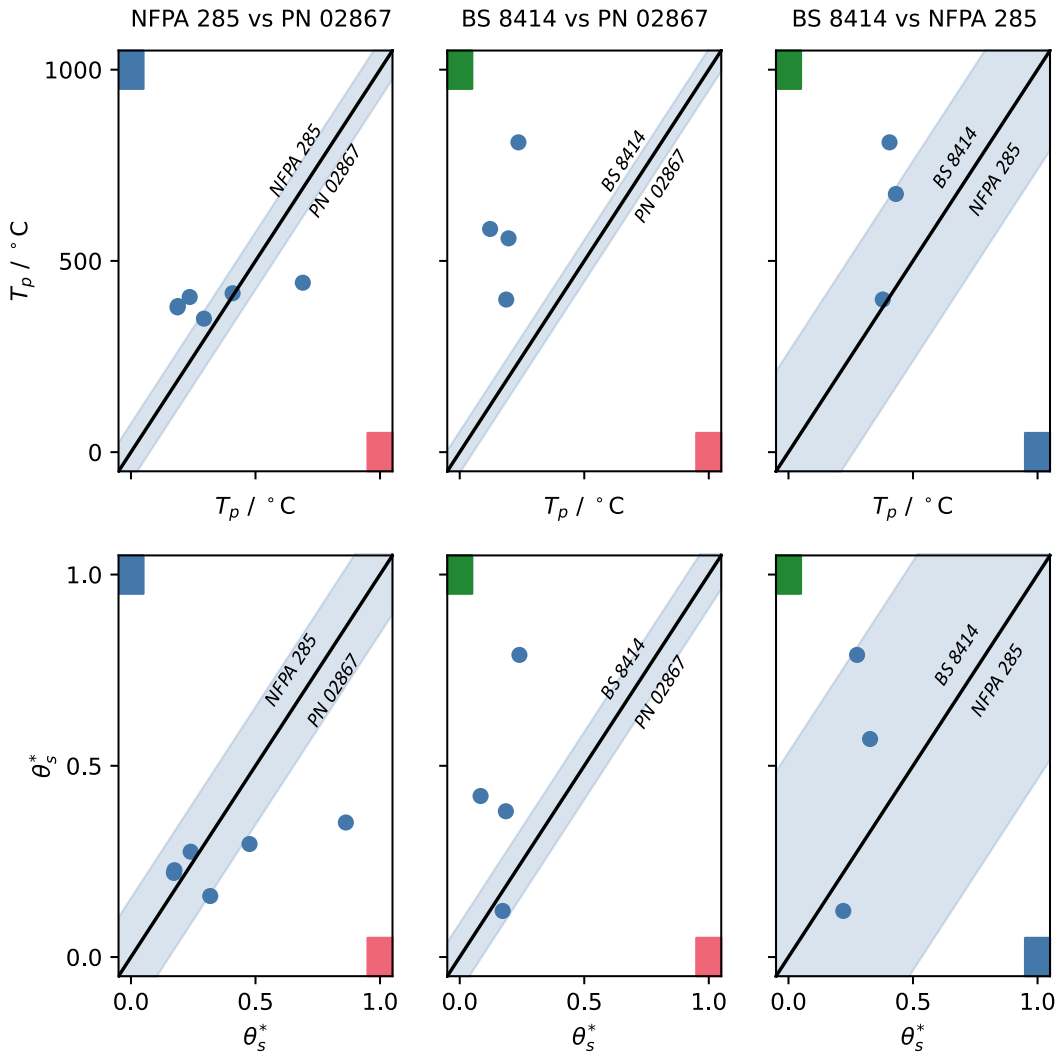

Figure 6.8 - Plots comparing the measurements of T_p and θ_s^* for tests of rainscreen facades with identical cladding and insulation materials across different test standards. Some facades appeared more than once in the same standard; in which case the point was taken as the mean value across these tests. The shaded area is the difference between the max and min values measured for identical facades within the same test standard. If 2 standards agree, then the points should fall on the 45° black line.

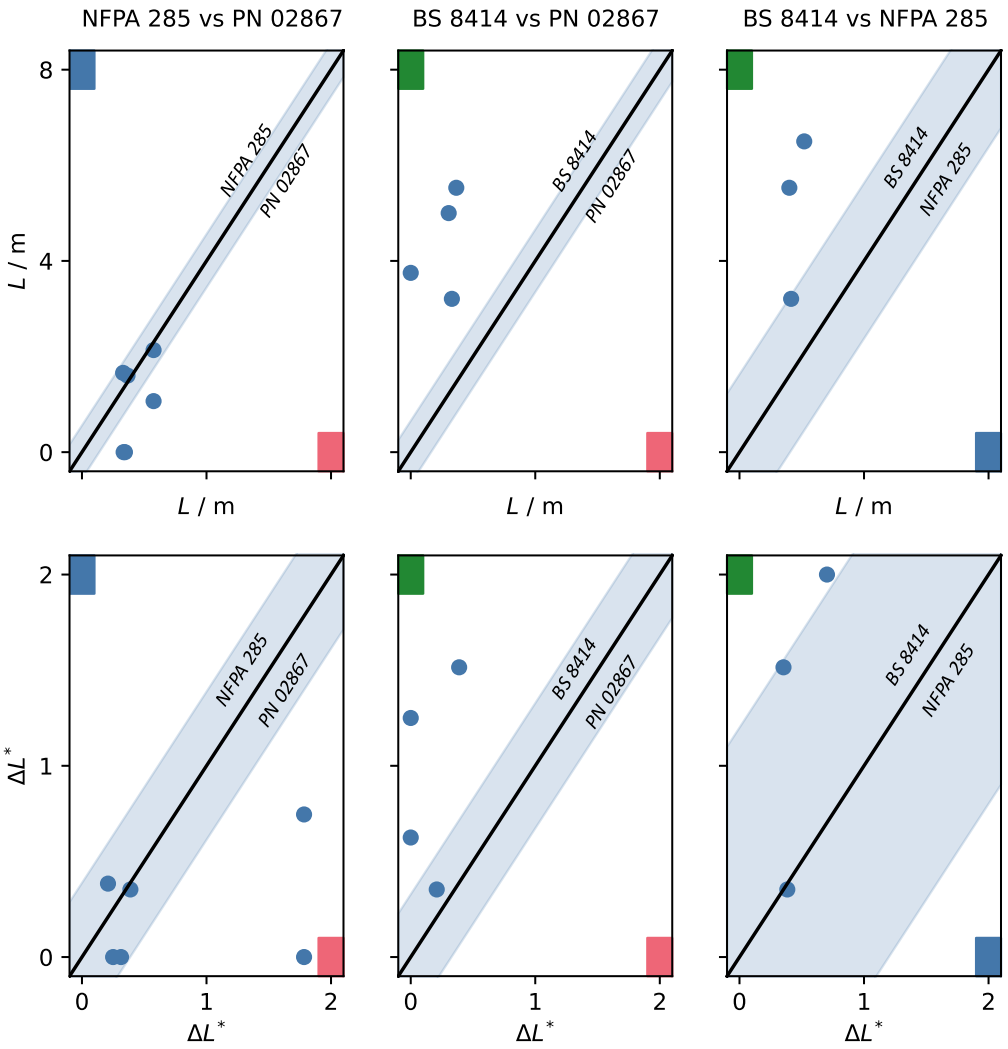

Figure 6.9 - Plots comparing the measurements of L and ΔL^* for tests of rainscreen facades with identical cladding and insulation materials across different test standards. Some facades appeared more than once in the same standard; in which case the point was taken as the mean value across these tests. The shaded area is the difference between the max and min values measured for identical facades within the same test standard. If 2 standards agree, then the points should fall on the 45° black line.

These results suggest that our method to remove the influence of the source did not succeed. Rainscreen facades with identical materials behaved very differently across the different standards. Some of these discrepancies may be due to the variation in commercial products of a particular type – not all fire retardant ACP will be equally fire retardant. However, the discrepancies are large enough that this seems unlikely to be the only reason. There are differences between these standards that cannot seem to be

captured using simple correlations. However, it may be possible to take into account the different behaviour between standards in another way.

6.4 Machine Learning

To test whether the output of the tests in KRESNIK II could be predicted using machine learning, a simple neural network was created – a kind of statistical model, inspired by the neurons within the human brain, that takes in large amounts of data and tries to predict non-linear relationships between input and output variables within that data. Machine learning and artificial intelligence (AI) have proved to be useful in a wide variety of situations, and have been used before in fire science to detect fire and smoke in images [114], [145]–[147] , aid wildfire modelling [148], [149], predict pyrolysis behaviour [150], predict compartment fire behaviour [88], [151], and assist with structural fire modelling [86], [87], [152]. Most relevant to this work, machine learning was applied to a database of 59 facade fire incidents to predict the severity of those incidents [153].

All of these papers used *supervised machine learning* to achieve their goals, in contrast to *unsupervised machine learning*. Supervised machine learning tries find a relationship between a collection of *features* and a series of *labels* (essentially inputs and outputs of the model). The features of a machine learning model are usually stored in an N x M matrix $\boldsymbol{X}$, where the M columns are different features, and the N rows are individual observations. These are related to an N x K matrix of labels for each observation, usually referred to as $\boldsymbol{Y}$. The role of a machine learning model is to find a function f such that:

$$f(\boldsymbol{X}) \approx \boldsymbol{Y} \tag{6.8}$$

Supervised machine learning models try to find the form of this function empirically, by fitting the model to a large subset of a dataset (referred to as *training* data), then seeing how well it compares to a separate subset of the same original dataset (referred to as *validation* data). Splitting the data like this is an attempt to maximise a model's ability to correctly predict a set of separate but related data, like it might be given in the future, rather than getting the best fit on a single dataset. Fitting very well to the training data but being unable to fit to validation data is known as *overfitting*.

Most algorithms for machine learning improve dramatically with increased data. This makes sense given that the functions they are fitting are often complex and non-linear, and so gaps between datapoints may miss crucial information on the required shape of the fit. These models also learn entirely by example, and so they cannot extrapolate to data that is dissimilar to the data they were originally trained on. This makes the size of the training dataset very important [154]. Although the size of KRESNIK II is relatively small compared to traditional AI datasets, which have thousands or even millions of datapoints, in previous fire safety literature the sample sizes have often been small. The dataset in [153] contained 59 entries, and the dataset in [88] contained only 14 entries. The 420 tests in KRESNIK II therefore represent the state of the art dataset for machine learning in facade fire safety.

To demonstrate the potential of using KRESNIK II for machine learning, a basic neural network was fit to the data, without any fine tuning. Neural networks are just one type of machine learning model, but they have proven to be a very powerful, and have been used in countless applications of AI. They can be represented abstractly by a series of nodes (or neurons) connected in a network. Each node represents an *activation function* that will change the change the number fed into the node based on a threshold value, referred to as its *bias*. The connections between each node contain *weights* that multiply the output of the previous node. The activation functions are specified in advance, along with the number of nodes and connection; these are referred to as the *hyperparameters* of the model. The weights and biases meanwhile are optimised to fit the data used to train the network; these are referred to as the *parameters* of the model. To achieve this optimisation, a *cost function* is specified that represents how far away the function $f(\boldsymbol{X})$ was from matching $\boldsymbol{Y}$. This cost function is then minimised. More detailed explanations of neural networks can be found in many books, including [155].

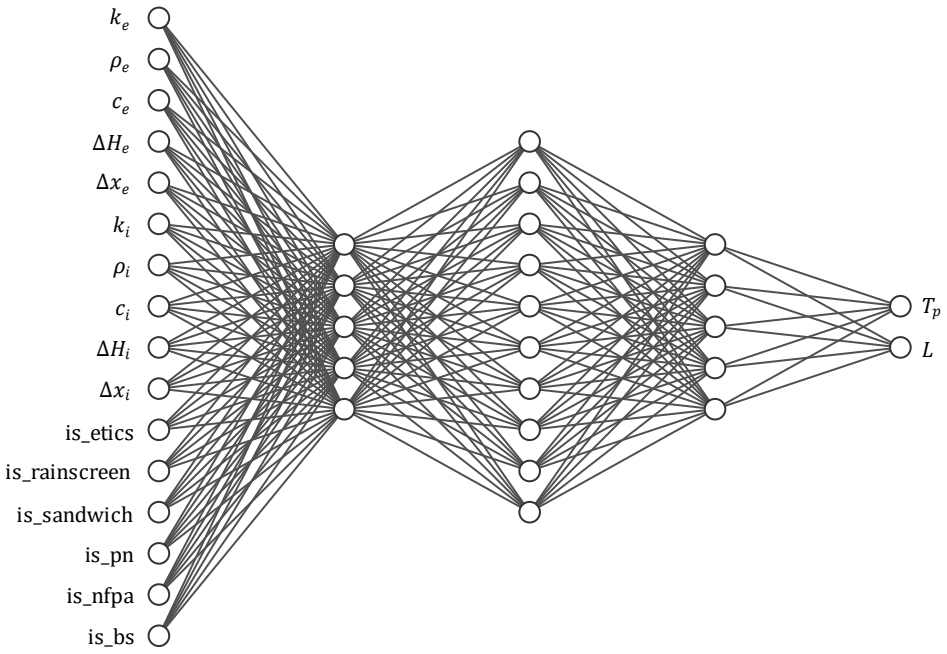

Figure 6.10 - Architecture of the sequential neural network fit to the KRESNIK II data, which we refer to as e-KRESNIK. Each circle represents a node with a ReLu (Rectified Linear Unit) activation function and a bias. Each connection has an associated weight. The network is sequential in that there are no loops to earlier nodes in the network, and dense in that the nodes in each layer are fully connected. Explanations of the inputs are given in Table 6.4.

The architecture of the neural network used here is given in Figure 6.10. It is a sequential neural network, with 16 inputs, 3 dense hidden layers, and 2 outputs. The inputs are given in Table 6.4. The network is sequential because there are no loops linking nodes from the right side of the network back to an earlier node in the network. Each node used an activation function called a *ReLu* function or *Rectified Linear Unit*. This is a very popular activation function in neural networks because it simplifies a lot of the maths used to optimise the network and speeds up training. The choice of this architecture was based on simplicity, and no work was done to tune the hyperparameters of this model. This exercise is purely to show the potential of using this sort of model with the data in KRESNIK II.

Table 6.4 – Explanation of the 16 inputs used in the neural network specified by Figure 6.10. If material properties were not available for a specific test (e.g., for tests where the cladding was labelled as simply ACP FR, not a specific composition) then the average value of the property for that generic material was used. Flammability depends on the external fire conditions, as well as the facade itself. These external conditions are taken into account in the variables defining the test method used (is_pn, is_nfpa, is_bs).

Input	Explanation
k_e	Thermal conductivity of external layer (either cladding, render, or external layer of a sandwich panel) in W/mK
ρ_e	Density of external layer in kg/m^3
c_e	Specific Heat of external layer in J/kgK
ΔH_e	Heat of Combustion of external layer in kJ/g
Δx_e	Thickness of external layer in mm
k_i	Thermal conductivity of insulation layer
ρ_i	Density of insulation layer
c_i	Specific heat of insulation layer
ΔH_i	Heat of Combustion of insulation layer
Δx_i	Thickness of insulation layer
is_etics	1 if ETICS facade, 0 otherwise
is_rainscreen	1 if rainscreen facade, 0 otherwise
is_sandwich	1 if sandwich panel facade, 0 otherwise
is_pn	1 if tested according to PN-B-02867, 0 otherwise
is_nfpa	1 if tested according to NFPA 285, 0 otherwise
is_bs	1 if tested according to BS 8414, 0 otherwise

The data was processed to create a matrix of the features listed in Table 6.4. After averaging the repeats from the PN-B-02867 test standard and removing the tests that had missing material data, we were left with 171 facades (88 of which were averaged from multiple tests). 10% of this data was put aside as *hold-out* data to test the

generalisability of the model after it had been trained and validated. This left us with a training set of 154 facades and a hold-out set of 17 facades. The network was trained using *mean absolute error* as a cost function and using the Adam gradient descent optimiser. K-fold cross validation was used instead of splitting the training data into a training and validation set, which gives a less biased estimate of model performance on smaller datasets [156]. Each of the inputs and outputs were also scaled to fall between 0 and 1 before being used to train the network. This is common practice in machine learning to improve model accuracy. This was implemented in Python using the Keras, Tensorflow, and Scikit-learn libraries [157]–[159].

The results of using the trained network on the hold-out data are shown in Figure 6.11. These plots show the predicted performance of the 17 facades in the hold-out dataset against their actual performance in the tests (due to shuffling the data, I do not know at this point which test method these facades were tested with). The distance from the 45° line represents the accuracy of the predicted results. The gray shaded area is the mean absolute error predicted from the cross-validation of the model. Most of the facades also fall within this range for both output variables. In total 85% of the data across the 2 outputs falls within this range. This suggests that although it was not possible to compare facade performance across tests using simple plume correlations, by using more complex, non-linear models with a lot of data, it is still possible to predict the performance of different facades across multiple test standards.

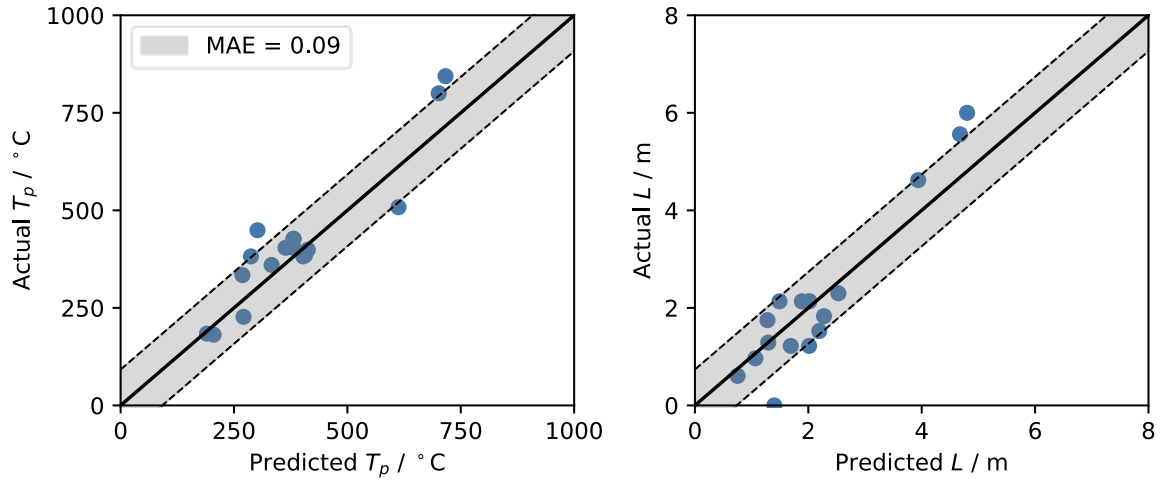

Figure 6.11 – Results of using the neural network in Figure 6.10, e-KRESNIK, trained on 154 facades, to predict the performance of the hold-out set of 17 facades. The mean absolute error (MAE) estimated through k-fold cross validation is given by the gray shaded area.

6.5 Conclusions

In this chapter, a methodology was developed to compare the results from 3 different facade fire test standards: PN-B-02867, NFPA 285, and BS 8414. Each standard used a fire source with a different heat release rate and geometry, which was accounted for using correlations developed for convective plumes above pool fires. 2 dimensionless parameters were defined, the peak excess temperature above the fire source $\Delta\theta_s^*$ and the excess flame height ΔL^*, defined in Equations 6.5 and 6.6, which scaled the outputs of the different standards by the size and diameter of their fire sources. It was hoped these dimensionless parameters would provide a way to translate results across the different standards, which would be an invaluable tool for fire safety engineering.

These new parameters were applied to the data in the updated KRESNIK II database, which now contained 384 different facade tests across the 3 standards. It was found that the frequency distributions of the peak temperatures and flame heights measured by the different standards were brought closer together by considering their dimensionless equivalents, which suggested that our methodology may have been successful. However, when considering tests of facades with the same materials performed across multiple standards, not only was there still a disparity in the measurements of each output between standards, but the standards did not even agree on the rank of each facade across each output. This suggests that different standards are not consistent in their assessments of facade safety, and that there is still no way to easily compare the results between them using fundamental knowledge of fire behaviour.

The final section of this chapter presented an alternative approach to predicting the behaviour of facades across different standards. By training a neural network on the data in KRESNIK II, considering the test standard used as an input to the model, it was possible to predict the test performance of the majority of facades in a set of hold-out data, without any fine-tuning of the model. This could be used to translate between standards by passing identical inputs to e-KRESNIK but changing only the test standard being considered. Unfortunately, these kinds of machine learning models can only be used to predict facades and test standards that are similar to those that were used to train the model, which is why this approach is only complementary to more traditional, bottom-up fire research. However, this chapter demonstrates the potential of such models, which could prove to be invaluable to designing safe facades in the future.

Chapter 7

Conclusions

This thesis is the first to study the possibilities of a top-down approach to facade fire safety, and the power of converting commercial facade tests into experiments – using them to develop our understanding of fire, rather than only show compliance with national laws.

Chapter 2 presented a literature review of previous research into facade fires. It explained how facade design is a multi-objective problem, with trade-offs having to be made between different objectives such as moisture control, facade thickness, and flammability. The end of the chapter discussed the value of *optimum design*, where different design objectives are explicitly quantified, allowing an engineer to understand whether a particular design is truly optimal in different objectives. Although previous work had been done to quantify the flammability of sandwich panels used in external walls [47], the previous research into facade fires was sparse and was insufficient to explicitly quantify the flammability of a facade using fundamental, bottom-up science. The research in this thesis therefore tried to take a complementary, top-down approach.

Chapter 3 demonstrated this top-down approach by creating and analysing a unique database, named KRESNIK, of 252 commercial facade fire tests performed according to the PN-B-02867 test standard. This chapter showed the advantages of converting the semi-structured data of the written reports produced by these tests into a fully structured relational database. By collapsing the complex data in these reports into single values of peak excess temperature, residence time, and flammability index, it was possible to identify trends in the data. Only facades with a cavity and some kind of combustible cladding promoted flame spread above 1.5 m or sustained burning of the facade these tests; however, this was not true for all facades of this kind. It was also the case that neither facade system level variable investigated (fuel load and U-Value) could predict its behaviour in the tests, with fuel load only explaining about 10% of the variation in output.

One of the limitations of the analysis in Chapter 3 was the limited measurements taken during the tests that related to facade flammability. Chapter 4 presented a novel methodology for using ordinary camera footage to estimate the rate of heat released by visible flaming from a turbulent fire, referred to as *visual fire power*, by estimating the volume of that fire. The methodology was compared to synthetic data in Blender as well as calibrated against experiments with a gas burner. This method could be used to improve the quality of data taken from standard facade tests, which are often filmed already, and was also used in the analysis of the experiments presented in Chapter 5.

The trends identified in Chapter 3 were examined further in Chapter 5 through a series of 20 parametric experiments on rainscreen facades, varying the Euroclass rank of the cladding and insulation materials used in these facades and whether or not the facade had a cavity. The choice to investigate these particular parameters was inspired in large part by the analysis done in Chapter 3, and demonstrated the potential of using top-down, system-level analysis on smaller sets of more detailed data. The experiments were performed in a similar way to the PN-B-02867 standard, used to test the facades in the data in Chapter 3. However, these experiments included additional temperature measurements on the surface and in the cavity, as well as recording the test using 4 cameras at different angles. These experiments found that varying each parameter had a different impact on the fire, and that looking at them individually could not explain the facade behaviour. However, the presence of a cavity did appear to dramatically increase the speed of flame spread. This work also demonstrated the possibility of measuring important parameters of a fire, such as the rate of flame spread and the visual fire power, from regular video footage. This could make the data recorded by standard fire tests more valuable, and almost all of these tests are already required to be filmed.

Chapter 6 examined how the kind of top-down analysis performed in Chapter 3, containing data only from the PN-B-02867 test standard, could be extended to compare the results between other international test standards. It included an updated version of the original KRESNIK database, named KRESNIK II, that contained a total of 384 tests across 3 different international test standards: PN-B-02867, NFPA 285, and BS 8414. Each of these standards expose facades to fire sources with different heat release rates and geometries, but they each measure the peak temperature at a point on the facade and the maximum flame height observed during a test. The chapter presented a potential method to remove the influence of the different fire sources in each standard

from these peak temperatures and flame heights by producing non-dimensional parameters of excess temperature and flame height above that of the fire source alone. Looking at tests involving facades with identical materials, it was found that similar facades performed significantly differently under the different standards in terms of both peak temperature and flame height (which are both connected to a facade's flammability), even after non-dimensionalising. The standards did not even agree on the flammability rank of each facade, suggesting that these standards may not be consistent in assessing what constitutes safe facade behaviour. However, it was possible to predict the performance of different facades across different standards using a neural network trained on the data in KRESNIK II. A predictive model similar to this network, referred to as e-KRESNIK, could be used to translate the results of a test across different standards, or as a way to quantify the performance of different facade designs prior to testing – which was mentioned in Chapter 2 as being crucial for optimum design. This is an example of artificial intelligence being used to aid problems when a fundamental understanding of the problem is incomplete.

The work in these chapters could be built upon in a number of ways. Most of the data in KRESNIK is publicly unavailable and had to be filled in by hand from written test reports. Identifying methods from natural language processing that could be used to automate this process, and finding ways to ensure commercial data security, are important steps for this kind of analysis to be used more broadly. The visual fire power methodology introduced in Chapter 4 should also go through further calibration across fires at different scales and a study of its sensitivity to different camera parameters, to allow it to be used more broadly as a tool for estimating heat release rates of turbulent fires. Chapter 6 also showed the difficulty of comparing the results of facades tested using different standards. Performing these different standards on truly identical facades would be an important step towards being able to make this comparison.

Taken as a whole, this thesis demonstrates the potential to transform standard facade fire tests into a source of scientific knowledge that could be used to take a top-down approach to understanding facade flammability. By combining the variables that relate to flammability into a single variable and then correlating this variable to different aspects of a facade design, it could be possible for engineers and designers to quantify and rank the flammability of different facade systems. The neural network presented in Chapter 6, e-KRESNIK, demonstrates that this approach can be used to predict two variables related to facade flammability, and by adopting new

measurements into standard tests, such as the *visual fire power* presented in Chapter 4, additional variables could be measured that more closely relate to facade flammability. Thousands of facade fire tests are performed internationally each year, the equivalent of millions of pounds of research. e-KRESNIK was trained on approximately 350 tests and predicted approximately 85% of the hold-out data correctly. These models improve dramatically with more data [154], meaning the potential of collecting these commercial fire test results is huge.

One application of such a model would be to help quantify facade behaviour in fire to aid the process of fire-safe facade design. In Chapter 2 we mentioned that explicitly quantifying different design objectives could allow an engineer to apply a process of optimum design. Figure 2.7 showed a hypothetical plot comparing different facades according to 2 objectives – a flammability index and the thermal transmittance, or U-value of the facade. The left image in Figure 7.1 shows a similar plot for the facades in KRESNIK II, with the maximum flame height L measured for a facade plotted against its U-value. The right image in Figure 7.1 shows a similar plot for randomly generated facades passed through the neural network from Chapter 5. Because the properties of these facades have been randomly generated, it may be that the facades cannot exist. However, this plot demonstrates that by using a machine learning model that can quantify the flammability of a facade, it would be possible to search the solution space of possible facades for potentially better solutions than what has been used previously. In the case of the right image in Figure 7.1, the new Pareto front has moved closer to the origin and therefore contains solutions that are more optimal than the Pareto front for the real facades in KRESNIK II.

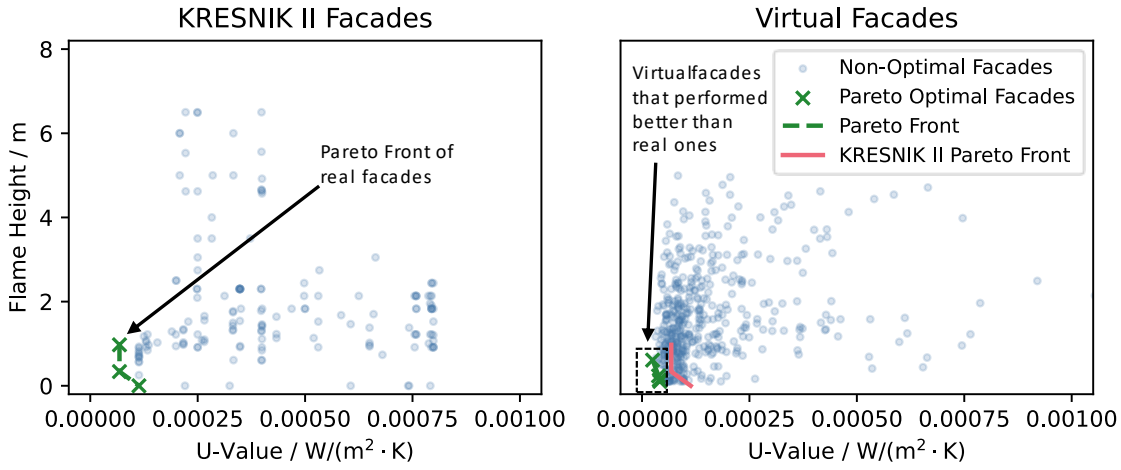

Figure 7.1 – Plots of flame height vs U-value for the facades in KRESNIK II (left) and for virtual facades generated by passing randomly generated inputs through the neural network trained in Chapter 6 (right). The virtual facades may contain materials that could not feasibly exist in reality. The Pareto front in the image on the right has moved closer to the origin, meaning it includes facades that are more optimal than the ones in KRESNIK II. This plot is similar to Figure 2.7

Designing a facade is a complex, multi-objective problem. Currently, many of the objectives that a facade has to achieve, such as its beauty, its moisture control, or its flammability, are difficult to quantify, making it challenging to consider these objectives and compare facades against each other. Being unable to quantify the flammability of facades has also made it difficult to scientifically interpolate or extrapolate the results of different facade safety tests, despite the necessity of small changes being made to facade designs in complex construction projects. However, in this research we have shown that, by collecting existing facade fire test data and applying a top-down approach to the problem, quantifying a facade's flammability could be possible, helping designers to construct safer high-rise buildings, and moving a step closer toward optimum design.

REFERENCES

[1] G. Zemella and A. Faraguna, *Evolutionary Optimisation of Facade Design*, First Edit. Springer-Verlag London, 2014.

[2] C. LAUTENBERGER, J. TORERO, and C. FERNANDEZ-PELLO, "1 - Understanding materials flammability," in *Flammability Testing of Materials Used in Construction, Transport and Mining*, V. B. Apte, Ed. Woodhead Publishing, 2006, pp. 1–21.

[3] "The Grenfell Tower Inquiry," 2018. [Online]. Available: https://www.grenfelltowerinquiry.org.uk/. [Accessed: 10-May-2018].

[4] B. Robert and P. Walker, "Boris Johnson accused of betraying homeowners over cladding crisis," *The Guardian*, Feb-2021.

[5] N. White and M. Delichatsios, "Fire Hazards of Exterior Wall Assemblies Containing Combustible Components: Final Report," *MATEC Web Conf.*, vol. 9, 2013.

[6] Wikipedia Contributors, "List of high-rise facade fires - Wikipedia, the Free Encyclopedia," 2020. [Online]. Available: https://en.wikipedia.org/w/index.php?title=List_of_high-rise_facade_fires&oldid=989716210. [Accessed: 12-Dec-2020].

[7] M. Bonner and G. Rein, "List of Facade Fires 1990 - 2020," 2020. [Online]. Available: https://doi.org/10.5281/zenodo.3743863.

[8] S. Colwell and T. Baker, *BR135: Fire performance of external thermal insulation for walls of multistorey buildings*, Third Edit. 2013.

[9] J. Torero, "Grenfell Tower: Phase 1 Report," *Rep. Grenfell Tower Inq.*, 2018.

[10] C. A. Wade and J. C. Clampett, "Fire Performance of Exterior Claddings," *Rep. from Build. Res. Assoc. New Zeal.*, 2000.

[11] BSI, *BS 8414-1:2015 Fire performance of external cladding systems. Test method for non-loadbearing external cladding systems applied to the masonry facade of a building*. 2015.

[12] BSI, *BS 8414-2:2015 Fire performance of external cladding systems. Test method for non-loadbearing external cladding systems fixed to and supported by a structural steel frame*. 2015.

[13] J. Schulz, D. Kent, T. Crimi, J. L. D. Glockling, and T. R. Hull, “A Critical Appraisal of the UK’s Regulatory Regime for Combustible Façades,” *Fire Technol.*, 2020.

[14] T. Herzog, R. Krippner, and W. Lang, *Facade Construction Manual*, Second. DETAIL Business Information, 2017.

[15] P. Oldfield, D. Trabucco, and A. Wood, “Five energy generations of tall buildings: An historical analysis of energy consumption in high-rise buildings,” *J. Archit.*, vol. 14, no. 5, pp. 591–613, 2009.

[16] D. Shearer and B. Anderson, “International comparison of energy standards in building regulations for non-domestic buildings: Denmark, Finland, Norway, Scotland, and Sweden,” *Rep. BRE Scotl.*, 2008.

[17] EU, “Directive 2010/31/EU of the European Parliament and of the Council of 19 May 2010 on the energy performance of buildings (recast),” *Off. J. Eur. Union*, pp. 13–35, 2010.

[18] HM Government, *Approved Document L - Conservation of fuel and power*. 2016.

[19] J. Hidalgo, S. Welch, and J. Torero, “Performance criteria for the fire safe use of thermal insulation in buildings,” *Constr. Build. Mater.*, vol. 100, pp. 285–297, Dec. 2015.

[20] G. Maria and D. J. Thorkild, “Roadshow Paris - Forward Looking Statement,” *Present. Rockwool Int.*, no. October, 2011.

[21] M. G. Moore, “The Contributions of Insulation to the U.S. Economy in 2017,” *Rep. Am. Chem. Counc.*, no. April, 2018.

[22] D. Bozsaky, “The historical development of thermal insulation materials,” *Period. Polytech. Archit.*, vol. 41, no. 2, p. 49, 2010.

[23] P. Petrus, “A Perspective On High Rise Building Fires Involving The Facade,” *Asia Pacific Fire*, 10-Apr-2017.

[24] M. Farrer and L. Barney, “Honolulu fire: three dead after blaze breaks out in high-rise building,” *The Guardian*, Jul-2017.

[25] B. Duval, “Monte Carlo Hotel Casino Fire,” *NFPA J.*, no. May/June, 2008.

[26] Kontakt 24, “Spalona elewacja, zniszczone okna. ‘Od parteru az po sam dach’ - [Burned facade, damaged windows. ‘From the ground floor to the roof’],” *tvn*

Warszawa, 2019. [Online]. Available: https://tvn24.pl/tvnwarszawa/najnowsze/spalona-elewacja-zniszczone-okna-od-parteru-az-po-sam-dach-297220. [Accessed: 08-Oct-2019].

[27] M. Chulov, K. Shaheen, and R. McKee, "Massive fire at Dubai skyscraper interrupts New Year's Eve fireworks," *The Guardian*, Jan-2016.

[28] HM Government, *Approved Document B - Fire Safety*. 2010.

[29] M. Smolka *et al.*, "Semi-natural test methods to evaluate fire safety of wall claddings: Update," *MATEC Web Conf.*, vol. 46, 2016.

[30] J. Anderson *et al.*, "European approach to assess the fire performance of façades," *Fire Mater.*, no. October 2019, pp. 1–11, 2020.

[31] B. Lars *et al.*, "Development of a European approach to assess the fire performance of facades," 2018.

[32] BBC Reporters, "Grenfell Tower: What happened," *BBC News*, 2018. [Online]. Available: https://www.bbc.co.uk/news/uk-40301289. [Accessed: 28-Aug-2019].

[33] J. Hackitt, "Building a safer future - Independent Review of Building Regulations and Fire Safety: Interim Report," 2017.

[34] HM Government, "November 2018 to April 2019 amendments to Approved Document B, Volume 1 and Volume 2," 2019.

[35] G. Genco, "Lacrosse Building Fire Report," Melbourne, 2015.

[36] P. Shergold and B. Weir, "Building Confidence," 2018.

[37] P. Johnson, D. Lange, J. Torero, A. Brinson, and M. Foley, "Fire Safety Engineering, The Final Report," Sydney, 2018.

[38] T. Nguyen and F. Meftah, "Behavior of clay hollow-brick masonry walls during fire. Part 1: Experimental analysis," *Fire Saf. J.*, vol. 52, pp. 55–64, 2012.

[39] T. Nguyen and F. Meftah, "Behavior of hollow clay brick masonry walls during fire. Part 2: 3D finite element modeling and spalling assessment," *Fire Saf. J.*, vol. 66, pp. 35–45, 2014.

[40] S. Russo and F. Sciarretta, "Masonry exposed to high temperatures: Mechanical behaviour and properties - An overview," *Fire Saf. J.*, vol. 55, pp. 69–86, 2013.

[41] S. Manzello, R. Gann, S. Kukuck, K. Prasad, and W. Jones, "An experimental

determination of a real fire performance of a non-load bearing glass wall assembly," *Fire Technol.*, vol. 43, no. 1, pp. 77–89, 2007.

[42] Q. Wang *et al.*, "Development of a dynamic model for crack propagation in glazing system under thermal loading," *Fire Saf. J.*, vol. 63, pp. 113–124, 2014.

[43] Y. Wang, Q. Wang, Y. Su, J. Sun, L. He, and K. M. Liew, "Experimental study on fire response of double glazed panels in curtain walls," *Fire Saf. J.*, vol. 92, pp. 53–63, 2017.

[44] J. Nam *et al.*, "Validation of a numerical model for curtain walls with MVHS during free burning," *Fire Saf. J.*, vol. 94, no. January, pp. 45–53, 2017.

[45] J. Hidalgo, S. Welch, and J. Torero, "Experimental Characterisation of the Fire Behaviour of Thermal Insulation Materials for a Performance-Based Design Methodology," *Fire Technol.*, vol. 53, pp. 1201–1232, 2017.

[46] B. Rogowski, "Fire Performance of Combustible Insulation in Masonry Cavity Walls," *Fire Saf. J.*, vol. 8, no. 2, pp. 119–134, 1985.

[47] J. Hidalgo, "Performance-based methodology for the fire safe design of insulation materials in energy efficient buildings," University of Edinburgh, 2015.

[48] F. Incopera, D. Dewitt, T. Bergman, and A. Lavine, *Foundations of Heat Transfer*, Sixth. John Wiley & Sons, 2013.

[49] Afipeb, Sipev, and Snmi, "Fire behaviour of EPS ETICS on concrete or masonry facades," *MATEC Web Conf.*, vol. 46, 2016.

[50] D. Bjegovic, I. Pecur, B. Milovanovic, M. Rukavina, and M. Bagaric, "Comparative full-scale fire performance testing of ETICS systems," *J. Croat. Assoc. Civ. Eng.*, vol. 68, no. 05, pp. 357–369, 2016.

[51] I. Kotthoff, S. Hauswaldt, O. Riese, and J. Riemesch-Speer, "Investigations of the performance of facades made of ETICS with polystyrene under external fire exposure and fire safety measures for their improvement," *MATEC Web Conf.*, vol. 46, 2016.

[52] M. Hajduković, N. Knez, F. Knez, and J. Kolšek, "Fire Performance of External Thermal Insulation Composite System (ETICS) Facades with Expanded Polystyrene (EPS) Insulation and Thin Rendering," *Fire Technol.*, vol. 53, no. 1, pp. 173–209, Jan. 2017.

[53] L. Zhou, A. Chen, X. Liu, and F. Zhang, “The Effectiveness of Horizontal Barriers in Preventing Fire Spread on Vertical Insulation Panels Made of Polystyrene Foams,” *Fire Technol.*, vol. 52, no. 3, pp. 649–662, 2016.

[54] Allianz Risk Consulting, “Sandwich panels,” *Tech Talk*, vol. Volume 17, 2015.

[55] G. M. E. Cooke, “Sandwich panels for external cladding – fire safety issues and implications for the risk assessment process,” *Rep. Eurisol*, 2000.

[56] ABI, “Technical Briefing: Fire Performance of Sandwich Panel Systems,” 2003.

[57] R. J. Crewe *et al.*, “Fire Performance of Sandwich Panels in a Modified ISO 13784-1 Small Room Test: The Influence of Increased Fire Load for Different Insulation Materials,” *Fire Technol.*, vol. 54, no. 4, pp. 819–852, Jul. 2018.

[58] Y. C. Wang and A. Foster, “Experimental and numerical study of temperature developments in PIR core sandwich panels with joint,” *Fire Saf. J.*, vol. 90, no. March, pp. 1–14, 2017.

[59] A. Foster, “Understanding , Predicting and Improving the Performance of Foam Filled Sandwich Panels in Large Scale Fire Resistance Tests,” University of Manchester, 2014.

[60] J. Kim, J. de Ris, and F. Kroesser, “Laminar burning between parallel fuel surfaces,” *Int. J. Heat Mass Transf.*, vol. 17, no. 3, pp. 439–451, 1974.

[61] V. Babrauskas, “The Grenfell Tower Fire and Fire Safety Materials Testing,” *Fire Eng.*, vol. 171, no. 1, 2018.

[62] A. Lacasta, J. Avellaneda, M. P. Giraldo, and C. Burgos, “Computer-simulation study on fire behaviour in the ventilated cavity of ventilated facade systems,” *MATEC Web Conf.*, vol. 9, 2013.

[63] K. Livkiss, S. Svensson, B. Husted, and P. van Hees, “Flame Heights and Heat Transfer in Façade System Ventilation Cavities,” *Fire Technol.*, vol. 54, no. 3, pp. 689–713, May 2018.

[64] C. Wahlquist, “Cladding in London high-rise fire also blamed for 2014 Melbourne blaze,” *The Guardian*, 2017.

[65] NFPA and Arup, “EFFECT: External Facade Fire Evaluation and Comparison Tool - User’s Guide,” *NFPA’s online tool based Methodol. Dev. by Arup*, no. February, 2018.

[66] G. Agarwal, “Evaluation of the Fire Performance of Aluminium Composite Material (ACM) Assemblies using ANSI/FM4880,” *FM Glob. Tech. Rep.*, 2016.

[67] E. Guillaume, T. Fateh, R. Schillinger, R. Chiva, and S. Ukleja, “Study of fire behaviour of facade mock-ups equipped with aluminium composite material-based claddings, using intermediate-scale test method,” *Fire Mater.*, vol. 42, no. December 2017, pp. 1–17, 2018.

[68] International Commitee of the Decorative Laminates Industry, “Fire behaviour of decorative high pressure laminates (HPL),” *Inf. Data Sheet*, 2009.

[69] J. Evans, “Bolton fire raises fresh questions over cladding safety,” *Financial Times*, Nov-2019.

[70] S. T. Mckenna *et al.*, “Fire behaviour of modern facade materials – Understanding the Grenfell Tower fire,” *J. Hazard. Mater.*, vol. 368, no. September 2018, pp. 115–123, 2019.

[71] M. S. Mclaggan *et al.*, “The Material Library of Cladding Materials.” The University of Queensland, 2019.

[72] M. S. McLaggan, J. P. Hidalgo, J. Carrascal, M. T. Heitzmann, A. F. Osorio, and J. L. Torero, “Flammability trends for a comprehensive array of cladding materials,” *Fire Saf. J.*, p. 103133, 2020.

[73] A. Čolić and I. B. Pečur, “Influence of Horizontal and Vertical Barriers on Fire Development for Ventilated Façades,” *Fire Technol.*, vol. 56, no. 4, pp. 1725–1754, 2020.

[74] E. Guillaume, “Grenfell Fire Reconstruction - First Lessons.” 2019.

[75] E. Guillaume, V. Dréan, B. Girardin, F. Benameur, and T. Fateh, “Reconstruction of Grenfell Tower fire. Part 1: Lessons from observations and determination of work hypotheses,” *Fire Mater.*, vol. 44, no. 1, pp. 3–14, 2020.

[76] E. Guillaume, V. Dréan, B. Girardin, M. Koohkan, and T. Fateh, “Reconstruction of Grenfell Tower fire. Part 2: A numerical investigation of the fire propagation and behaviour from the initial apartment to the façade,” *Fire Mater.*, vol. 44, no. 1, pp. 15–34, 2020.

[77] E. Guillaume, V. Dréan, B. Girardin, F. Benameur, M. Koohkan, and T. Fateh, “Reconstruction of Grenfell Tower fire. Part 3—Numerical simulation of the Grenfell Tower disaster: Contribution to the understanding of the fire propagation

and behaviour during the vertical fire spread," *Fire Mater.*, vol. 44, no. 1, pp. 35–57, 2020.

[78] S. Lay, "Fire safety for high-rise facades," *Struct. Eng.*, no. October, pp. 30–33, 2007.

[79] W. An, J. Sun, K. Liew, and G. Zhu, "Effects of building concave structure on flame spread over extruded polystyrene thermal insulation material," *Appl. Therm. Eng.*, vol. 121, no. October 2014, pp. 802–809, 2017.

[80] E. K. Asimakopoulou, D. I. Kolaitis, and M. A. Founti, "Assessment of Fire Engineering Design Correlations Used to Describe the Geometry and Thermal Characteristics of Externally Venting Flames," *Fire Technol.*, vol. 53, no. 2, pp. 709–739, 2017.

[81] J. Ji, Y.-F. Li, W.-X. Shi, and J.-H. Sun, "Numerical studies on smoke spread in the cavity of a double-skin facade," *J. Civ. Eng. Manag.*, vol. 22, no. 4, pp. 470–479, 2016.

[82] C. Chow, "Spread of smoke and heat along narrow air cavity in double-skin façade fires," *Therm. Sci.*, vol. 18, no. SUPPL.2, pp. 405–416, 2014.

[83] W. Chow and W. Hung, "Effect of cavity depth on smoke spreading of double-skin façade," *Build. Environ.*, vol. 41, no. 7, pp. 970–979, 2006.

[84] DCLG, *Fire Performance of Green Roofs and Walls*, no. August. 2013.

[85] L. Mazziotti, P. Cancelliere, G. Paduano, P. Setti, and S. Sassi, "Fire risk related to the use of PV systems in building facades," *MATEC Web Conf.*, vol. 46, 2016.

[86] M. Z. Naser, "Fire resistance evaluation through artificial intelligence - A case for timber structures," *Fire Saf. J.*, vol. 105, no. September 2018, pp. 1–18, 2019.

[87] M. Z. Naser, "AI-based cognitive framework for evaluating response of concrete structures in extreme conditions," *Eng. Appl. Artif. Intell.*, vol. 81, no. March, pp. 437–449, 2019.

[88] A. Dexters, R. R. Leisted, R. Van Coile, S. Welch, and G. Jomaas, "Testing for knowledge: Application of machine learning techniques for prediction of flashover in a 1/5 scale ISO 13784-1 enclosure," *Fire Mater.*, no. October 2019, pp. 1–12, 2020.

[89] M. Spearpoint, I. Fu, K. Frank, and I. Fu, "Façade fire incidents in tall buildings,"

CTBUH J., vol. 1, no. 2, pp. 34–39, 2019.

[90] R. Evins, S. C. Joyce, P. Pointer, S. Sharma, R. Vaidyanathan, and C. Williams, "Multi-objective design optimisation: Getting more for less," *Proc. Inst. Civ. Eng. Civ. Eng.*, vol. 165, no. 5, pp. 5–10, 2012.

[91] J. Kim, "A Methodology for Daylight Optimisation of Facades: An investigation of the opening design strategy with Cellular Automata for an office building," *Emerg. Technol. a Smarter World*, 2012.

[92] R. Shan, "Optimization for heating, cooling and lighting load in building façade design," *Energy Procedia*, vol. 57, pp. 1716–1725, 2014.

[93] J. Arora, *Introduction to Optimum Design*, Second Edi. Elsevier Academic Press, 2004.

[94] PKN, "PN-B-02867:2013-06," 2013.

[95] ISO, "ISO 13785-1:2002," 2002.

[96] P. Sulik and B. Sedlak, "Spreading Fire by The ETICS Facade," *Conf. Proc. Fifteenth Int. Interflam Conf.*, vol. 2, 2019.

[97] R. Elmasri and S. B. Navathe, *Database Systems: Models, Languages, Design, And Application Programming*, Sixth Edit. Pearson, 1989.

[98] Lucidchart, "Entity-Relationship Diagram Symbols and Notation," 2019. [Online]. Available: https://www.lucidchart.com/pages/ER-diagram-symbols-and-meaning. [Accessed: 04-Jun-2019].

[99] D. Drysdale, *An Introduction to Fire Dynamics*, Third Edit. 2011.

[100] M. Foley and D. Drysdale, "Heat transfer from flames between vertical parallel walls," *Fire Saf. J.*, vol. 24, no. 1, pp. 53–73, 1995.

[101] L. Bisby, "Grenfell Tower Inquiry Phase 1 - Expert Report," 2018.

[102] D. McFadden, "Conditional logit analysis of qualitative choice behavior," *Front. Econom.*, 1973.

[103] L. Orloff and J. de Ris, "Froude Modeling of Pool Fires," *Symp. Combust.*, vol. 19, no. 1, pp. 885–895, 1982.

[104] J. L. De Ris and L. Orloff, "Flame heat transfer between parallel panels," *Fire Saf. Sci.*, pp. 999–1010, 2005.

[105] B. J. Stratton, M. Spearpoint, and C. Fleischmann, “Determining Flame Height And Flame Pulsation Frequency And Estimating Heat Release Rate From 3D Flame Reconstruction,” University of Canterbury, NZ, 2005.

[106] G. Cox, *Combustion Fundamentals of Fire*. London: Academic Press, 1995.

[107] Y. Xin, “Estimation of chemical heat release rate in rack storage fires based on flame volume,” *Fire Saf. J.*, vol. 63, pp. 29–36, 2014.

[108] L. Audouin, G. Kolb, J. L. Torero, and J. M. Most, “Average centreline temperatures of a buoyant pool fire obtained by image processing of video recordings,” *Fire Saf. J.*, vol. 24, no. 2, pp. 167–187, 1995.

[109] T. H. Chen, P. H. Wu, and Y. C. Chiou, “An early fire-detection method based on image processing,” *Proc. - Int. Conf. Image Process. ICIP*, vol. 3, pp. 1707–1710, 2004.

[110] T. Çelik, H. Demirel, H. Ozkaramanli, and M. Uyguroglu, “Fire Detection in Video Sequences Using Statistical Color Model,” *2006 IEEE Int. Conf. Acoust. Speech Signal Process. Proc.*, vol. 2, 2006.

[111] B. C. Ko, K. H. Cheong, and J. Y. Nam, “Fire detection based on vision sensor and support vector machines,” *Fire Saf. J.*, vol. 44, no. 3, pp. 322–329, 2009.

[112] P. S. Mason, C. M. Fleischmann, C. B. Rogers, A. E. McKinnon, K. Unsworth, and M. Spearpoint, “Estimating thermal radiation fields from 3D flame reconstruction,” *Fire Technol.*, vol. 45, no. 1, pp. 1–22, 2009.

[113] J. Chen and Q. Bao, “Digital image processing based fire flame color and oscillation frequency analysis,” *Procedia Eng.*, vol. 45, pp. 595–601, 2012.

[114] T. Xuan Truong and J. M. Kim, “Fire flame detection in video sequences using multi-stage pattern recognition techniques,” *Eng. Appl. Artif. Intell.*, vol. 25, no. 7, pp. 1365–1372, 2012.

[115] A. K. K. Wong and N. K. Fong, “Experimental study of video fire detection and its applications,” *Procedia Eng.*, vol. 71, pp. 316–327, 2014.

[116] T. B. Maynard and J. W. Butta, “A Physical Model for Flame Height Intermittency,” *Fire Technol.*, vol. 54, no. 1, pp. 135–161, 2018.

[117] K. Li, S. Mao, and R. Feng, “Estimation of Heat Release Rate and Fuel Type of Circular Pool Fires Using Inverse Modelling Based on Image Recognition

Technique," *Fire Technol.*, vol. 55, no. 3, pp. 667–687, 2019.

[118] A. E. Çetin *et al.*, "Video fire detection - Review," *Digit. Signal Process. A Rev. J.*, vol. 23, no. 6, pp. 1827–1843, 2013.

[119] A. Gaur, A. Singh, A. Kumar, A. Kumar, and K. Kapoor, "Video Flame and Smoke Based Fire Detection Algorithms: A Literature Review," *Fire Technol.*, vol. 56, no. 5, pp. 1943–1980, 2020.

[120] D. Graham, "Tomographic Reconstruction of a Swirling Flame," Imperial College London, 2016.

[121] G. Bradski and A. Kaehler, *Learning OpenCV: Computer vision with the OpenCV library*. O'Reilly Media, Inc., 2008.

[122] P. Mason, "Estimating Thermal Radiation Fields From 3D Flame Reconstruction," Lincoln University, 2003.

[123] G. Bradski, "The OpenCV Library," *Dr. Dobb's J. Softw. Tools*, 2000.

[124] A. Mordvintsev and K. Abid, "OpenCV Camera Calibration Tutorial," 2013. [Online]. Available: https://opencv-python-tutroals.readthedocs.io/en/latest/py_tutorials/py_calib3d/py_calibration/py_calibration.html. [Accessed: 02-Jul-2020].

[125] Otsu and N., "A threshold selection method from gray-level histograms," *IEEE Trans. Syst. Man Cybern.*, vol. 9, no. 1, pp. 62–66, 1996.

[126] Blender Online Community, "Blender - a 3D modelling and rendering package." Blender Foundation, Amsterdam, 2018.

[127] M. M. Khan, A. Tewarson, and M. Chaos, "Combustion Characteristics of Materials and Generation of Fire Products," in *SFPE Handbook of Fire Protection Engineering 5th Edition*, 2016, pp. 1143–1233.

[128] BSI, *BS EN 13501-1, Fire classification of construction products and building elements. Part 1: classification using data from reaction to fire tests*. 2009.

[129] N. Papaioannou, F. Leach, and M. Davy, "Effect of Thermocouple Size on the Measurement of Exhaust Gas Temperature in Internal Combustion Engines," *SAE Tech. Pap.*, vol. 2018-Septe, no. 1, pp. 1–12, 2018.

[130] D. D. Drysdale, A. J. R. Macmillan, and D. Shilitto, "The King's Cross fire: Experimental verification of the 'Trench effect,'" *Fire Saf. J.*, vol. 18, no. 1, pp. 75–

82, 1992.

[131] F. E. Harell Jr., *Regression Modeling Strategies*, Second. Springer, 2015.

[132] B. Garvey, "Experimental study on the interaction of cladding materials in the fire performance of facades," University of Queensland, 2018.

[133] B. Garvey *et al.*, "Experimental methodology to study the fire contribution of cladding materials," in *Proceedings of the 15th International Interflam*, 2019.

[134] NFPA, *NFPA 285 Standard Fire Test Method for Evaluation of Fire Propagation Characteristics of Exterior Non-Load-Bearing Wall Assemblies Containing Combustible Components*. 2012.

[135] B. McCaffrey, "Purely buoyant diffusion flames: some experimental results, NBSIR 79-1910," *National Bureau of Standards*. 1979.

[136] S. Yokoi, "Study on the prevention of fire spread caused by hot upward current.," Tokyo, 1960.

[137] Y. P. Lee, M. A. Delichatsios, and Y. Ohmiya, "The physics of the outflow from the opening of an enclosure fire and re-examination of Yokois correlation," *Fire Saf. J.*, vol. 49, pp. 82–88, 2012.

[138] G. Heskestad, "Peak gas velocities and flame heights of buoyancy-controlled turbulent diffusion flames," *Symp. Combust.*, 1981.

[139] F. Ren, L. Hu, and X. Sun, "Experimental Investigation on Lateral Temperature Profile of Window-Ejected Facade Fire Plume with Ambient Wind," *Fire Technol.*, vol. 55, no. 3, pp. 903–913, 2019.

[140] L. M. Yuan and G. Cox, "An experimental study of some line fires," *Fire Saf. J.*, vol. 27, no. 2, pp. 123–139, 1996.

[141] "Kingspan BS 8414 Tested Systems." [Online]. Available: https://www.kingspan.com/gb/en-gb/fire-safety/kingspan-bs-8414-tested-systems. [Accessed: 10-Dec-2020].

[142] HM Government, "Fire test reports: DCLG BS 8414 tests no. 1-7," 2018.

[143] N. Jones *et al.*, "Burning behaviour of rainscreen façades," *J. Hazard. Mater.*, vol. 403, 2021.

[144] H. Emmons, "Fire Research Abroad," *Fire Res. Abstr. Rev.*, vol. 10, no. 2, 1968.

[145] G. Lin, Y. Zhang, G. Xu, and Q. Zhang, “Smoke Detection on Video Sequences Using 3D Convolutional Neural Networks,” *Fire Technol.*, vol. 55, no. 5, pp. 1827–1847, 2019.

[146] W. Mao, W. Wang, Z. Dou, and Y. Li, “Fire Recognition Based On Multi-Channel Convolutional Neural Network,” *Fire Technol.*, vol. 54, no. 2, pp. 531–554, 2018.

[147] S. M. Nemalidinne and D. Gupta, “Nonsubsampled contourlet domain visible and infrared image fusion framework for fire detection using pulse coupled neural network and spatial fuzzy clustering,” *Fire Saf. J.*, vol. 101, no. August, pp. 84–101, 2018.

[148] M. Polinova, L. Wittenberg, H. Kutiel, and A. Brook, “Reconstructing pre-fire vegetation condition in the wildland urban interface (WUI) using artificial neural network,” *J. Environ. Manage.*, vol. 238, no. March, pp. 224–234, 2019.

[149] J. L. Hodges and B. Y. Lattimer, “Wildland Fire Spread Modeling Using Convolutional Neural Networks,” *Fire Technol.*, vol. 55, no. 6, pp. 2115–2142, 2019.

[150] O. Cepeliogullar, I. Mutlu, S. Yaman, and H. Haykiri-Acma, “A study to predict pyrolytic behaviors of refuse-derived fuel (RDF): Artificial neural network application,” *J. Anal. Appl. Pyrolysis*, vol. 122, pp. 84–94, 2016.

[151] J. L. Hodges, B. Y. Lattimer, and K. D. Luxbacher, “Compartment fire predictions using transpose convolutional neural networks,” *Fire Saf. J.*, vol. 108, no. November 2018, 2019.

[152] M. Z. Naser, “Deriving temperature-dependent material models for structural steel through artificial intelligence,” *Constr. Build. Mater.*, vol. 191, pp. 56–68, 2018.

[153] I. Fu, M. Spearpoint, and K. Frank, “Façade Fire Incidents in Tall Buildings Fire and Safety,” *CTBUH J.*, no. Ii, pp. 34–39, 2019.

[154] A. Halevy, P. Norvig, and F. Pereira, “The unreasonable effectiveness of data,” *IEEE Intell. Syst.*, vol. 24, no. 2, pp. 8–12, 2009.

[155] I. Goodfellow, Y. Bengio, and A. Courville, *Deep Learning*. MIT Press, 2016.

[156] S. Rogers and M. Girolami, *A first course in machine learning*. 2011.

[157] F. Chollet, “Keras.” 2015.

[158] M. Abadi *et al.*, “TensorFlow: A system for large-scale machine learning,” in *Proceedings of the 12th USENIX Symposium on Operating Systems Design and Implementation, OSDI 2016*, 2016.

[159] F. Pedregosa *et al.*, “Scikit-learn: Machine learning in Python,” *J. Mach. Learn. Res.*, 2011.

Appendix

This appendix presents the details of the entity relationship diagram for KRESNIK I, shown in Figure 3.2. The Datatype column mentions factors. These are not a datatype in computing but are a structure in R that is used to deal with categorical data, and so I have separated them from other string/character variables for clarity. All material properties were taken from measurements at room temperature.

Entity	Variable	Datatype	Description
PNB02867	droplets	Boolean	True/False: were droplets observed during the test?
	L1_temp	Boolean	True/False: did the temperature measured at L1 exceed 450℃?
	L2_temp	Boolean	True/False: did the temperature measured at L2 exceed 350℃?
	L1_burn	Boolean	True/False: was burning observed at or above line L1 after the wood crib was removed?
	L2_burn	Boolean	True/False: was burning observed at or above line L2 after the wood crib was removed?
	burn_after	Boolean	True/False: was burning observed anywhere on the facade after the test had concluded?
	peak_temp	Numeric	What was the maximum temperature measured during the test by any thermocouple (after averaging the thermocouple data over 30 s)? Measured in ℃
	residence_time	Numeric	After subtracting the wood crib thermocouple curves from the test thermocouple data, for how long did at least one of the thermocouples measure

			at least 100℃ above these wood crib curves?
	pass	Boolean	True/False: was the outcome of this test a pass or a fail?
Test	source	String	What organisation provided this test data?
	standard	Factor	Which standard was used in this test?
Facade	type	Factor	4 options: was this facade ETICS, Rainscreen, Sandwich Panel, or Other.
	comments	String	A field to add any comments that may be important. Used if the facade or test scenario are unusual in some way.
Cavity	cavity_width	Numeric	Width of the air cavity in mm.
	cavity_barriers	Boolean	True/False: Were cavity barriers present in this test?
Cladding	cladding_thickness	Numeric	Thickness of the exterior cladding in mm.
SandwichExterior	s_exterior_thickness	Numeric	Thickness of the thin outer layers of the sandwich panel in mm.
Render	render_density	Numeric	Application density of render used on ETICS facade in kg/m^2.
	render_thickness	Numeric	Thickness of render in mm.
Insulation	ins_density	Numeric	Density of insulation in kg/m^3. If not provided in the test report then the value from the MaterialProperties table is used.
	ins_thickness	Numeric	Thickness of insulation in mm.
MaterialProperties	material_name	Factor	Generic name of the material (product names forbidden in order to preserve anonymity).

	heat_of_combustion	Numeric	Chemical heat of combustion of the material in MJ/kg. Taken from literature.
	density	Numeric	Density of the material in kg/m^3. Taken from literature.
	specific_heat	Numeric	Specific heat capacity of material in J/kg*K. Taken from literature.
	thermal_conductivity	Numeric	Thermal conductivity of material in W/m*k. Taken from literature.